Journal of the
OPTICAL SOCIETY
of AMERICA

VOLUME 40, NUMBER 8 AUGUST, 1950

The Combined Effect of Infra-Red Radiation and Intensification upon the Photographic Latent Image*

L. FORTMILLER, T. H. JAMES, R. F. QUIRK, AND W. VANSELOW
Kodak Research Laboratories, Eastman Kodak Company, Rochester, New York

(Received December 5, 1949)

The developability of some latent-image centers can be destroyed by the absorption of infra-red radiation (Herschel effect). Absorption of one quantum per center is sufficient to destroy the developability of some centers, indicating that the removal of one silver atom or *F*-center is sufficient to destroy the developability of such a center. Experiments have been carried out on motion-picture positive film to determine whether the developability of such centers can be restored by any of the various known methods of latensification. Experiments were also carried out to determine what effect latensification prior to the infra-red exposure has upon the Herschel effect. Both physical and direct development were employed. The degree of stabilization attained when latensification preceded infra-red exposure was calculated in terms of percent difference between the change of density of the control and of the latensified film. The degree of restoration attained when latensification followed infra-red exposure was calculated in a similar way. All latensifying agents investigated except perborate caused either partial or complete stabilization for both direct and physical development. Perborate treatment prior to infra-red exposure increased the Herschel effect. Gold and mercury produced increased infra-red sensitivity. Of the agents studied, only low intensity light and water showed any restoration for physical development. For complete direct development, no restoration was observed except for bisulfite which produced total restoration. These results indicate that, with the exception of bisulfite treatment, latensification procedures will not make developable any significant number of subimage centers which originally were smaller by one unit than the critical size necessary for initiating development.

A PHOTOGRAPHIC latent-image center in a silver halide grain probably is built up during exposure by the successive addition of silver atoms to a pre-existing sensitivity speck or by the successive addition of *F*-centers to a growing *F*-center aggregate. When a certain critical condition is reached or exceeded, the grain becomes developable. Our knowledge of the nature of this critical condition is inadequate. At least three factors have been considered as possibly contributing to its achievement. One is that of size. It is often stated that the growing center acquires the power to initiate development when it reaches a certain critical size. Sheppard has suggested, however, that mere size may be of secondary importance to the properties of the interface between the center and the surrounding silver halide. We may be justified in speaking of a critical size only in connection with otherwise equal interface conditions. A third possibility is that the configuration of the units in the center may influence its ability to promote development, and one arrangement of a given number of units may constitute a development center, whereas some other arrangement of the same number of units may not promote development.

In practice, the only way in which we can determine the number of grains which have acquired latent-image centers as a result of a given exposure is to develop the photographic material and count the number of grains which have developed, or measure the optical density of the developed deposit. The latter procedure is valid only when conditions are such that a known relationship exists between the density and number of developed grains per unit area.

The number of developed grains per unit area depends upon both the development time and the composition of the developing solution, even when suitable corrections have been made for "fog" grains, i.e., grains which have been reduced by the developer without reference to exposure. Any specification of the number of grains which contain latent-image centers, therefore, should be qualified in terms of the prescribed development conditions.

* Communication No. 1301 from the Kodak Research Laboratories.

It has been assumed[1,2] that when, as a result of a uniform exposure, only a fraction of the available silver halide grains becomes developable, at least some of the remaining grains contain "sub-image specks" which are thermally stable, but cannot promote development under the conditions employed. The evidence for the existence of such specks rests upon the observation that it is often possible by suitable post-exposure treatment to increase the number of developable grains. Such treatment has been termed "latensification."

Latensification can be brought about in several ways. One in which the effect must be ascribed to conversion of sub-image specks into full-image specks by increase in size makes use of a secondary exposure to light of low intensity. The basis of this type of latensification is illustrated by some experiments of Webb and Evans in which an emulsion was given a series of equal energy exposures, each exposure consisting partly of an intensity such as to give about the optimum photographic effect, *optimum intensity*, and partly of an intensity 1000 times lower, *low intensity*. It was found that if the optimum intensity exposure is applied first, the low intensity part of the exposure is always rendered more efficient. In fact, under the particular conditions employed, if the optimum intensity exposure was given first and amounted to as much as one-fourth the total exposure, the low intensity part of the exposure was rendered just as efficient as if the exposure had been made entirely at the optimum intensity, i.e., there was no reciprocity-law failure for the low intensity exposure. On the other hand, if the order of exposures was reversed, the low intensity part being applied first, the drop in efficiency of the low intensity exposure was very marked. The interpretation was given that the reciprocity-law failure at low intensities takes place primarily in the initial stages of the exposure while the speck is still very small. If the rate of addition of silver atoms or *F*-centers to the aggregate is very low, the chance that the first unit to be added will "evaporate" off before a second is added becomes large, and the formation of latent-image speck in a virgin grain by the low intensity exposure is a very inefficient process. If a sufficient amount of exposure is given at the optimum intensity, a stable speck is established, even though it is not yet capable of initiating development. This speck can be efficiently built up to a full latent-image speck with the low intensity light. This type of double-exposure technique has been used extensively by Burton and Berg[2] to study the properties of the "sub-image."

A second method in which latensification probably is brought about by an increase in size of the sub-image nuclei involves treatment of the exposed material in an atmosphere of mercury vapor. In this method, however, the increase in size is brought about by condensation of mercury atoms on the nuclei rather than by the addition of silver atoms to it. The mechanisms of other methods of latensification are more in doubt. These methods include bathing the photographic material in a solution of aurous thiocyanate, in a solution of potassium bisulfite, and in a solution of sodium perborate. Any experiments which would reveal a fundamental difference in the behavior of the latent image subjected to different methods of latensification would be of value in consideration of the mechanism or mechanisms of latensification. Such differences might show up in the retention or lack of retention of latensification on prolonged development in an active solution, or in the behavior of a latent-image speck which had been reduced in *size* by a controlled amount and then subjected to latensification.

Experimental results[3] showed that latensification by low intensity light was markedly reduced with prolonged development. Recent work[4] has shown that latensification by low intensity light is not obtained with a simple motion-picture positive film when development is carried to completion in an energetic developer, even though conditions are such that marked latensification is obtained for the more normal, incomplete development. Moreover, latensification obtained with other agents and incomplete development disappeared when development was carried to completion. Thus, the latensification experiments give no evidence of the formation, during exposure, of a nucleus which is thermally stable but which cannot be developed by prolonged bathing in an energetic developer. Neither do they show a difference in the behavior toward complete development of a latent image intensified in different ways.

The search for a stable, non-developable speck was continued by approaching it from the opposite direction, namely, by decreasing the size of developable latent-image specks. This presumably could be accomplished in a controlled manner by making use of the Herschel effect, since the work of Kornfeld and James[5] had indicated that the developability of some latent-image centers could be destroyed by the absorption of one quantum each of infra-red radiation. The direct effect of such absorption would be the loss of a silver atom or *F*-center by each nucleus. Kornfeld and James had used incomplete development in a solution of only moderate activity. However, subsequent work[6] showed that a Herschel effect persisted with complete development in an energetic developer, even at relatively low infra-red exposures. In the present work, we have determined whether a latent-image center destroyed by the removal of one silver atom or of one *F*-center could be restored to any extent by sub-

[1] J. H. Webb and C. H. Evans, J. Opt. Soc. Am. **28**, 431 (1938).
[2] P. C. Burton and W. F. Berg, Phot. J. **86B**, 2 (1946).
[3] W. H. Carnahan, C. N. Nelson, and L. A. Jones, private communication (1941).
[4] T. H. James and W. Vanselow, PSA Journal **15**, 688 (1949).
[5] G. Kornfeld and T. H. James, J. Opt. Soc. Am. **33**, 615 (1943).
[6] W. Vanselow and T. H. James, PSA Journal (Part II, Phot. Sci. Tech.) **16B**, 21 (1950).

sequent treatment with any of the various latensifying agents. With a single exception, it could not.

A second aim of the present investigation was to determine what effect latensification of an actinic light exposure would have upon the subsequent action of infra-red radiation. The results varied. Gold and mercury latensification stabilized the latent image toward the action of the infra-red exposure and actually sensitized the emulsion toward the formation of the latent image by that exposure. Treatment in sodium perborate solution resulted in an increase in the destruction of the latent image by the infra-red exposure. Low intensity light exposure and treatment in bisulfite solution produced incomplete stabilization. These phenomena were studied with both direct and physical development.

EXPERIMENTAL PROCEDURE

All experiments were made with motion-picture positive film. Unless otherwise stated, exposures were made using the Eastman IIb (time-scale) Sensitometer, with the positive lamp, a color-temperature-correcting filter for 3000°K, and a neutral density of 0.4 in the light path for experiments with direct development. The neutral density was omitted for the exposures for the physical-development experiments. These exposures will be designated as *sensitometer exposures*.

The light source for making the *infra-red* (*Herschel*) *exposures* consisted of a 500-watt tungsten-filament projection lamp at a distance of 75 cm. The radiation which passed through a combination of two Kodak Wratten No. 87 and one Kodak Wratten No. 25 filters[7] produced the Herschel effect. One of the two sensitometer wedges on each film strip was exposed to the infra-red; the other was masked and served as the control.

Auxiliary low intensity light exposures, hereafter designated as *low intensity light*, were made under the following conditions: A 6-watt, 115-volt, white, frosted bulb was housed in a safelamp behind a 5- by 7-inch piece of flashed opal glass having an opening 11 cm by 5.2 cm. The film was exposed at a distance of 142 cm from the bulb, or 128 cm from the flashed opal glass. A neutral density of 2.0 was used to adjust the light intensity. All low intensity light exposure times were 15 minutes.

Mercury-vapor treatment was carried out in a large wooden container, coated with paraffin on the inside. The liquid mercury was in glass dishes on the bottom of the box. The air was stirred mechanically 1 minute out of every 15. A similar container, but *without* mercury, was used for storing the control films. The treatment lasted for 2 days at 20°C and 50 percent relative humidity. For the "decay" experiments, the strips (mercury-treated and control) were pinned onto wooden racks and stored in separate metal boxes at about 20°C (relative humidity was not controlled).

Strips of film were gold-latensified by bathing them for 10 minutes in a solution containing 0.04 g $KAuCl_4$, 0.5 g KCNS, and 0.6 g KBr per liter at *p*H approximately 4.2. The corresponding control strips were bathed in a solution containing the same quantities of KCNS and KBr. After bathing, the strips were dried.

Film samples were bisulfite-latensified by bathing for 1 minute in a solution of potassium metabisulfite containing 50 g per liter at *p*H approximately 4.5, and then dried rapidly in air at room temperature.

For perborate latensification, solutions containing 0.2 g per liter of sodium perborate, with and without potassium bromide at *p*H 6, were used. Films were bathed for 1 minute before drying, or washing and drying, as the experiments dictated.

The investigation covered (A) direct development of 4 minutes in Kodak D-16 Developer, (B) postfixation physical development, and (C) direct development over a time range of 2 to 32 minutes in Kodak D-19 Developer containing 0.5 g of α-picolinium-β-phenylethylbromide.

The procedure for physical development consisted in immersing the exposed and treated photographic film in a fixing bath composed of 5 percent sodium thiosulfate pentahydrate and 0.5 percent potassium hydroxide by weight. The fixing bath had previously been freed of oxygen by bubbling through it continuously for 30 minutes "high purity" nitrogen. The bubbling of nitrogen was continued during the 5-minute time of fixation at a rate of about 8 cc per second. After fixation, the film was washed 30 minutes at 20°C. Physical development was carried on in 500-cc graduated cylinders with the same type of nitrogen agitation as was used during fixation. The formula for the physical developer used is as follows:

Part A		
p-Phenylenediamine dihydrochloride	11.04	g
Sodium sulfite (desiccated)	20.0	g
Water	320	cc
Part B		
Silver nitrate	12.0	g
Water	140	cc
Part C		
Sodium sulfite (desiccated)	288	g
Water	1300	cc
0.1 *M* borax	160	cc

Part B was added to Part C when both were completely in solution. Part A was added directly before use. Development was carried on for 2 hours at 20°C, after which the strips were lightly swabbed with cotton, washed for 30 minutes, and then dried.

EXPERIMENTAL RESULTS

(A) Direct Development

Restoration

The first set of experiments was carried out to determine the relative effect of the various latensification

[7] J. H. Webb and C. H. Evans, J. Opt. Soc. Am. **28**, 258 (1938).

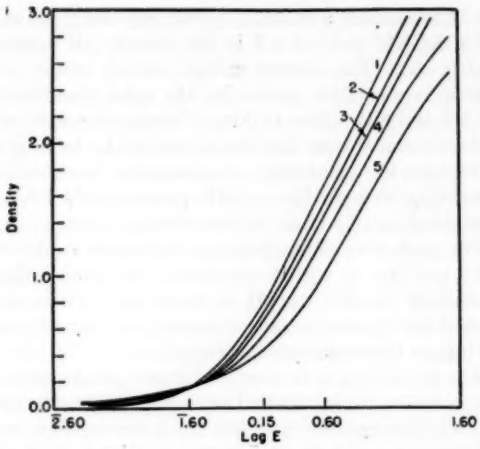

FIG. 1. Characteristic curves, untreated motion-picture positive film. Curves 1, 2, 3, 4, and 5 represent, respectively, 0, 3, 10, 30, and 90 minutes' infra-red exposure.

treatments on film which had been exposed first to actinic light in the sensitometer and then to infra-red light to produce a partial destruction of the latent image formed in the sensitometer exposure. Four durations of infra-red exposure were employed: 3, 10, 30, and 90 minutes. The extent of the Herschel effect produced by such exposures is shown in Fig. 1, where the family of characteristic curves given corresponds to a sensitometer exposure and subsequent infra-red exposures of 0, 3, 10, 30, and 90 minutes. Development was for 4 minutes in D-16.

In the latensification experiments, similar sets of characteristic curves were obtained for each latensifying agent, the treatment of the film being exactly the same, except that in each case the latensifying treatment was given to the film after the infra-red exposure but before development.

TABLE I. Restoration by low intensity light or mercury treatment of latent image partially destroyed by infra-red exposure.

Infra-red exposure (minutes)	Initial density	Density after infra-red exposure and subsequent treatment by: None (control)	Low intensity light	Mercury	Restoration (percent) by Low intensity light	Mercury
10	Fog	0.02	0.08	0.05		
	0.4	0.33	0.33	0.35	0	28
	1.0	0.83	0.83	0.87	0	23
	2.0	1.75	1.73	1.82	−8	28
	2.7	2.40	2.38	2.43	−7	10
30	Fog	0.03	0.09	0.06		
	0.4	0.28	0.28	0.36	0	67
	1.0	0.73	0.69	0.80	−14	26
	2.0	1.59	1.61	1.70	5	26
	2.7	2.24	2.25	2.35	2	24
90	Fog	0.05	0.10	0.10		
	0.4	0.27	0.24	0.39	−23	92
	1.0	0.56	0.56	0.73	0	39
	2.0	1.31	1.39	1.49	12	26
	2.7	1.97	2.05	2.20	11	31

The data were evaluated as follows: Four density values, 0.4, 1.0, 2.0, and 2.7 (column 2, Table I) were chosen and the corresponding sensitometer exposure values were determined from the characteristic curve corresponding to no infra-red exposure and no latensification treatment. The densities corresponding to these particular exposures were then determined from the characteristic curves for the various times of infra-red exposure. These densities are termed the control densities (column 3) and represent the Herschel effect without latensification. From the series of characteristic curves obtained in the experiments with low intensity light latensification, the same four initial densities (0.4, 1.0, 2.0, and 2.7) were chosen and the exposures required to obtain them in the absence of infra-red exposure were determined. These exposures will, in general, be less than the ones required in the absence of latensification, but the *same number of developed grains* will be involved in the two sets of experiments, and hence common reference points will be established in determining the relative effect of the infra-red exposure in the two sets of experiments. The corresponding densities obtained for various times of infra-red exposure and subsequent low intensity latensifications were then determined (column 4, Table I). We are now in a position to calculate the extent to which the latensification treatment has restored developability to grains which had been made undevelopable by the infra-red exposure. As an example, consider the data for 30-minute infra-red exposure and an initial density of 2.0. The control density is 1.59; the density after latensification is 1.61. Assuming that density is proportional to the number of developed grains, the percentage of grains "restored" to developability by the latensification treatment is $100(1.61-1.59)/(2.00-1.59)=5$. (This calculation is intended only to be illustrative of the method used. Actually, a restoration of 5 percent is too small to be con-

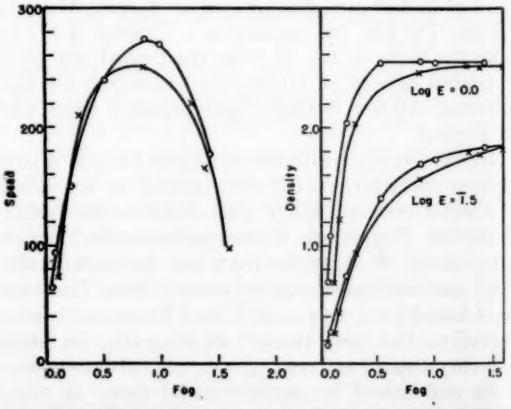

FIG. 2. Speed and density *vs.* fog plots for direct development of untreated film; ○ = values are for white-light exposure alone; × = values are for white-light exposure, followed by 30-min. infra-red exposure.

TABLE II. Restoration by gold, perborate, and bisulfite treatment of latent image partially destroyed by infra-red exposure.

Infra-red exposure (minutes)	Initial density	Density after infra-red exposure and subsequent treatment by: Gold control KBr–KCNS	Gold	Perborate control (KBr)	Perborate	Bisulfite control (H_2O)	Bisulfite	Restoration (percent) by: Gold	Perborate	Bisulfite
10	Fog	0.06	0.07	0.04	0.05	0.02	0.13			
	0.4	0.37	0.35	0.30	0.37	0.33	0.38	(−67)	70	70
	1.0	0.87	0.88	0.77	0.95	0.83	0.91	8	78	47
	2.0	1.77	1.81	1.67	1.88	1.75	1.82	17	63	28
	2.7	2.36	2.40	2.29	2.51	2.38	2.48	12	53	31
30	Fog	0.07	0.11	0.05	0.07	0.03	0.14			
	0.4	0.31	0.34	0.27	0.35	0.30	0.38	33	61	80
	1.0	0.68	0.79	0.65	0.86	0.71	0.87	34	60	55
	2.0	1.57	1.60	1.55	1.75	1.57	1.81	7	44	56
	2.7	2.19	2.22	2.16	2.35	2.21	2.33	5	35	24
90	Fog	0.10	0.13	0.07	0.09	0.05	0.16			
	0.4	0.35	0.33	0.28	0.31	0.27	0.39	−40	25	92
	1.0	0.60	0.67	0.54	0.67	0.55	0.81	17	28	58
	2.0	1.34	1.32	1.26	1.47	1.31	1.57	− 3	28	38
	2.7	1.95	1.83	1.94	2.16	1.95	2.15	−16	29	27

sidered of significance, since the density difference of 0.02 is within the limits of experimental error.)

Data for the mercury-latensification experiments are given in column 5 of Table I. The control densities are identical with those for the low intensity light experiments and are not repeated in the table. The calculated restorations produced by low intensity light and by mercury are given in columns 6 and 7. Restoration by the low intensity light is zero within the limits of experimental error, but a genuine positive effect appears in the data for mercury.

Table II gives data obtained in the experiments with gold, bisulfite, and perborate latensification, together with data for the corresponding control treatments (in KBr–KCNS solution, KBr solution, and water, respectively). Percentage restoration is calculated on the basis of the corresponding control. However, the densities for the various control treatments are all equal, within the limits of experimental error, to the corresponding densities for the dry control given in Table I.

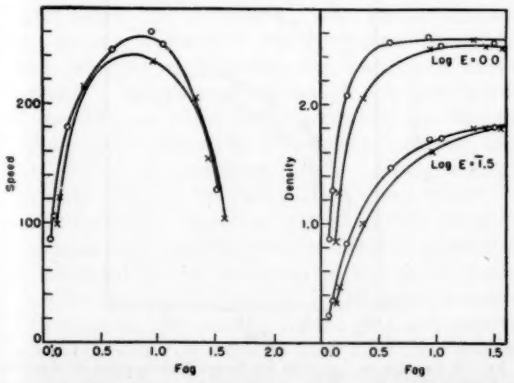

FIG. 3. Speed and density *vs.* fog plots for direct development of mercury-latensified film; ○ = values are for white-light exposure and subsequent mercury treatment; × = values are for white-light exposure, 30-min. infra-red exposure, and mercury treatment.

The data in Tables I and II show that for development of 4 minutes in D-16 the degrees of restoration for low intensity light and gold are practically zero, while for mercury, restoration averages 35 percent, for bisulfite 51 percent, and for perborate 48 percent. A study was then made to determine to what extent this restoration persisted upon complete development in an active developer. Development was carried out over a time range of 2 to 32 minutes in D-19 containing 0.5 g of α-picolinium-β-phenylethyl bromide per liter. Some of the data are presented graphically in Figs. 2 to 4. Figure 2 shows (left) emulsion speed *versus* fog for an infra-red exposure of 30 minutes and for the controls with no infra-red exposure; and (right) density *versus* fog for the two exposure levels of $\log E = 0$ and $\bar{1}.5$, all with no latensification treatment. Similar plots are given in Fig. 3 for the mercury-latensification experiments.

In Table III are listed the maximum densities, corresponding to complete development, obtained for two values of white-light exposure and for 10 and 30 minutes' infra-red exposure. For a given exposure treatment, the densities obtained with the various latensification procedures are essentially equal to that obtained with no latensification, with the single exception of the bisulfite latensification. This high bisulfite value may be a result, at least in part, of solvent action.

It had been observed that holding exposed film which had been treated with bisulfite affects the results. A short development-time series was carried out in which a $3\frac{3}{4}$-hour holding period at 20°C and 50 percent relative humidity was introduced after the customary rapid drying period following the bisulfite treatment. The curves in Fig. 4 present the data. For equal fog values for the controls, there still exists a Herschel effect[5] (compare curves 1 and 2). Further, the latensifying action of the bisulfite had eliminated the Herschel effect; curve 4 appears to be an extension of curve 3.

TABLE III. Maximum densities obtained on prolonged development of film subjected to latensification treatment.

Latensifying agent	Highest density attained when $\log E = 0$: Control	Infra-red exposure (10 minutes)	Control	Infra-red exposure (30 minutes)
None	2.49	2.49	2.54	2.49
Bisulfite	2.57	2.57	2.69	2.69
Perborate	2.54	2.54	2.57	2.51
Control for mercury	2.44	2.44	2.55	2.51
Mercury	2.44	2.45	2.54	2.50
Highest density attained when $\log E = \bar{1}.5$				
None	1.76	1.75	1.81	1.80
Bisulfite	1.79	1.82	1.82	1.87
Perborate	1.74	1.75	1.75	1.76
Control for mercury	1.70	1.70	1.82	1.81
Mercury	1.69	1.76	1.81	1.80

TABLE IV. Stabilization of the latent image toward infra-red exposure.

Infra-red exposure (minutes)	Initial density	Density after infra-red exposure with pretreatment by: None (control)	Low intensity light	Mercury	Water	Stabilization (percent) by: Low intensity light	Mercury	Water
10	Fog	0.02	0.08	0.09	0.02			
	0.4	0.33	0.38	0.46	0.37	71	185	57
	1.0	0.83	0.88	1.02	0.90	30	112	41
	2.0	1.75	1.77	1.96	1.88	8	84	52
	2.7	2.40	2.41	2.60	2.51	3	67	37
30	Fog	0.03	0.09	0.15	0.04			
	0.4	0.28	0.38	0.51	0.39	83	191	92
	1.0	0.73	0.82	1.04	0.87	33	115	52
	2.0	1.59	1.65	1.96	1.71	15	90	29
	2.7	2.24	2.29	2.60	2.32	11	78	17
90	Fog	0.05	0.12	0.28	0.10			
	0.4	0.27	0.35	0.65	0.46	61	290	146
	1.0	0.56	0.70	1.09	0.85	32	120	66
	2.0	1.31	1.44	1.95	1.67	19	93	52
	2.7	1.97	2.04	2.52	2.24	10	75	37

The difference observed between bisulfite-treated film developed at once (after the customary rapid drying period) and treated film kept for $3\frac{3}{4}$ hours might be explained on the basis of a time factor required for (a) a solvent action, possibly involving a reorientation of silver sulfite complex over the surface of the grains, or (b) reduction of Ag^+ ion to Ag atoms through the action of the bisulfite. The fact that there is no effect of the bisulfite treatment on the Herschel effect with physical development (see subsequent section) favors the solvent hypothesis over the reduction hypothesis. The solvent-action hypothesis could be based upon the fact that the infra-red exposure causes a redistribution of the latent-image silver toward the interior, with the assumption that the solvent action of the bisulfite would make the newly formed internal specks again accessible to the developer.

Again referring to Table III, it is seen that a common density has been attained by prolonged development by the various treatments, including the initial controls and infra-red controls. In the previous paper by Vanselow and James,[5] it was stated that the Herschel effect was not eliminated by prolonged development. This was verified in the present investigation for the 90-minute infra-red exposure, although for the 30-minute infra-red exposure (see Table III), the D_{max} loss was only about 0.05 and for the 10-minute infra-red exposure, no loss was observed.

Stabilization

In a second series of experiments, the effect of latensification treatment applied before the infra-red exposure was examined. The experimental procedure was the same as before except that the order of the latensification treatment and the infra-red exposure was reversed, i.e., the film which had been exposed in the sensitometer was latensified, then exposed to the infra-red radiation, and developed. The data were treated in the same manner as before, and the degree of *stabilization* toward infra-red radiation produced by the latensification was calculated. Data for the various latensification treatments are given in Tables IV and V.

All of the latensification treatments, with the exception of the perborate, result in an apparent stabilization of the latent image toward the destructive action of the infra-red exposure. The result obtained with low intensity latensification is a simple partial stabilization of the latent image. The situation is more complex with mercury and gold latensification. Here, the "fog" data show that the latensification treatment has produced an appreciable sensitization of the film to infra-red. This sensitization acts to oppose the normal destructive effect of the infra-red exposure, and the "stabilization" calculated by the procedure adopted in this paper will actually include both genuine stabilization, if any, and sensitization. If sensitization were independent of the

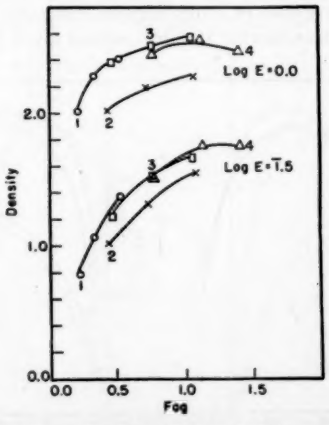

FIG. 4. Density *vs.* fog plots for direct development of bisulfite-latensified film after $3\frac{3}{4}$-hour storage; ○ = white-light exposure, storage; × = white-light exposure, 90-min. infra-red exposure, storage; □ = white-light exposure, bisulfite treatment, storage △ = white-light exposure, 90-min. infra-red exposure, bisulfite treatment, storage.

TABLE V. Stabilization of the latent image toward infra-red exposure.

Infra-red exposure (minutes)	Initial density	Density after infra-red exposure with pretreatment by: Gold control KBr–KCNS	Gold	Perborate control (KBr)	Perborate	Bisulfite control (H_2O)	Bisulfite	Stabilization (percent) by: Gold	Perborate	Bisulfite
10	Fog	0.04	0.10	0.04	0.03	0.02	0.15			
	0.4	0.34	0.48	0.33	0.29	0.37	0.39	230	− 57	67
	1.0	0.84	1.07	0.82	0.77	0.90	0.97	144	− 28	70
	2.0	1.74	2.02	1.70	1.80	1.88	1.93	107	33	42
	2.7	2.46	2.71	2.32	2.50	2.51	2.59	103	47	42
30	Fog	0.06	0.19	0.05	0.04	0.04	0.16			
	0.4	0.31	0.62	0.32	0.19	0.39	0.39	340	− 160	0
	1.0	0.70	1.22	0.69	0.51	0.87	0.91	173	− 58	31
	2.0	1.62	2.14	1.52	1.46	1.71	1.77	137	− 12	21
	2.7	2.25	2.78	2.12	2.25	2.32	2.42	117	22	26
90	Fog	0.11	0.48	0.11	0.05	0.10	0.20			
	0.4	0.36	1.00	0.39	0.11	0.46	0.43	(1000)	(−1000)	—
	1.0	0.64	1.51	0.69	0.26	0.85	0.84	240	− 140	−7
	2.0	1.39	2.31	1.33	0.92	1.67	1.71	150	− 61	12
	2.7	2.03	2.93	1.90	1.78	2.24	2.37	134	− 15	28

presence or absence of a latent image, a fog-correction could be made on the density data to isolate the pure Herschel effect, and , hence, a true value for stabilization could be calculated. However, such independence does not exist for the gold-latensified film, since the "corrected" image densities increase with increasing infra-red exposure, even when correction is made by straight subtraction of fog from image density. It may be doubtful if the independence exists for mercury. Hence, correction has not been attempted, and the apparent stabilization values (all over 100 percent) only are recorded.

The gold, bisulfite, and perborate treatments involve a complication not present in the mercury and low intensity light treatments, namely, the bathing of the film in an aqueous solution which alters the amount of soluble salts present in the emulsion. (This complication existed, of course, in the previous experiments on restoration, but the change of salt content of the film in these experiments was of little or no consequence to the results obtained.) Simple bathing of the film in water before the infra-red exposure greatly decreased the amount of Herschel effect produced by a given infra-red exposure. This decrease is largely or entirely a result of the decrease in bromide ion concentration in the film, an effect noted previously by Narbutt.[8] Stabilization produced by the bisulfite treatment, therefore, should be considered strictly as only that produced in excess of the stabilization which results from an equivalent treatment in water alone. The percentage stabilization by bisulfite given in Table V, accordingly, is calculated on the water-treated film as the control. Data for film treated in a KBr–KCNS solution and in a KBr solution (the controls for the gold and perborate latensifications, respectively) show that these solutions have relatively little influence upon the Herschel effect.

The perborate latensification results in an increase in the Herschel effect, i.e., the perborate treatment has decreased the stability of the latent image toward the action of infra-red radiation. This sensitization of the Herschel effect is dependent upon the presence of perborate in the film during the infra-red exposure. When the perborate-latensified film was batch-washed (so that the bromide content of the film remained essentially constant) in $10^{-4}M$ KBr solution and dried prior to the infra-red exposure, the Herschel effect was considerably decreased. No significant difference was obtained between film washed for 20 minutes and that for 1 hour. Results with the washed film indicate that the perborate latensification produced some stabilization of the latent image in the higher white-light exposure areas but that some loss in stability persisted in the low exposure areas. Spectral-absorption data for an aqueous solution of sodium perborate show that absorption occurs between 700 and 1000 mμ,* and data for solid sodium perborate in Nujol show a major band at about 2900 mμ.†

A series of experiments was carried out on the influence of keeping the mercury-latensified strips for various times before applying the infra-red exposure. Results are shown in Fig. 5. Data for control tests on untreated film are plotted in Fig. 5A. Two exposures were chosen which gave densities of 1.00 and 2.00 for the freshly exposed film. Curves B and C represent the densities obtained for these exposures as a function of the duration of keeping the exposed strips before development. Curves B′ and C′ represent the densities for the same white-light exposures kept for the specified times, then exposed 75 minutes to infra-red light before development. Curves A and A′ give the corresponding fog values. It will be seen that the latent image becomes much less susceptible to the Herschel effect the older it is. At the same time, the sensitivity of the film to infra-red radiation has increased considerably. As a result of this increased sensitivity, the characteristic curve for

[8] J. Narbutt, Zeits. f. wiss. Phot. 28, 191 (1930).

* Measured by Dr. R. H. Lambert, of these Laboratories.
† Measured by Dr. A. L. Geddes, of these Laboratories.

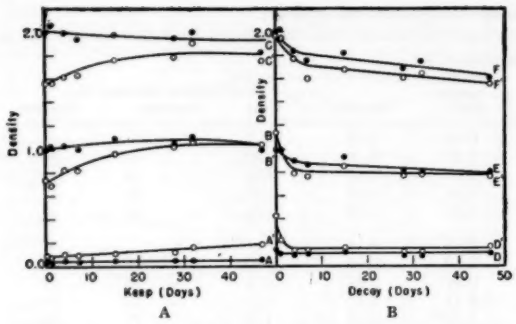

FIG. 5. Density *vs.* time of storage of control and mercury-latensified film; (A, B, C)—(●) untreated, white-light-exposed film; (A′, B′, C′)—(○) white-light-exposed film, stored for time indicated and then exposed 75 minutes to infra-red; (D, E, F)—(●) white-light exposure with mercury latensification; (D′, E′, F′)—(○) white-light exposure, mercury latensification, storage for specified time, then exposed 75 minutes to infra-red radiation.

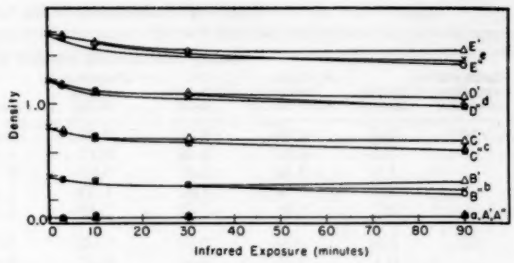

FIG. 6. Density *vs.* infra-red exposure for physical development of untreated and of KCNS–KBr-treated film; curves a, b, c, d, e (×) represent white-light exposure, followed by infra-red exposure of untreated film; curves A′, B′, C′, D′, E′ (△) represent white-light exposure, KCNS–KBr treatment, infra-red exposure; curves A″, B″, C″, D″, E″ (○) represent white-light exposure, infra-red exposure, KCNS–KBr treatment.

the 48-day-old strip without infra-red exposure and that for the strip with infra-red exposure actually cross at a density of about 1.0.

The corresponding curves for the mercury-latensified film are given in Fig. 5B. Curves E and F show that a rapid drop in the density of the mercury-latensified film occurs within the first four days of keeping. The decrease with longer keeping is small. Fog, however, remains essentially constant (curve D). The infra-red sensitivity drops to a minimum within four days (curve D′) and remains essentially constant for longer keeping. Curve E′ shows that a Herschel effect is obtained with mercury-latensified film which has been kept four days before the infra-red exposure, and that for longer times of keeping the density of the infra-red-exposed film is independent of the time of keeping. At the 4-day keeping time, the Herschel effect obtained with the mercury-latensified film is considerably less than that obtained with the corresponding untreated film, again indicating that the mercury treatment has acted to stabilize the latent image toward the Herschel effect. At the long times of keeping, the latent image of the nonlatensified film is stabilized to an extent comparable to that of the latensified film.

The increase in infra-red-sensitivity of the untreated film with time of keeping is unexpectedly large and has not been accounted for.

(B) Physical Development

The experiments on restoration and stabilization were repeated using physical in place of direct development. The strips were developed after fixation in the *p*-phenylenediamine physical developer for 2 hours. In general, the other experimental procedures, except for fixation and development, were like those described in Part A. The data were analyzed in much the same manner as for direct development, except that plots were made of the densities obtained when various infra-red exposures were superimposed upon initial sensitometer exposures which gave densities of 0.4, 0.8, 1.2, and 1.6 without the infra-red treatment. From these data, relative to the various controls, are derived the degree of stabilization when latensification preceded infra-red exposure and the degree of restoration when latensification followed infra-red exposure.

Although the same agents were investigated with physical development as with direct development, only the gold data will be presented in detail. The data for the KCNS–KBr treatment (control for the gold latensification) are given graphically in Fig. 6, where the curves marked a···e (cross data points) are for untreated film, the curves marked A′···E′ (triangle data points) are for treatment prior to infra-red exposure, and the curves marked A″···E″ (circle data points) are for treatment following infra-red exposure. Curves a, A′ and A″ coincide, showing that the fog was independent of the treatment. Moreover, no significant fog increase occurs with increasing infra-red exposure. Curves B″···E″ practically coincide with curves b···e, showing that KCNS–KBr treatment following infra-red exposure causes no significant change in the Herschel effect. However, comparison of curves B′···E′ with curves b···e shows that the Herschel effect is decreased considerably by the KCNS–KBr treatment prior to the infra-red exposure.

Gold treatment (preceding fixation) of the film used in this investigation produced but little latensification for postfixation physical development. When the treatment followed the infra-red exposure, it produced no significant restoration of the latent image, as shown by the data in Table VI. When the gold treatment preceded the infra-red exposure, however, it resulted in an even more marked sensitization to infra-red than previously noted for direct development. Some of the data are included in Table VI. The induced infra-red sensitivity is much greater in the image areas than in the portions of the film which had received no initial white-light exposure. This is shown in Fig. 7, which gives the characteristic curves for the gold-treated film

with no infra-red exposure (curve 1) and with infra-red exposures of 3, 10, 30, and 90 minutes (curves 2 to 5, respectively), following the gold treatment. For example, with 30 minutes' infra-red exposure, the fog density increased by only 0.03, whereas the density for log $E=0.47$ increased from 0.40 to 0.87. This effect could not be duplicated by exposure of the treated film to low intensity white light instead of the infra-red.

The degree of restoration and stabilization obtained by the various latensification procedures and physical development, together with sensitometric data on the effect of the various latensifying agents in the absence of infra-red exposure, are summarized in Table VII.

CONCLUSIONS

The results of the present investigation on the interaction of latensification and infra-red exposure are summarized in Table VIII. The percentages of stabilization and restoration given in the table represent the averages of the percentages calculated for 10, 30, and 90 minutes' infra-red exposure and initial densities of 0.4, 1.0, 2.0, and 2.7 for direct development, and of 0.4, 0.8, 1.2, and 1.6 for physical development.

The low intensity light exposure produced a fair amount of stabilization. This is in accord with current latent-image theory[9] that the low intensity-exposure latensification is a result of an increase in the size of specks which would not otherwise serve as development centers under the conditions employed. This building up of pre-existing small specks is a much more efficient process than the formation of new centers, and many of the pre-existing specks may be built up to appreciably greater size than that corresponding to the critical size for a development center. With the infra-red exposures employed, it is probable that most of the latent-image specks have not absorbed more than one quantum apiece,[4] and, hence, have not been decreased in size by more than one silver atom or one F-center. Accordingly, we may assume that, as a result of the auxiliary exposure, more nuclei which were at the critical threshold have been built up to beyond this size than subnuclei have been built up to just the critical size.

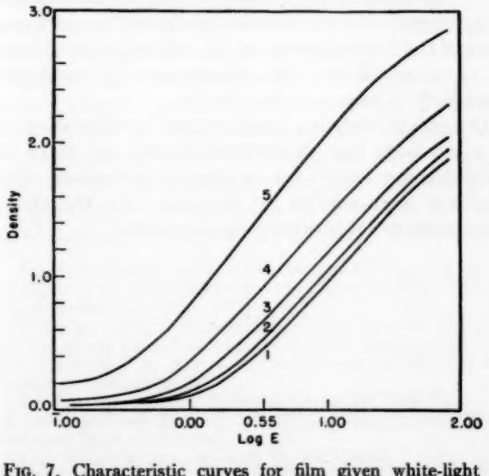

FIG. 7. Characteristic curves for film given white-light exposure, gold treatment, infra-red exposure, and postfixation physical development; curves 1, 2, 3, 4, 5 represent, respectively, 0, 3, 10, 30, and 90 minutes' infra-red exposure.

[9] C. E. K. Mees, *Theory of the Photographic Process* (The Macmillan Company, New York, 1942), pp. 248–249.

TABLE VI. Stabilization and restoration data for gold treatment and physical development.

Infra-red exposure (minutes)	Latensification before infra-red exposure: Initial density	Control density (KBr–KCNS)	Density	Stabilization (%)	Latensification after infra-red exposure: Control density (KBr–KCNS)	Density	Restoration (%)
10	0.40	0.33	0.61	400	0.33	0.35	29
	0.80	0.72	1.00	350	0.72	0.74	25
	1.20	1.11	1.39	310	1.11	1.09	−22
	1.60	1.53	1.77	340	1.52	1.47	−63
30	0.40	0.33	0.87	770	0.31	0.30	−11
	0.80	0.70	1.27	570	0.69	0.67	−18
	1.20	1.08	1.64	470	1.08	1.04	−33
	1.60	1.45	1.97	350	1.43	1.39	−24
90	0.40	0.33	1.34	1450	0.24	0.29	31
	0.80	0.68	1.82	950	0.59	0.58	− 5
	1.20	1.05	2.25	800	0.98	0.95	−14
	1.60	1.44	2.58	710	1.33	1.29	−15

Mercury and gold produce extensive apparent stabilization. Gold, which produces complete stabilization, replaces silver in the latent image, or gold is formed by reduction of aurous ions by electrons from the F-centers, and we might assume that the gold image is not susceptible to the Herschel effect. On the other hand, prolonged treatment with gold is known to increase markedly the size of the latent-image nuclei as a consequence of physical development, and the brief treatment may result in an increase in size amounting to a few atoms per nucleus. A mere increase in size of this order should be sufficient to stabilize the nucleus toward the infra-red exposure.

Mercury may increase the size of the latent-image specks by amalgamation. Another mechanism which has been suggested is that the mercury reduces silver ions to silver atoms,[10] which then augment the size of the latent-image centers and subcenters. If this mechanism applies, however, we must assume that very few of the subcenters have been increased to just the critical size by the mercury treatment, whereas the great majority of the specks of just critical size have been increased to beyond the critical size by the mercury treatment. On the other hand, we would not expect a latent-image speck composed of mercury and silver to react toward the infra-red exposure in the same way as a simple silver speck.

The apparent stabilization by gold and mercury may be at least partly due to infra-red sensitivity induced by the mercury and gold treatments. The sensitizing

[10] V. I. Shiberstov, J. Tech. Physics (USSR) **16**, 395 (1946).

TABLE VII. Stabilization and restoration obtained for physical development with various latensifying treatments.

Agent	Effect of latensification before infra-red exposure (stabilization) (percent)	Effect of latensification after infra-red exposure (restoration) (percent)	No infra-red exposure % speed compared with dry control	% gamma compared with dry control	Fog
Gold	100 (625)*	−10	118	110	0.04
Mercury	100 (125)*	3	265	86	0.07
Low intensity light	20	20	150	91	0.05
Perborate	−37	3	266	78	0.04
Bisulfite	†	−10			
Water	100 (108)	16	~120	100	0.04

* Values denote stabilization (if any) plus red sensitization.
† Control shows insufficient Herschel effect for calculation of stabilization.

TABLE VIII. Summary of stabilization and restoration data for direct and physical development.

Agent	Effect of latensification before infra-red exposure (stabilization) (percent) Direct	Physical	Effect of latensification after infra-red exposure (restoration) (percent) Direct		Physical
	(4 min. in D-16)		(4 min. in D-16)	(Complete)	
Low intensity light	31	20	−2		20
Mercury	100	100	35	(0)	3
Gold	100	100	<10		−10
Water	55	100	−1		16
Bisulfite	31		51	100	−10
Perborate	Increase	−37	48	(0)	3

by gold as revealed by physical development is especially large, and it would seem that the infra-red exposure causes a very large number of subimage specks to be increased to, or past, the developability threshold. This is surprising, considering the low degree of latensification for physical development produced by the gold treatment alone.

Water, which causes only slight latensification, produced a stabilization of the latent image toward the Herschel effect. This stabilization, however, is due, at least in part, to the well-known effect of silver ion concentration. With increasing silver ion concentration, the probability that an excess silver ion will be near to, or adsorbed by, a silver nucleus at the time the latter absorbs an infra-red quantum increases. Likewise, the probability that the center will capture another electron before it loses the excess silver ion created by ejection of an electron will increase. The water treatment also increases the infra-red sensitivity and this accounts in part for the stabilizing action. This spectral sensitization does not appear when the water contains 0.01*M* KBr.

Bisulfite stabilizes the latent image in excess of that caused by water alone. This stabilization is about the same in percentage as that caused by low intensity light exposure.

Perborate increases the Herschel effect. We cannot state with certainty from the present data whether or not this sensitized Herschel effect results from absorption of infra-red radiation by the perborate. The absorption spectrum of the perborate shows some absorption between 700 and 1000 mμ, but a major band does not appear until about 2900 mμ.

Of the various latensifying agents, only the low intensity light produced restoration for physical development, and that was slight. With incomplete direct development, restoration was obtained with mercury, bisulfite, and perborate. However, the restoration by mercury and perborate disappeared when direct development was pushed to completion in an active solution. This was to be expected from the previous results, which showed that no latensification is obtained when development is complete. The results obtained with the bisulfite, however, cannot be explained on this basis. No restoration was obtained for physical development, indicating that the bisulfite treatment has not increased the number of developable centers for physical development. However, the bisulfite-treated film which had been held four hours after treatment showed complete restoration for prolonged direct development. This suggests that the bisulfite treatment has uncovered some of the internal image which may have been formed by an action of the infra-red exposure in transferring some surface images to the interior.

In general, omitting bisulfite from consideration, we may conclude that latensification will not make developable any significant number of subcenters which originally were smaller by one unit than the critical size necessary for initiating development.

A Ratio-Recording Double-Beam Infra-Red Spectrophotometer with Automatic Slit-Control*†

D. F. Hornig, G. E. Hyde,‡ and W. A. Adcock§
Metcalf Research Laboratory, Brown University, Providence, Rhode Island

(Received April 14, 1950)

A simple scheme by which any spectrometer is readily converted to a direct ratio-recording spectrophotometer is described. The optics consist of a double-beam "slit illuminator" which passes light from a common source area alternately over two identical paths to the spectrometer entrance slit. The optical arrangement allows great flexibility in the use of samples since it includes foci for small samples and sufficient space for low temperature cells, gas cells, etc. Common paths make the use of filters, polarizers, etc., convenient and accurate. Spectrometer optics, detector and amplifier are common to both signals and hence non-critical. The electrical signals from the two beams are amplified, "sorted" and rectified by synchronous switches, compared potentiometrically and their ratio recorded. Details of the amplifier and ratio circuits are included. A simple method is described by which errors in the ratio caused by the frequency characteristics of the detector, input transformer, or amplifier are eliminated. The energy in the comparison beam is kept constant at any predetermined level while a spectrum is scanned by means of a simple servo slit-width control. This arrangement is much more convenient and flexible than cams, particularly when interchangeable prisms are used.

INTRODUCTION

ANY method of measuring the spectral transmission of a substance involves the comparison of the light transmitted by the substance at a given frequency with some standard. The most convenient method of making such a measurement continuously is probably the double-beam instrument, in which one beam is passed through the sample and the other is used as a reference,[1] although it is possible to design "memory" devices which will compare the light transmitted by the sample with a blank run previously.[2] The most straightforward double-beam instrument might consist of two completely separate spectrometers, although the necessity of matching all of the optical, detecting and recording components would make such a device impracticable. Any scheme which is to be simple and accurate must involve the matching of as small a number of critical components as possible. Conversely, the two beams must have, if possible, all critical elements, such as spectrometer optics, detector and amplifier, in common. Several spectrometers embodying these principles have been described[3–5] but in each case the two beams are not quite equivalent in that they "see" different areas of the source and that one of the beams is modified by a "comb" which is used in balancing the two beams. Recently an ingenious instrument has been described[6] in which the two beams are very nearly equivalent but in which one beam uses the top half of the spectrometer slits and the other the bottom. It would seem very difficult to match the top and bottom of such critical components as the slits, particularly when they are very narrow (e.g., 0.01 mm is a normal operating slit-width near 3000 cm^{-1}) or when their width is varied.

The instrument described here may properly be called a "slit illuminator" in that, since the entire spectrometer is used in conjunction with both beams, it can be used as a simple attachment to any infra-red spectrometer. It involves two beams which originate on the same area of source, pass through essentially identical optical paths and alternately illuminate the slit of the spectrometer. The output of the single detector is amplified by a single amplifier and only then are the signals "sorted" by synchronous switches and compared potentiometrically. A unique circuit arrangement makes the accurate measurement of transmission quite independent of the detector characteristics or of distortion by the amplifier, provided that the system is linear. Finally, a simple servo slit-control keeps energy in the comparison beam constant, once it has been set at any predetermined level.

THE DOUBLE-BEAM OPTICAL SYSTEM

A schematic diagram of the optical arrangement is given in Fig. 1. The radiation beam from the Globar source, G, is interrupted at a frequency of about six cycles per second by the rotating shutter, S. The pulses of radiation all pass to the spherical mirror M1 (5 cm diameter, 19.6 cm radius of curvature), and are then sent alternately along two optically identical paths to the entrance slit of the spectrometer. This is accomplished by two rotating plane mirrors, M5 and M6,

* Based on a thesis submited by George E. Hyde in partial fulfillment of the requirements for the degree of Doctor of Philosophy, Brown University, 1950.

† While not directly supported by ONR, the work described here was closely connected with the program supported by Contract N6ori-88, T. O. 1 and we are indebted to ONR for considerable indirect assistance.

‡ Du Pont Postgraduate Fellow in Chemistry, 1948–50.

§ Present address: Research Laboratory, Stanolind Oil and Gas Company, Tulsa, Oklahoma.

[1] V. Z. Williams, Rev. Sci. Inst. **19**, 155 (1948).

[2] W. M. Avery, J. Opt. Soc. Am. **31**, 633 (1941).

[3] N. Wright and L. W. Herscher, J. Opt. Soc. Am. **37**, 211 (1947).

[4] Baird, O'Bryan, Ogden, and Lee, J. Opt. Soc. Am. **37**, 754 (1947).

[5] J. U. White and M. D. Liston, J. Opt. Soc. Am. **40**, 29; 36; 93 (1950).

[6] A. Savitzky and R. S. Halford, Rev. Sci. Inst. **21**, 203 (1950).

geared to the shutter in such a way that when the pulse from M1 passes between the two sectors of M5 it goes through a focal point, on to a second spherical mirror, M2 (which is identical with M1), through another focus to M6 which reflects it to the spherical mirror M4 (again identical with M1), and is finally focused on the entrance slit. Alternately, if the pulse is reflected from M5 it passes to the spherical mirror M3, which sends it between the sectors of M6 to M4 which again focuses it on the entrance slit. The two alternate paths are indicated in the diagram by the broken and dashed lines, respectively. The solid lines indicate the common parts of the two optical paths. If a sample absorbing 50 percent of the radiation were placed in one of the two beams, the radiation intensity as a function of time would appear as in Fig. 2.

This arrangement uses five reflecting surfaces and three moving parts but it has a number of advantages, and in two years of continuous use it has produced no difficulties. This is primarily due to the fact that all of these optical parts are completely non-critical, their only function being to focus an image of the Globar (which is $\frac{1}{4}$ inch in diameter) on the entrance slit of the spectrometer, in our case a Perkin-Elmer Model 12B. For this reason inexpensive spherical optics have proved quite satisfactory and after the initial installation it has never been necessary to realign any of the mirrors.

This arrangement guarantees an equal source intensity for both paths since the same emitting area is used for both. The complete equivalence of paths makes

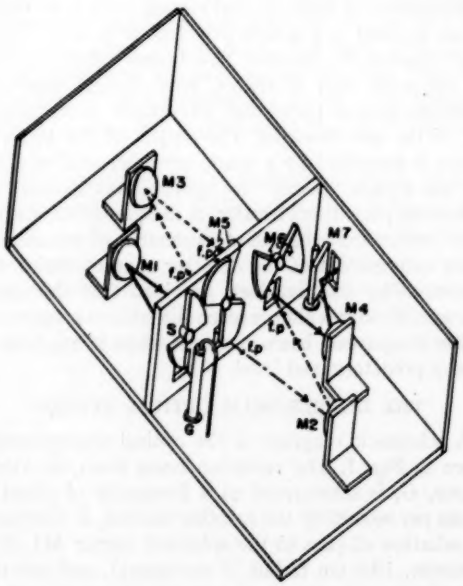

FIG. 1. Schematic diagram of double beam arrangement. Optical parts are: globar source, G; rotating shutter, S; spherical mirrors, M1, M2, M3, M4; rotating sector mirrors, M5, M6; plane mirror, M7. Dashed lines indicate comparison paths, solid lines the common paths and f.p. the focal points.

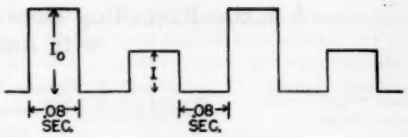

FIG. 2. Light intensity vs. time at entrance slit of spectrometer when $I=I_0/2$.

it possible to eliminate atmospheric absorption from the spectra. The shutter S, which is ordinarily opaque, provides true reference zeros and thus serves in principle to distinguish radiation from the Globar from any other radiation, such as that which might be introduced by a hot sample cell. In the arrangements of Wright and Herscher[3] or of Baird *et al.*,[4] for example, radiation from a hot sample cell acts as an apparent negative absorption by the sample. In this instrument, because of the "signal mixing" to be discussed later, there is still a small residual hot cell effect. If a shutter is used which is opaque in the wave-length region being studied but transparent at shorter wave-lengths, the effects of stray short wave-length radiation can be largely eliminated since they do not contribute to the alternating component of the light intensity. As an example, a silver chloride shutter may be used in the *KRS*-5 region. The introduction of zeros in the radiation intensity (and hence the shutter) is essential for potentiometric comparison of the beam intensities as well as for the absolute measurement of I_0 which is the basis for the automatic slit-control; it must be recognized, however, that it decreases the signal to noise ratio by a factor 2 at 100 percent transmission and $\sqrt{2}$ at 0 percent compared with instruments using "comb" balancing without zeros.

This particular optical arrangement allows great flexibility in the use of samples. The presence of foci in the paths makes it possible to use small samples of liquids or solids if they are placed at or near the focal points. On the other hand, it is possible to accommodate a 5-cm diameter, 10-cm long gas cell between M5 and either M2 or M3. In Fig. 3, a photograph of the apparatus with a cell for use at liquid air temperatures is shown. In Fig. 4, a 30-cm gas cell designed to operate at pressures up to 5 atmospheres is shown in position. In this case the mirror M2 is contained inside the cell. Both M2 and M3 are positioned by removable pins so that cells such as that shown in Fig. 4 may be readily inserted and removed. No difficulties have been encountered in the removal and subsequent insertion of these mirrors.

The presence of common paths makes it possible to insert filters, polarizers, etc., without affecting the balance between the two beams.

Despite the number of moving parts, this geometry is mechanically simple. A 1/12 h.p., 1725 r.p.m. motor drives a single shaft on which are mounted the worm gears which drive the shutter, the mirrors and the synchronous switches which subsequently sort the

signal. The particular mechanical arrangement shown in Fig. 1 is cumbersome in that the mechanical parts interfere to some extent with the placing of samples in the beams. It was used because it was desired to enclose the entire system in a single box, a "slit illuminator," which could be placed on the spectrometer base instead of the usual source without modifying the rest of the spectrometer at all. The mechanical parts could equally well be mounted *beneath* the spectrometer base in which case no mechanical parts would intrude in the optical area.

SPECTROMETER AND DETECTOR

In the instrument described here, the pulses of light from the double beam "slit illuminator" fall on the entrance slit of a Perkin-Elmer Model 12B spectrometer. However, any other infra-red spectrometer, including grating instruments, would do as well and if the Globar were replaced by a suitable source the same optics could also be used for visible or ultraviolet spectra. After passing through the dispersing system of the spectrometer, the radiation falls on a detector; the only requirement for optimum performance is that its time constant should not exceed approximately 30 percent of the duration of each light pulse, and at the present time a number of thermocouples and bolometers, as well as the Golay detector, which are sufficiently fast are available.[1] Thermocouples with a time constant of approximately 0.03 sec. were used in the present instrument; however, as will be described later, accurate percentage transmissions can be obtained even when the response time is several times as great as the pulse length.

PREAMPLIFIER

The problem of suitable low noise level amplifiers has been treated by several authors.[5,7,8] The critical part of any such amplifier is the initial stage, which in our case is housed in a preamplifier mounted immediately beneath the spectrometer. In this way the length of the thermocouple cable is kept to about six inches, reducing the difficulty from pick-up in the input circuit. The circuit of this preamplifier is given in Fig. 5. Because the inherent noise level of a vacuum tube amplifier is considerably greater than the inherent thermal noise in a low resistance thermocouple, an input transformer was used between the thermocouple and the first preamplifier grid. The transformer used[9] had a turns ratio of 447 and was designed to operate at 5 c.p.s. from a 5-ohm thermocouple. Its low frequency response was not as good as might be desired for the present purpose and the pulses decayed about 50 percent in 0.08 sec. The appearance of the optical signal of Fig. 2 after it had been converted to an electrical signal by the thermocouple and passed through the transformer is shown in Fig. 6.

The first amplifier stage is designed primarily to have a minimum noise and pick-up level. The filament is run at reduced current, the screen grid and the plate at low voltage. Grid bias is obtained by using essentially a "floating grid," the cathode being connected directly to B^-. The plate supply voltage for this stage is decoupled from the rest of the amplifier by the use of a voltage regulator tube and this simple arrangement has proved satisfactory.

In order to avoid possible ground loops all B^- returns from the thermocouple, the input transformer and the vacuum tube were made to a single point which was connected to a water pipe. The thermocouple was not connected to the spectrometer base and the shield of the thermocouple cable was grounded only at the preamplifier. All other circuits were connected to this same ground via the B^- leads to the power supply and

FIG. 3. Double-beam spectrophotometer with low temperature cell in place.

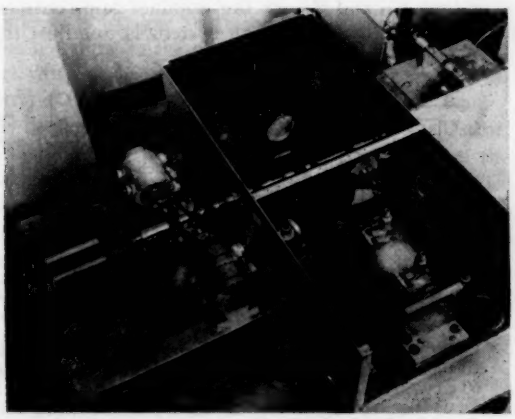

FIG. 4. Double-beam spectrophotometer showing 30-cm path, high pressure gas cell in position.

[7] L. C. Roess, Rev. Sci. Inst. **16**, 172 (1945).
[8] C. B. Aitken and W. C. Welz, Electronics **20**, 124 (1947).
[9] United Transformer Company, New York, New York, Type B-6630.

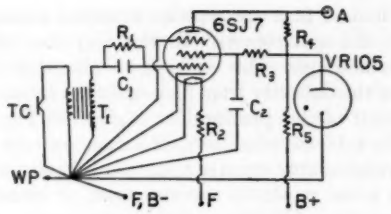

FIG. 5. Preamplifier. TC, thermocouple; T_1, *UTC*, *B*-6630; WP, ground connection to water pipe; B⁻, common element of all circuits via power supply; B⁺, 250 v.; F, F, 6 v. d.c.; A, output to amplifier; R_1, 45 megohms; R_3, 10 ohms, 2 watt; R_4, 0.8 megohm, wire wound; R_4, 0.18 megohm, wire wound; R_5, 10,000 ohms, 10 watt; C_1, 0.25 microfarad; C_2, 1.0 microfarad.

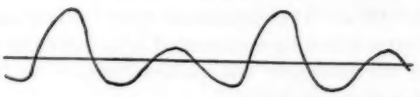

FIG. 6. Voltage at preamplifier grid when $I = I_0/2$.

isolated from their chassis which were grounded separately via the spectrometer table.

AMPLIFIER

The remainder of the amplifier is fairly conventional and straightforward and is shown in Fig. 7. It is laid out with inline sequence of stages to insure adequate separation of high and low level stages. The cathode resistors are not bypassed because of the excessively large condensers that would be required; moreover, the negative feedback thus obtained improves the linearity. The network R_9, R_{10} and C_6 in the first stage is a phase-shift network,[10] which approximately corrects the phase shift arising in the input transformer and coupling circuits at low frequencies. Condensers C_4, C_8, C_{14}, C_{17} and C_{19} serve to attenuate the high frequencies which are not needed and which might cause instability and oscillation. R_{14} and R_{18} are the amplifier gain controls; their function in the over-all system is to adjust the slit-width, as will be explained later. Between the first and second stages a *T* network[11] which is tuned to 60 cycles is incorporated to reduce the effects of pick-up at this frequency. Within limits 60-cycle/sec. pick-up does no harm; since it arises largely in the input transformer it may be further reduced by properly orienting or further shielding the transformer.

The filaments are all lighted from a storage battery. This reduces 60-cycle pick-up and insures a stable voltage. The power supply for the amplifier and preamplifier is mounted in a separate chassis. It employs degenerative voltage stabilization but at one time *VR* tubes were tried with apparently equally good results.

The output circuit consists of two balanced cathode followers which provide low impedance sources, G and H, of opposite polarity for the ratio circuit. The degree of balance of the cathode followers is non-critical.

RATIO CIRCUIT

The function of the ratio circuit is to convert the amplifier output to a measurement of the ratio of the light intensity in the two beams. The circuit employed to do so is given in Fig. 8. Each of the two amplifier outputs, G and H, is separated in time by switches S_1 and S_2, the signals being sent to switch S_3 when the sample is in the optical path and to switch S_4 when the standard is in the optical path. The voltages on the two contacts of S_3 (and also S_4) are then of opposite polarity. Rectification is accomplished by switches S_3 and S_4 which operate at 6 cycles per sec., twice the frequency of switches S_1 and S_2. It is important that all of the switches be so adjusted that the amplifier outputs, G and H, are never shorted to each other. (It is possible for this to happen when the switches are so constructed that each S.P.D.T. switch is in fact a pair of S.P.S.T. switches, as is the case with those used here.) The exact phasing of these switches is adjusted empirically for maximum d.c. output since it depends on the detailed wave shape. The switches[12] are war surplus

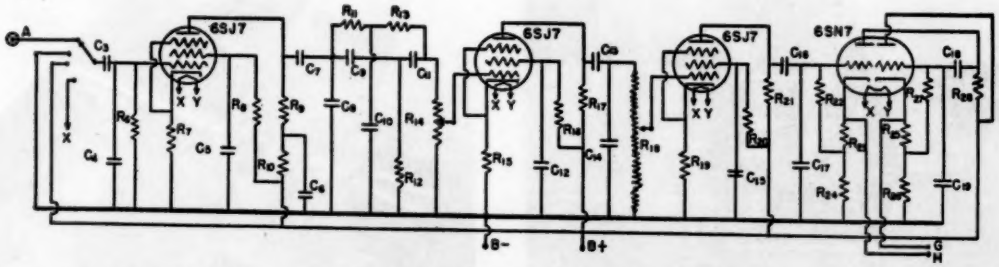

FIG. 7. Amplifier. A, input from preamplifier; B⁻, B⁺, 250 v.; G, H, output to ratio circuit; R_4, 5 megohms; R_7, R_{15}, R_{19}, 2000 ohms; R_8, R_{16}, R_{20}, R_{22}, R_{27}, 2 megohms; R_9, 50,000 ohms; R_{10}, R_{17}, R_{21}, 0.5 megohm; R_{11}, R_{13}, 0.5 megohm, tune to 60 c.p.s.; R_{12}, 2.5 megohms; R_{14}, continuous gain control, 5 megohm potentiometer; R_{18}, stepwise gain control, 5 megohm total; R_{23}, R_{25}, 5000 ohms; R_{24}, R_{26}, 15,000 ohms; R_{28}, 22,000 ohms; C_3, C_7, C_{13}, C_{16}, C_{18}, 0.5 microfarad; C_4, C_{14}, C_{17}, C_{19}, .004 microfarad; C_5, C_{12}, C_{15}, 8 microfarad; C_6, 1.0 microfarad; C_8, .04 microfarad; C_9, C_{11}, .005 microfarad; C_{10}, .01 microfarad.

[10] F. E. Terman, *Radio Engineers Handbook* (McGraw-Hill Book Company, Inc., New York, 1943), p. 414.
[11] W. N. Tuttle, Proc. I. R. E. 28, 23 (1940).
[12] Yagi antenna switching units from *SCR* 521 or similar airborne radar sets, labelled Signal Switch, Auto-lite part No. *SWB* 4002.

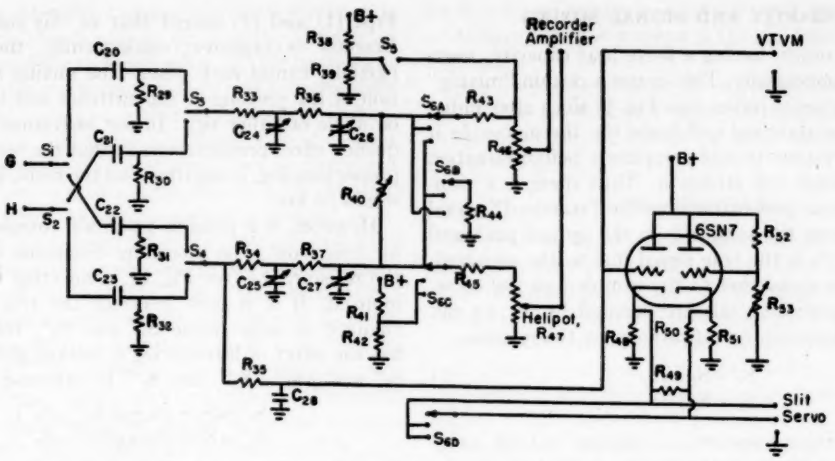

FIG. 8. Ratio and slit-control circuit. G, H, inputs from amplifier; VTVM, vacuum tube voltmeter; B^+, 250 v.; R_{29}, R_{30}, R_{31}, R_{32}, 0.18 megohm, one percent precision; R_{33}, R_{34}, R_{35}, R_{36}, R_{37}, 0.10 megohm, one percent precision; R_{38}, 5 megohms; R_{41}, one megohm; R_{39}, 47 ohms; R_{40}, one-megohm potentiometer; R_{42}, 1000 ohms; R_{43}, R_{45}, 30,000 ohms, one percent precision; R_{44}, 31,000 ohms; R_{46}, 1000-ohm potentiometer; R_{47}, 1000-ohm precision potentiometer (Helipot); R_{48}, R_{51}, 10,000 ohms; R_{49}, 23 ohms; R_{50}, 25,000 ohms; R_{52}, 0.5 megohm; R_{53}, 10,000-ohm potentiometer; C_{20}, C_{21}, C_{22}, C_{23}, 0.5 microfarad; C_{24}, C_{25}, 4, 12, 12, 50, 100 microfarads; C_{26}, C_{27}, 20, 50, 100, 100, 200 microfarads; C_{28}, 0.25 microfarad; S_1, S_2, S_3, S_4, synchronous switches; S_5, S.P.S.T. switch; S_{6A}, S_{6B}, S_{6C}, S_{6D}, ganged selector switch.

units similar to those previously used by Savitzky and Halford, and in a year of continuous operation at 180 and 360 r.p.m. they have been quite satisfactory.

The outputs from switches S_3 and S_4 are directly proportional, aside from signal "mixing" which will be discussed later, to the radiation intensity in the sample and standard beams. The pulsating d.c. from these switches is then smoothed by two-section RC filters. The two filters are carefully matched, precision resistors and wire-wound potentiometers (except R_{40}) being used. Due to the long time constants, it is necessary to use electrolytic condensers and there is some evidence that they occasionally produce small errors, but not greater than one percent.

These filters determine the speed of response of the instrument. A series of condensers (C_{24} to C_{28}) are available on a ganged selector switch so that the time for 90 percent response can be varied from 3 to 50 seconds. Increasing the time constant of the filter gives slower response but reduces the noise level.

The ratio of the smoothed voltages is obtained from a conventional potentiometer circuit. The voltage representing the standard beam is placed across R_{47}, a "Helipot" 1000-ohm ten-turn precision potentiometer,[12] which is coupled mechanically to the pen of the Brown Electronik recorder.¶

The voltage obtained from the movable contact thus represents some fraction of the standard voltage. This voltage and the corresponding voltage representing the sample beam (across R_{46}) are fed to the amplifier of the recorder, which adjusts the movable contact until they are equal. The pen then indicates the ratio. The resistor, R_{46}, serves to vary the divider from which the "sample" voltage is taken, thus varying the pen position when the two beams are balanced; it is, therefore, the "100 percent control."

In order to obtain optimum response of the pen to changes in the transmission of the sample the gain of the amplifier in the recorder must be set properly. If it is too high, there tends to be more noise and some hunting; if too low the response is slow and the pen does not come to the correct position.

A three position switch, S_6, makes it possible to record not only the ratio of the voltages derived from the two beams but also either of them individually; that is, a "single-beam" record may be obtained for either the sample or the standard beam. To do so, a fixed reference voltage, obtained from the B^+ voltage, is applied to the Helipot through switch S_{6C} and the voltage derived from the beam in question is applied to R_{46} through S_{6A} and compared with this fixed voltage. While the spectrometer is ordinarily used as a ratio instrument in obtaining spectra, single-beam operation is often of use in calibration and testing.

S_5, a push button switch located near the wavelength drum, is used to superimpose a small voltage on R_{46}, producing a sharp spike or pip on the record for indexing purposes. A simple vacuum tube voltmeter measures the radiation level in the standard beam. It is a useful accessory.

[12] The Helipot Corporation, S. Pasedena, California.

¶ The Brown Instrument Company, Philadelphia, Pennsylvania. Any other self-balancing potentiometer recorder such as the Speedomax Type G, Leeds and Northrup Co., would do as well. In the case of the Speedomax which can be obtained with a 400-ohm slide wire the Helipot is unnecessary.

LINEARITY AND SIGNAL MIXING

A thermocouple, having a finite heat capacity, heats and cools exponentially. This causes a certain "mixing" of the two types of pulses (see Fig. 6) since after radiation from the standard cell heats the thermocouple it does not have time to cool completely before radiation from the sample cell strikes it. Thus there is a component of signal proportional to the "standard" signal during the time the sample is in the optical path and *vice versa*. If S_1 is the true signal due to the standard, S_2 is the true signal due to the sample and the corresponding apparent signals are denoted by S′, we can express this behavior quantitatively by the relations

$$\begin{aligned} S_1' &= S_1 + fS_2 \\ S_2' &= S_2 + fS_1. \end{aligned} \tag{1}$$

The same mixing constant, f, applies in both cases because of the identical treatment of the two signals, both optically and electrically. In this case the apparent ratio of intensities is given by the expression

$$R' = \frac{S_2 + fS_1}{S_1 + fS_2} = \frac{R+f}{fR+1}. \tag{2}$$

The apparent transmission, R′, is not proportional to the true transmission, R. This behavior is typical, not only for thermal lags but for response times due to any cause.

Mixing of signals is also caused by the limited frequency response and the phase shift of the amplifier and input transformer. Poor high frequency response has an effect exactly like that of the thermocouple. A more important effect arises from the poor response and phase shift at low frequencies introduced by the coupling circuits and, most important, by the input transformer. This effect is approximately corrected by the network in the first stage of the amplifier. The resulting error in the apparent ratio is exactly like that expressed in Eqs. (1) and (2) except that in this case the mixing constant is negative; consequently, the two effects partially cancel each other. The mixing is also a function of the phasing of the switches and this effect can be made of either sign. In our instrument the low frequency effect predominates so that the resultant f, with proper phasing, is negative and the ratio, if uncorrected, would be low.

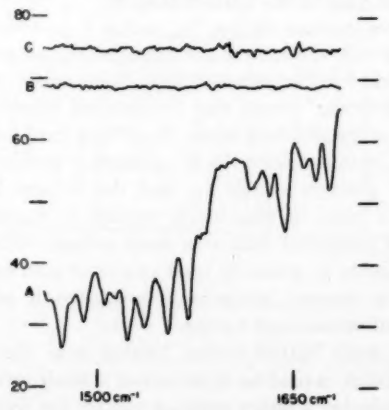

FIG. 9. (A) Atmospheric water absorption near 6μ on "single beam," NaCl prism, 0.05-mm slit. (B) 100 percent line on double-beam under same conditions using automatic slit-width control. (C) Same as (B) but fixed slit, 0.05 mm.

However, it is possible to obtain complete correction for this error. The preceding discussion obtains when the resistor, R_{40} (see Fig. 8), connecting the circuits is omitted. If it is now inserted, the two voltages are changed to some value S_1'' and S_2'', respectively. It has the effect of introducing a voltage $g(S_2''-S_1'')$ into S_1'' and $g(S_1''-S_2'')$ into S_2''. In this case we have

$$\begin{aligned} S_1'' &= S_1 + fS_2 + g(S_2''-S_1'') \\ S_2'' &= S_2 + fS_1 + g(S_1''-S_2''). \end{aligned} \tag{3}$$

These equations are readily put into the form

$$\begin{aligned} (1+2g)S_1'' &= aS_1 + bS_2 \\ (1+2g)S_2'' &= aS_2 + bS_1, \end{aligned} \tag{4}$$

where

$$a = 1+g+fg;\ b = f+g+fg \tag{5}$$

so that

$$R'' = \frac{aR+b}{a+bR}. \tag{6}$$

The condition that R″ is equal to R at all values of R is simply that $b=0$. Consequently, R_{40} must be so adjusted that $g=-f/(f+1)$. Since, as we have mentioned before, f is negative in our instrument this is always possible.

It is then possible, by adjustment of R_{40}, to eliminate errors in the measured ratio caused by signal mixing. It is important to realize that exact correction may thus be obtained for signal mixing but that error due to non-linearity in the amplifier is not corrected; however, amplifier linearity is readily obtained. In practice, R_{40} is adjusted to give the correct transmission when screens of known transmission are placed in the sample beam. When this has been done the ratio as indicated by the recorder is within one percent of the true optical ratio as established by a set of calibrated screens for all ratios from 0 to 100 percent.

We have tested this principle by operating the instrument with a thermocouple having a time constant of 0.2 sec. when the pulse width was only 0.08 sec. When R_{40} was adjusted it was still accurate to one percent over the entire range. It is, therefore, possible to increase the scanning speed considerably if desired, although it would be done at the expense of signal to noise ratio. This correction method might well be applied to quite different situations. It is especially attractive because of its simplicity and complete correction.

AUTOMATIC SLIT WIDTH CONTROL

The tremendous variation with wave-length of the energy emitted by infra-red sources makes it necessary

to change the slit-width frequently while a spectrum is being recorded. This is usually done by the operator or with some sort of cam arrangement. In this instrument the adjustment is made continuously and automatically in any spectral region by a simple, convenient and extremely flexible arrangement. Essentially the same method was used by Coor and Smith[15] in an ultraviolet spectrograph but its utility is far greater in the infra-red region. The circuit by which control is effected is included in Fig. 8. The pulsating d.c. voltage at switch S_4 which represents the radiation through the standard cell is smoothed by R_{35} and C_{28} and compared with a reference voltage through a balanced cathode follower. The reference voltage is derived from B^+ through a resistance divider. The difference between the two voltages is taken from the cathodes and applied to the input of a Brown amplifier. The amplifier drives a small Brown motor which is directly coupled to the slit-control knob of the spectrometer. The amplifier and motor are components of a Brown Elektronik recorder.

The motor adjusts the slit at all times so that the radiation level through the standard beam is constant, producing an output voltage equal to the reference voltage which is normally about 1.1 volt. The reference voltage is set with R_{53}. It is adjusted for best performance and thereafter seldom touched. If it is too high the amplifier will be non-linear in its final stages; if too low the voltages in the ratio circuit will be too low for proper operation of the recorder. The usable region is quite broad, however.

In operation, the radiation level is kept constant within 10 percent, once it has been set initially, even when passing through deep atmospheric absorption bands. The initial slit-width adjustment is made manually by adjusting the amplifier gain controls, R_{14} (continuous) and R_{18} (stepwise). If the gain is reduced the slit-width automatically increases to restore the original balance of the amplifier output and reference voltage; similarly, if the gain is increased the slit-width decreases.

The balanced cathode follower reduces the impedance to a suitable value for feeding the Brown amplifier. It is also inherently stable and quite free of drift. The gain control of the Brown amplifier is adjusted for optimum performance. If it is too low the slit response is sluggish, if too high there is a tendency for the slit to hunt.

A few details are worth mentioning. A switch in the 110-volt line of the amplifier allows the slit-control to be turned off if manual slit-control is desired. Switch S_{6D} shorts the output of the cathode follower and makes the circuit inoperative during single-beam operation. A mechanical coupling is used between the slit motor and slit knob which uncouples if the motor attempts to drive the slit knob too far in either direction. Since the slit knob is on a screw, the coupling must also allow the knob to travel axially as it rotates. It is then impossible to damage the spectrometer if the slit-control functions improperly.

This arrangement is much preferable to cams, especially in a spectrometer with interchangeable prisms. It has proved to be one of the most useful features of this instrument.

[15] T. Coor, Jr. and D. C. Smith, Rev. Sci. Inst. 18, 173 (1947).

PERFORMANCE

Since all of the infra-red spectroscopic work of this laboratory for the last year has been done on the instrument described here, examples of its performance will appear in the literature in other connections. However, it seems worthwhile to include some typical data.

A primary purpose of a double-beam instrument is to eliminate atmospheric absorption from the record. Figure 9 illustrates (A) a portion of the water vapor spectrum near 6μ, taken on "single-beam," (B) the 100 percent line when scanning the same region with the slit-control operating and (C) the same with fixed slit width. The records were taken with an NaCl prism, the Globar operating at 225 watts and a slit-width of 0.05 mm in A and C (in B it was 0.05 mm when there was no absorption). As may be seen, the 100 percent line is constant in either case to within one percent.

As a measure of the accuracy of the absorption measurements, Mr. G. H. Meguerian has used the instrument to perform a large number of analyses of thiophenol during a chemical reaction; using a CaF_2 prism and a slit-width of 0.125 mm at 2680 cm^{-1}, the absorption was reproducible to 0.3 percent and he obtained analyses which were reproducible to within 0.3 percent of the total sample. The signal to R.M.S. noise ratio under these conditions was 610. In addition to being accurate the instrument is also capable of fairly fast scanning for survey purposes. At the fastest response speed it can trace the entire region from 2μ to 15μ on the NaCl prism in just under nine minutes, although at some loss of resolution. However, it is still possible to resolve the doublet with 3 cm^{-1} separation which occurs in the ammonia spectrum at 950 cm^{-1}.

Some minor problems still remain in the instrument. For example, the ratio measured is slightly dependent on the amplifier output level if R_{40} is not changed correspondingly. In changing the voltage at the vacuum tube voltmeter from 0.4 to 1.3 volts, the measured ratios changed an average of 1.3 percent before R_{40} was adjusted. Changes of from 0.5 to 1.0 percent have also been observed when different sets of filter condensers (C_{24-28}) were used. Development is continuing on this instrument but in its present form it is a very satisfactory research tool.

ACKNOWLEDGMENT

We should like to thank Dr. E. L. Wagner for the use of Fig. 1 and to acknowledge the skilled assistance of Mr. T. L. Dawson in the design and construction of the mechanical parts for the instrument.

A New Mounting for an Echelette Diffraction Grating

J. H. GREIG AND W. F. C. FERGUSON
Department of Physics, New York University, Washington Square, New York, New York
(Received May 2, 1950)

With this mounting a single ruled echelette grating may be used "in the blaze" over a very wide range of wave-lengths. This is accomplished by tilting the grating with respect to the incident light as in a Littrow mounting, and then rotating the grating about an axis perpendicular both to the grating elements and the incident beam. By this rotation the path difference between beams of light reflected from successive elements of the grating may be varied from a maximum value, the ordinary blaze wave-length, to zero. The spectrum reflected from the grating may then be reflected from a plane mirror, rotating with the grating, to produce a constant deviation mounting. The image of the slit is found to be tilted as the grating rotates. This can be compensated by a rotation of the slit. In a trial, using an echelette designed for the near infra-red, all orders of the sodium *D*-lines from the fifth to the first were caused to pass an observing telescope, successively in the blaze, by a 55-degree rotation of the grating mounting.

INTRODUCTION

THE main reason for using an echelette grating is its high intensity in the blaze. In order to make use of this intensity over a wide range of wave-lengths, more than an octave, it is customary to change the groove shape, either by changing gratings or by having each element of the grating movable as was done by Cleeton[1] and Williams and by Coates.[2] With the present mounting a single ruled grating may be used in the blaze over a very wide range of wave-lengths. This is accomplished by tilting the grating with respect to the incident light as in a Littrow mounting, and then rotating the grating about an axis perpendicular both to the grating elements and the incident beam. General analytical equations for the positions of the interference maxima, etc. are derived in the following section.

DERIVATION OF GRATING FORMULAS

It seems a little surprising that the grating equation is always derived in texts with the restriction that the elements of the grating be parallel to the incident wave front, i.e., it is derived in two dimensions. If we remove this restriction the problem must be solved in three dimensions, but the derivation is still quite simple.

To derive the equations in three dimensions we will choose a coordinate system fixed with respect to the grating, so that one element of the grating is along the X-axis and the normal to the grating is along the Y-axis as shown in Fig. 1. In order to have an interference maximum for a wave-length λ the path difference between two rays diffracted from corresponding parts of different grating elements must be an integral number of wave-lengths. One ray starts on the incident wave front at $P_0(x_0, y_0, z_0)$, is diffracted at the pth grating element at $P_1(x_1, 0, pd)$ and ends on the emergent wave front at $P_2(x_2, y_2, z_2)$; where d is the grating constant and p is an integer. The corresponding points on the other ray are denoted by the same letters and subscripts with primes.

If the distance from P_0 to P_1 is A and the direction cosines of the incident ray are $\cos a_1$, $\cos b_1$, $\cos c_1$ we can find expressions for x_0, y_0, and z_0 in terms of x_1 and p.

$$\begin{aligned} x_0 &= A\cos a_1 + x_1 \\ y_0 &= A\cos b_1 \\ z_0 &= A\cos c_1 + pd. \end{aligned} \tag{1}$$

Similarly, if the distance from P_1 to P_2 is B and the direction cosines of the emergent ray are $\cos a_2$, $\cos b_2$, and $\cos c_2$,

$$\begin{aligned} x_2 &= B\cos a_2 + x_1 \\ y_2 &= B\cos b_2 \\ z_0 &= B\cos c_2 + pd. \end{aligned} \tag{2}$$

Since any ray is perpendicular to the wave front,

$$(x_0-x_0')\cos a_1+(y_0-y_0')\cos b_1+(z_0-z_0')\cos c_1=0 \tag{3}$$

and

$$(x_2-x_2')\cos a_2+(y_2-y_2')\cos b_2+(z_2-z_2')\cos c_2=0. \tag{4}$$

Substituting (1) and the corresponding set of primed equations into (3), we get, since $\cos^2 a_1+\cos^2 b_1+\cos^2 c_1=1$,

$$A-A'+(x_1-x_1')\cos a_1+(p-p')d\cos c_1=0. \tag{5}$$

Similarly from (2) and (4) we get,

$$B-B'+(x_1-x_1')\cos a_2+(p-p')d\cos c_2=0. \tag{6}$$

Now if n is the order of interference,

$$(p-p')n\lambda=A+B-(A'+B') \tag{7}$$

is the condition for an interference maximum. Adding (5) and (6) and using (7) we get,

$$(p-p')[n\lambda+d(\cos c_1+\cos c_2)]+(x_1-x_1'),\quad (\cos a_1+\cos a_2)=0. \tag{8}$$

This must be true independent of $(p-p')$ and (x_1-x_1') therefore,

$$n\lambda=-d(\cos c_1+\cos c_2), \tag{9}$$

and

$$\cos a_1=-\cos a_2. \tag{10}$$

In the two-dimensional derivation $\cos a_1=0$, $\cos c_1=-\sin i$, and and $\cos c_2=-\sin j$, so (9) becomes;

$$n\lambda=d(\sin i+\sin j), \tag{11}$$

where i is the angle of incidence and j is the angle of diffraction.

In terms of the angles used to describe the present mounting $\cos a_1=\sin\theta$, where θ is measured in a horizontal plane and c_1 and c_2 are given by

$$\cos c_1=-\sin i\cos\theta, \tag{12}$$

and

$$\cos c_2=\cos i\cos\varphi-\sin i\sin\varphi\cos\theta, \tag{13}$$

where i is the angle from the Z-axis to the vertical and φ is the angle from the vertical to the emergent ray. Now (9) becomes

$$n\lambda=d(\sin i\cos\theta+\sin i\sin\varphi\cos\theta-\cos i\cos\varphi). \tag{14}$$

If we use the fact that φ is nearly 90 degrees and note that $\sin i=s/d$ and $\cos i=h/d$ as in Fig. 2(a), (14) becomes,

$$n\lambda=2s\cos\theta-h\cos\varphi. \tag{15}$$

The equation for the tilt of the image of a slit can be obtained by differentiating Eq. (14). Since rays of the same wave-length

[1] C. E. Cleeton, Physics **6**, 207 (1935).
[2] R. J. Coates, Rev. Sci. Inst. **19**, 586 (1948).

from the two ends of the slit strike the grating at slightly different angles, θ and $\theta+d\theta$. They must leave with slightly different angles φ and $\varphi+d\varphi$, a_2 and a_2+da_2. Since $da_2=-da_1=d\theta$, the angle of tilt T will be given by

$$\tan T=d\varphi/d\theta=-[\sin i\sin\theta(1+\sin\varphi)]/[\cos i\sin\varphi-\sin i\cos\varphi\cos\theta]. \quad (16)$$

Again, expressing i in terms of s and h and neglecting the difference between $\sin\varphi$ and 1, (16) becomes,

$$\tan T=(2s/h)\sin\theta. \quad (17)$$

DESCRIPTION OF MOUNTING

In the use of a reflecting diffraction grating in a Littrow mounting the usual fundamental relation for the first-order spectrum, $\lambda=d(\sin i+\sin j)$, becomes: $\lambda=2s$. λ is the wave-length for which constructive interference occurs; d, the width of a grating element (in the plane of the grating); $i=j$, the angle of incidence = the angle of emergence of the ray; and $s=d\sin i=d\sin j$, is half the path difference between disturbances emerging from successive elements of the grating. These relations are shown in Fig. 2(a).

In an idealized echelette grating, used in a Littrow mounting,[3] the groove form is such that s is the actual

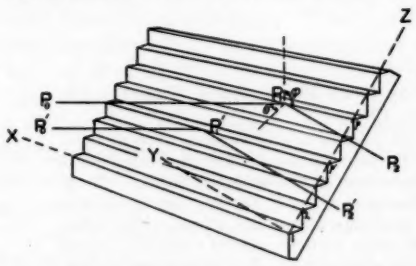

FIG. 1. Coordinate system used to derive the grating equation.

width of a step between two successive elements; so that the light incident in the direction of s emerges in the reverse direction with a path difference of $2s$ between disturbances from successive elements. The other side of the groove, h, is normal to the incident light and gives essentially specular reflection for the blaze wavelength. Tan $i=s/h$.

In the present mounting the rulings of the echelette are horizontal, slit also horizontal, and the echelette is tilted backward to its normal blaze angle, i. The incident and emergent beams are then in a horizontal plane for the blaze wave-length. Now the grating is rotated through an angle θ about a vertical axis through its center. The path difference becomes $2s\cos\theta$, or the "effective" width of a step becomes $s\cos\theta=s'$. The effective width of the grating element is now $d'=(h^2+s'^2)^{\frac{1}{2}}$, and the effective blaze angle, between the normal to d' and the horizontal plane of incidence and emergence, is $i'=j'=\tan^{-1}s'/h$. This is equivalent to tilting each element from i to i'. These effects are indicated in Fig. 2(b).

[3] R. F. Stamm and J. J. Whalen, J. Opt. Soc. Am. 36, 2 (1946).

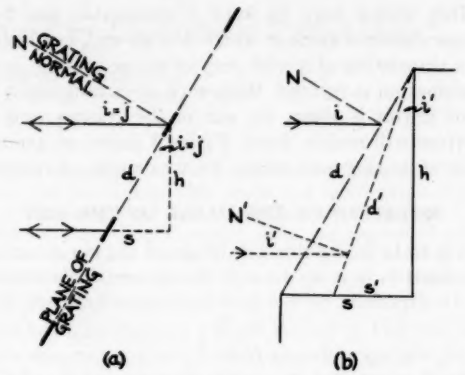

FIG. 2(a). Reflection grating in Littrow mounting, defining the terms used in the text. (b) An element of an echelette grating showing the effect on the constants of rotating the grating.

With these effective values the usual relations, stated above, become: $\lambda=d'(\sin i'+\sin j')$; and $\lambda=2s'$.

The dispersion $dj'/d\lambda$ becomes $1/h$ for the first order.

The resolving power $\lambda/d\lambda$ is, as usual, equal to the number of grating elements, in the first order.

It is seen that the usual properties of the grating for spectroscopic purposes have not been changed. But the path difference, $2s'$, for the wave-length that will emerge at the blaze angle will vary as the cosine of the angle of rotation of the grating. The wave-lengths that are reflected from the grating, always in the blaze and always in a horizontal plane, may be continuously varied from the normal blaze wave-length to a very small value. The spectrum moves vertically as θ varies.

ARRANGEMENT FOR CONSTANT DEVIATION

Obviously the emergent beam moves in a horizontal plane through twice the angle of rotation of the grating. To avoid the necessity of the observer's following this

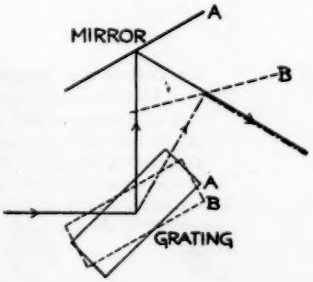

FIG. 3. Grating and mirror in positions A for angle of rotation, $\theta=45°$; in positions B, $\theta=60°$. The mirror, rotating with the grating, requires translation only, as the positions are changed.

beam it is reflected from a plane mirror, held vertically, which is rotated with the grating. This provides a constant deviation mounting; the beam may be directed constantly in any direction. If the plane mirror is fixed at any angle to the rulings of the grating, its aperture must be very large to accommodate the beam from the grating for large angles of rotation; and also the emergent aperture shifts.

This mirror may be kept a reasonable size by a proper choice of angle at which it is set and, in addition, by a translation of it with respect to the grating, as the combination is rotated. With such an arrangement the plane mirror is about the size of the grating, and the aperture will remain fixed. Figure 3 shows an arrangement of grating and mirror for two angles of rotation.

ROTATION OF THE IMAGE OF THE SLIT

It is to be noted that the image of the horizontal slit is rotated in passing through the system. This rotation can be explained by the fact that monochromatic light from the end of the slit strikes the grating at an angle $\theta+d\theta$, slightly different from θ. As a consequence the angle of emergence in a vertical plane will be slightly different from j'. The tilt of the image, T, will be defined as $\tan^{-1}dj'/d\theta$. Combining the equations for dispersion, $dj'=(1/h)d\lambda$, and the differential of the fundamental equation, $d\lambda=2s\sin\theta d\theta$, one obtains: $\tan T=(2s/h)\sin\theta=2\tan i\sin\theta$. $\sin\theta$ will not usually be varied by more than a factor of two; so it is not difficult to rotate either the entrance slit or the exit slit to compensate for this tilt.

EXPERIMENTAL ARRANGEMENT

The mounting described here was set up as in Fig. 3 using an echelette grating with 3610 lines per inch, a plane mirror, collimator, and telescope. The grating, ruled by R. W. Wood, was blazed near the sixth order of $\lambda 5461$, the blaze angle, for a Littrow mounting, being about 13 degrees. All orders from the fifth to the first of the sodium D-lines were observed to pass the telescope, successively in the blaze, as the rotation of the grating and mirror proceeded from $\theta=24.5$ to 79.5 degrees. The image of the slit was tilted from $T=9.5$ to 26 degrees.

Réunions d'Opticiens (Assembly of Opticians). Compiled by Pierre Fleury, André Maréchal, and Claire Anglade. Éditions de la "Revue d'Optique," Paris, 1950.

This volume contains the works presented at the Réunions d'Opticiens held in October, 1946 at Paris. Beginning the book are four discussions: "Theories of Light" by Jean Cabannes; "On the Formation of Images in Corpuscular Optics" by Louis de Broglie; "The Production of Non-spherical Surfaces" by F. Twyman: "Degree of Coherence and the Method of Coherent Background" by F. Zernike. The 126 articles are grouped into 12 sections: Theories and fundamental ideas, teachings; aberrations, corresponding calculations; structure and properties of images; optical instruments; glass, surfaces, optical materials; control and optical measurements; sources, photometry, physical receivers, photography; physiological optics, color; glasses, ophthalmology; spectroscopy, molecular optics, polarimetry; astronomical, atmospheric, geodesic, metrological optics; corpuscular optics.

La Théorie des Images Optiques (Theory of Optical Images). Compiled by Pierre Fleury, André Maréchal, and Claire Anglade. Éditions de la "Revue d'Optique," Paris, 1949.

A compilation of 46 papers presented at an international colloquium on the theory of optical images, held at the time of the Réunions d'Opticiens, October, 1946 at Paris. The articles have been arranged in six chapters: Aberrations, attempts to classify and to reduce systematically; aberrations, applications and development of general methods; possibilities of using non-spherical surfaces; new research on diffraction; combined effects of diffraction and geometrical aberrations; phase contrast; intervention of the receiver (primarily the eye, photographic emulsion).

JOURNAL OF THE OPTICAL SOCIETY OF AMERICA VOLUME 40, NUMBER 8 AUGUST, 1950

The Attenuation of Brightness Contrast Caused by Atmospheric Optical Haze*

HOWARD S. COLEMAN AND HAROLD E. ROSENBERGER
The Optical Research Laboratory, The University of Texas, Austin, Texas
(Received January 3, 1950)

Two physical processes causing the attenuation of brightness contrast of objects by the atmosphere have been isolated. One of these is related to scattering by the particles in the atmosphere and the other is related to convection currents of small local air masses of a variety of optical densities which cross a line of sight during the observation of an object through the atmosphere. These small air masses momentarily deflect the line of sight from the object to its background, thereby changing the apparent contrast of the object viewed. This attenuation process is designated as "optical haze" to distinguish it from reduction in contrast caused by scattering processes. Some authors have referred to this as "shimmer." In the case of a black object viewed against the horizon as a background, the intensity of optical haze has been found to vary with time throughout the day. This temporal variation of optical haze was found to have at least one minimum during the day, usually after sunrise and before sunset. During the afternoon minimum, the optical haze was found to practically vanish at which time scattering alone was responsible for the atmospheric attenuation of brightness contrast and hence the two attenuation processes could be isolated on days in which the scattering was reasonably constant. On such days, studies of the relative importance of the two physical attenuation processes mentioned have indicated that as much as fifty percent of the atmospheric attenuation of brightness contrast can be attributed to optical haze. This suggests a need for modifying the theoretical treatment of the subject of atmospheric attenuation (to make allowances for optical haze which is ordinarily not considered as a factor).

INTRODUCTION

THE obscuration of objects by the atmosphere is an important topic from the point of view of many civil and military operations. There is one factor of obscuration about which almost no objective studies have been made. This factor is referred to as "optical haze" (sometimes referred to as "shimmer"). Optical haze is distinct from the molecular and nuclei types of atmospheric scattering which are generally considered in discussing the attenuation of brightness contrast by the atmosphere. Optical haze is caused by small-scale convection currents which result in the frequent crossing of the line of observation of small air masses of different optical density for regions of the atmosphere in which there is turbulence. This difference in optical density causes minute deviations of light passing from an object toward an observer so that momentarily the light from the surround is directed along the line of sight and the light from the object directed elsewhere. This can result in a change of the apparent contrast of objects if the action of the optical haze is sufficiently rapid to result in an integrated response on the photosensitive receptor used in the observation of the object. In the case of a dark object viewed against a bright surround, the apparent contrast would be decreased as a result of optical haze. In the case of a bright object viewed against a dark surround, no change in apparent contrast would be caused by optical haze.

It is the purpose of this paper to describe a method by means of which it is possible to measure and to evaluate the importance of optical haze with respect to its contribution to the attenuation of brightness contrast by the atmosphere.

APPARATUS AND PROCEDURE

The apparatus used in the experiments described in this paper consisted of a photoelectric telephotometer, seven black and seven white visibility targets, the details of which have been described in a previous paper.[1] For purposes of discussion in this paper, the targets can be regarded as plane white rectangular objects having a black circular disk on them subtending an angle of 1.86 minutes of arc with respect to point of observation. The telephotometer was adjusted such that the entrance pupil to the photoelectric tube used was only slightly smaller than the image formed of a black target. As optical haze causes a momentary deflection of the image of the black target from the entrance pupil to the photoelectric tube and directs the image of a portion of its surround (the white portion of the target) into the photoelectric tube, an increase in apparent luminance of the black target results. This effect is illustrated schematically in Fig. 1.

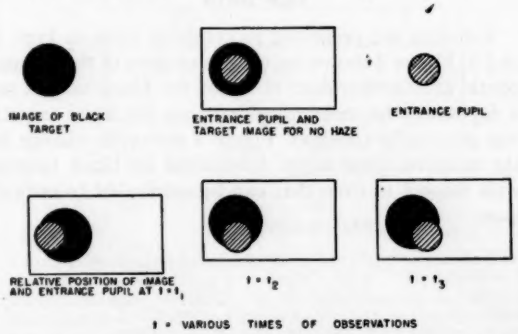
IMAGE OF BLACK TARGET
ENTRANCE PUPIL AND TARGET IMAGE FOR NO HAZE
ENTRANCE PUPIL
RELATIVE POSITION OF IMAGE AND ENTRANCE PUPIL AT $t = t_1$
$t = t_2$
$t = t_3$
t = VARIOUS TIMES OF OBSERVATIONS

FIG. 1. Schematic diagram showing the random temporal displacements of the image of a target with respect to the location of the entrance pupil to the photoelectric tube in the telephotometer as a result of atmospheric optical haze.

* The work described in this paper was performed, in part, under terms of Task IX of Contract N6onr-266 between the ONR and The University of Texas.

[1] Coleman, Morris, Rosenberger, and Walker, J .Opt. Soc. Am. 39, 515 (1949).

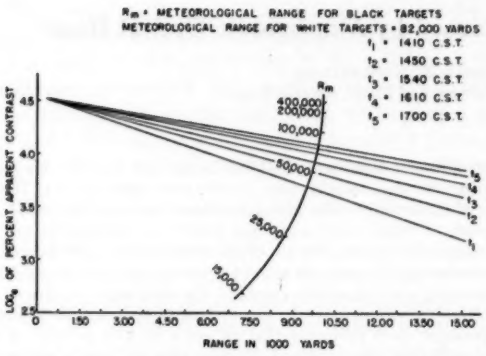

FIG. 2. Basic data showing the change in atmospheric attenuation of brightness contrast as a result of changes in optical haze during the part of a day in which the meteorological range for white targets did not change appreciably.

Since the influence of optical haze changes throughout the day, the procedure consisted simply in measuring the change in a quantity referred to as "meteorological range." This quantity is defined to be the range at which the brightness contrast of an object is reduced by the atmosphere to two percent of its inherent value. In addition the meteorological range was obtained for the white targets. These measurements were made using a filter in the telephotometer that rendered its spectral response similar to that of the human eye. The isolation of the contribution of optical haze from contributions by scattering to the attenuation of brightness contrast can be made by observing the difference in meteorological range determined by the black targets and that determined by the white targets (which changes only slightly by comparison with the black targets because of their greater size). Results thus obtained can be used to determine the loss in "visible" range of objects that can be attributed to atmospheric optical haze.

THE DATA

The data are presented in graphical form in Figs. 2 and 3. Figure 2 shows the change of slope of the atmospheric attenuation data obtained for black targets on a day when the meteorological range for white targets was practically constant. Figure 3 shows the change in the meteorological range determined by black targets with respect to time that can be attributed to optical haze.

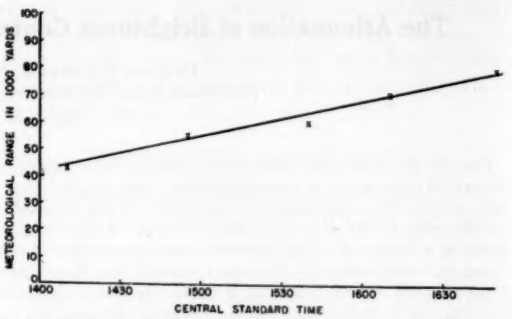

FIG. 3. The variation in meteorological range caused by temporal changes in optical haze as determined by the use of black targets.

DISCUSSION AND CONCLUSIONS

It is evident from the data presented in this paper that the optical haze in the atmosphere is an appreciable factor in limiting the visibility of objects. This type of haze is a complex quantity, the apparent intensity of which depends to a large extent upon the conditions of observation, particularly with respect to the variations in luminosity of the region immediately surrounding an object under examination. The apparent ill effects caused by optical haze on the visibility of objects through the atmosphere depend upon the observing mechanism involved. For example, in the cases of experiments described in this paper, the more nearly the size of the image of the object under consideration approaches the size of the entrance pupil to the photosensitive receptor used, the more apparent obscuration of vision occurs. In addition the relative size of the object with respect to the surround in which it is located is a major factor. For example, an object of very small subtense in a bright surround would suffer more obscuration with respect to its brightness contrast than an object having a relatively large subtense with respect to its surround. This suggests the possibility of developing an "optical haze meter" using a black target in the center of a white surround of large subtense with respect to the black target.

The data presented in this paper suggest a need for refinement of the theoretical treatments of the subject of atmospheric attenuation of brightness contrast to make allowances for optical haze as well as scattering by atmospheric particles.

On the Existence of "Sub-Bands" in the Luminescence Emission Spectrum of Manganese Activated Zinc Silicate*

CLIFFORD C. KLICK AND JAMES H. SCHULMAN
Crystal Branch, Naval Research Laboratory, Washington, D. C.

(Received May 5, 1950)

Failure of the luminescence decay of manganese-activated zinc silicate to follow an exact exponential curve has been cited as evidence for the presence of two different emitting centers with different decay rates. However, the shapes of the spectral emission curves taken at different times after excitation are identical, showing that if two centers exist their emissions are the same. The luminescence emission of this phosphor has also been measured at 4°K and shows a single peak a few hundred angstroms wide. There is little observed change in the emission between 90°K and 4°K. The width of the room temperature emission is therefore the result of the temperature-broadening of an already broad band. No experimental evidence is found for bands predicted on the assumption that emission spectra are formed by the superposition of bands having the shape of Gauss error curves. Theoretical work on the shape of emission and absorption bands is reviewed and does not support the Gauss error curve theory.

THE emission of manganese-activated zinc silicate was measured as part of a survey of important phosphors at liquid helium temperatures to give information on the effects of temperature on luminescence; the interaction of impurity centers and host lattice; and the presence or absence of fine structure in emission. This phosphor is of special interest because its emission is not symmetrical about the peak frequency but has a pronounced long wave-length tail.

When the emission spectrum of a luminescent material is complex it has been accepted practice to ascribe this to the simultaneous occurrence of several emission bands each with its own central wave-length. Each peak in the emission curve is evidence of a band and even structure in the side of an emission curve, though not a peak, is frequently taken as evidence of a separate emission band if the absolute value of the slope shows a minimum.

In several recent papers[1–5] an attempt has been made to apply a different method of analysis. This method assumes that complicated spectra are caused by the occurrence of various emission bands; but, in addition, it assumes that each emission band has the shape of a Gauss error function. Using this method of analysis bands are found not only at positions close to those derived from the older method but also in smoothly varying portions of the emission curve that do not follow a Gauss error function. Thus, it is suggested by those using this method of analysis that many emission spectra are much more complicated than had previously been supposed.

The use of a mathematical function to represent the emission spectrum of a band would be a very powerful analytic tool. It was to check the validity of this procedure that the low temperature emission spectrum of manganese-activated zinc silicate was determined. For low manganese concentrations this phosphor has a single peak in its emission and smoothly falling sides as shown in curves "a"[6] and "c"[7] of Fig. 1. There is, however, a long wave-length tail to the emission which is analyzed as the contribution of a submerged band in

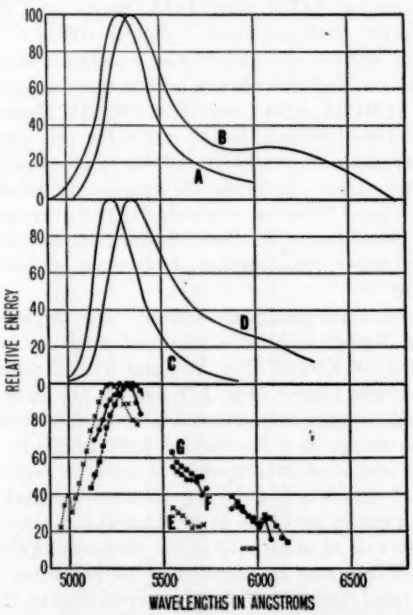

FIG. 1. Spectral emission of Zn_2SiO_4:Mn phosphors. a. Zn_2SiO_4–Mn_2SiO_4 5 percent (Kroger, −180°C). b. Zn_2SiO_4–Mn_2SiO_4 20 percent (Kroger, −180°C). c. Zn_2SiO_4–Mn_2SiO_4 4.7 percent (Schulman *et al*, −150°C). d. Zn_2SiO_4–Mn_2SiO_4 26 percent (Schulman *et al*, −150°C). e. Zn_2SiO_4–Mn_2SiO_4 0.46 percent (Nagy, −180°C). f. Zn_2SiO_4–Mn_2SiO_4 5.6 percent (Nagy, −180°C). g. Zn_2SiO_4–Mn_2SiO_4 10.7 percent (Nagy, −180°C).

* This paper was presented at the Cleveland meeting of the Electrochemical Society.

[1] G. Szigeti and E. Nagy, Publications of the Univ. for Tech. Sciences, Budapest 1, 115 (1948).

[2] K. H. Butler, J. Electrochem. Soc. 93, 143 (1948).

[3] E. Nagy, J. Opt. Soc. Am. 39, 42 (1949).

[4] H. Brinkman and C. C. Vlam, Physica 14, 650 (1949).

[5] C. C. Vlam, Physica 15, 609 (1949).

[6] F. A. Kroger, thesis, "Luminescence in Solids Containing Manganese" (van Campen, Amsterdam, 1940), p. 19.

[7] J. H. Schulman, R. J. Ginther, and E. W. Claffy, J. Electrochem. Soc. 96, 57 (1949).

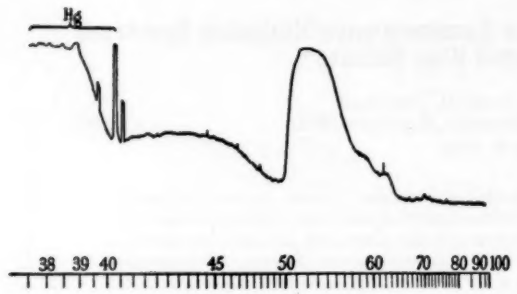

FIG. 2. After Randall. Densitometer trace of the emission spectrum of Zn_2SiO_4–Mn_2SiO_4 0.5 percent at liquid hydrogen temperature (20°K).

the Gauss curve scheme. If this does exist as predicted, and if the broadening of the band could be eliminated by cooling to liquid helium temperature (4°K), this long wave-length band should appear as a separate peak.

Actually the Gauss error curve analysis seems to predict a number of bands for this phosphor. Butler[2] has made an analysis plotting energy against frequency of emission and finds bands centering at 5250A, 5450A, and 5780A. Brinkman and Vlam[4] have also analyzed energy *versus* frequency curves for this phosphor and find bands at 5220A and 5430A. Nagy,[3] and Szigetti and Nagy[1] have analyzed a slightly different curve plotting number of emitted photons against frequency of emission, and they conclude that there are emission bands at 5000A, 5250A, 5690A, and 6030A. There seems to be little difference in the curve for this phosphor whether plotted as energy or number of photons against frequency since the range of emission frequencies is small. Vlam,[5] however, maintains that in tungstates a single Gauss curve fits the emission data better when energy, rather than number of photons, is used as an ordinate.

The emission spectrum found by Nagy[3] differs from that of Butler[2] and Brinkman and Vlam[4] as well as from that of Kröger[6] (Fig. 1, a and b) and Schulman, Ginther, and Claffy[7] (Fig. 1, c and d). His data taken at liquid nitrogen temperatures have been converted to relative energy as a function of wave-length to correspond to the other data reported here and are reproduced in Fig. 1 curves e, f, and g. It will be noted that Nagy finds a peak in his curve at 6030A which is very likely near the end of sensitivity of his photo-multiplier, but which, if real, may be ascribed to the beginning of the 6100A band found by Kröger (curve b, Fig. 1). A more serious deviation occurs in the 5800A peak. Curves f and g, both show this effect for manganese silicate concentrations of 5.6 and 10.7 mole percent Mn_2SiO_4 in the phosphor, respectively. (Manganese content is given as mole percent Mn_2SiO_4 throughout this paper.) These curves may be compared to Kröger's data at the same temperature (curve a, Fig. 1) and Schulman, Ginther and Claffy's results (Curve c, Fig. 1). In contrast to the other experimenters, Nagy did not use a filter to absorb the visible lines of the mercury arc exciting source. The gaps in his data are a result of the interference of the green and yellow lines reflected from the phosphor. The gaps are approximately 150 angstroms wide. Since the resolution of the instrument is given as 15 angstroms, one may conclude that the source produced quite broad lines which might overlap even in the region where data are reported, thus causing an apparent peak in the phosphor emission.

In addition to the bands variously predicted on the Gauss error curve theory, Randall[8] and Shrader[9] have found fine structure in the emission of this phosphor. Randall reports that at liquid hydrogen temperatures (20°K) there is a moderately strong continuum from 4000 to 5000A, a weak line at 5070A, a weak line at 5100A, a strong line at 5155A, a moderately strong line at 5180A, and a weak band from 5900 to 6300A. The densitometer trace of his film is given in Fig. 2. Shrader has measured the emission of manganese-activated zinc silicate at liquid nitrogen temperatures with an instrument of high resolution and finds some evidence for a line at 5150A.

EXPERIMENTAL EQUIPMENT

Figure 3 shows the experimental arrangement for the low temperature measurements. The exciting source was a 10-watt, low pressure, mercury discharge lamp equipped with a Corning No. 9863 filter. This furnished a strong source of fairly pure 2537A radiation. A quartz lens focused the irradiating light on the phosphor which had been deposited on the inside sloping end of a long glass tube. The top of this tube was closed by a quartz plate sealed on with DeKhotinsky cement. Two stopcock-controlled entrances were provided into the tube so that it might first be evacuated and then filled with helium gas. Surrounding the glass tube was a bath of liquid helium held in a strip silvered Pyrex Dewar flask (*B*). Cooling of the phosphor was provided by conduction through the glass on which the phosphor was deposited and by the atmosphere of helium gas in thermal equilibrium with the tube immersed in the liquid helium. Gas convection was negligible because of the relatively small diameter of the tube and the tendency of the cool gas to remain at the bottom. The liquid helium level was always from 6 to 10 inches above the phosphor and runs were not started until 10 minutes after the Dewar flask (*B*) was filled. After this time boiling of the liquid helium was normal, indicating that temperature equilibrium had been reached. In order to prevent undue boiling of the liquid helium, the helium Dewar (*B*) and its contents were precooled with liquid nitrogen. Under these conditions approximately three liters of liquid helium filled the Dewar. Runs were taken for as long as four hours with only half of the liquid helium boiling off in that time. Surrounding the helium Dewar (*B*) was another Dewar

[8] J. T. Randall, Proc. Roy. Soc. **170**, 272 (1939).
[9] R. E. Shrader, J. Opt. Soc. Am. **39**, 699 (1949).

(*A*) containing liquid nitrogen to reduce heat losses from the helium Dewar. Dewar (*A*) was also strip silvered, and the transparent strips lined up with those of the helium Dewar (*B*) so that the phosphor could be observed and its emission photographed with a Gaertner spectrometer. A Lucite jacket surrounded the whole system to protect the operator should a Dewar fail. An exposure was also made with a plaque of the phosphor immersed directly in the liquid helium so that the phosphor would be at as low a temperature as possible.

A preliminary experiment was run to determine whether a monochromator and photo-cell combination could be made as sensitive as the spectrographic method. The Gaertner instrument that was used could be adapted for either purpose. When used as a spectrograph it was equipped with Eastman Kodak Type II-F film. When used as a monochromator the exit slit was adjusted to give the same resolution achieved when the instrument was used as a spectrograph. An RCA 1P21 photo-multiplier with high gain and low noise was used with a d.c. amplifier and recording milliammeter. Later this arrangement was modified so that the light into the monochromator was chopped and the photo-multiplier used with a high gain a.c. amplifier and voltmeter. Neither arrangement of the monochromator gave as satisfactory an emission spectrum as a one-hour exposure with the spectrograph. Since we were primarily interested in finding fine structure and poorly resolved bands, the spectrographic method was adopted even though the monochromator and photo-cell have the advantage of being easily calibrated to give relative energy.

The wave-length calibration was made by photographing the spectrum of a low pressure mercury arc without filter. The spectra reported here were taken with a resolution of approximately 15 angstroms as shown by the resolution of the yellow lines of the mercury spectrum. A Leeds and Northrup recording densitometer was used to analyze the film. Each picture was run through the densitometer at three different rates of speed so that overshoots of the recorder could be separated from true fine structure. All the spectra but one were taken on a single film so that variation in film and developing were minimized.

In addition to the densitometer traces of the film several observers examined it under a travelling microscope for evidence of structure.

EXPERIMENTAL RESULTS

Densitometer traces of the emission spectra as a function of temperature are given in Fig. 4 for Zn_2SiO_4–Mn_2SiO_4 6.8 percent. Trace *a* is the room temperature emission; trace *b* is the emission at liquid nitrogen temperature (90°K); and trace *c* is the emission at liquid helium temperature (4°K). Figure 5 gives the densitometer traces of several exposures taken at liquid helium temperature. Curve *a* is a two-hour exposure; curve *b* is a trace of the same exposure with a five-fold increase in densitometer sensitivity for the center section of the curve. Curve *c* is a one-hour exposure and curve *d* a one-half hour exposure. Curve *e* was taken with the phosphor immersed directly in liquid helium and is a one-hour exposure. The two peaks in this curve at about 5200 and 5380A are due to spots on the film. Curve *e* is on a different film from the other curves of Figs. 4 and 5. Several exposures were taken at low temperatures in order to have a more comprehensive picture of the emission spectrum and also to aid in separating fine structure from background fog and film scratches.

Our results at helium temperature do not show the line structure found by Shrader and by Randall at 5150A. Nor do we find the other lines reported by Randall. This may indicate that our resolution was not adequate or that our film was too "noisy." However, inspection of Randall's densitometer trace in Fig. 2 shows that the structure he reports is very small. In Fig. 5 four vertical lines are drawn at 5230A, 5250A, 5270A, and 5310A. These seem to mark small but recurrent structure in each of the traces. In view of the lack of agreement in the position of the "lines" between the present work and that of Randall and of Shrader, and because of the small magnitude of the "line"

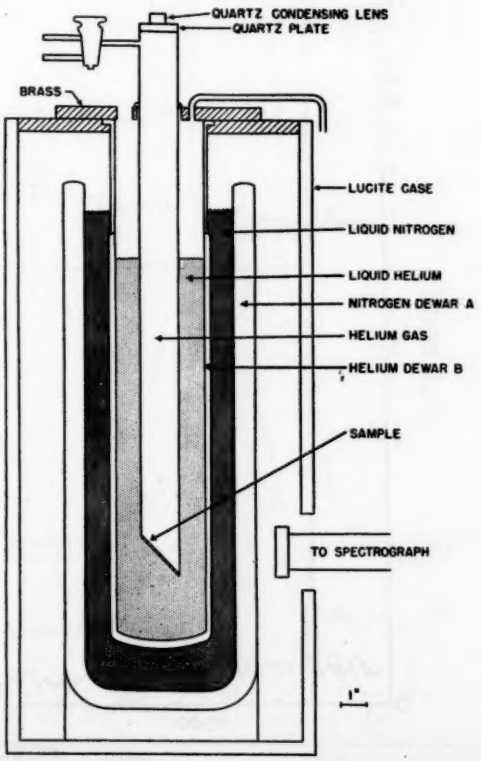

FIG. 3. Helium Dewar for spectral emission measurements.

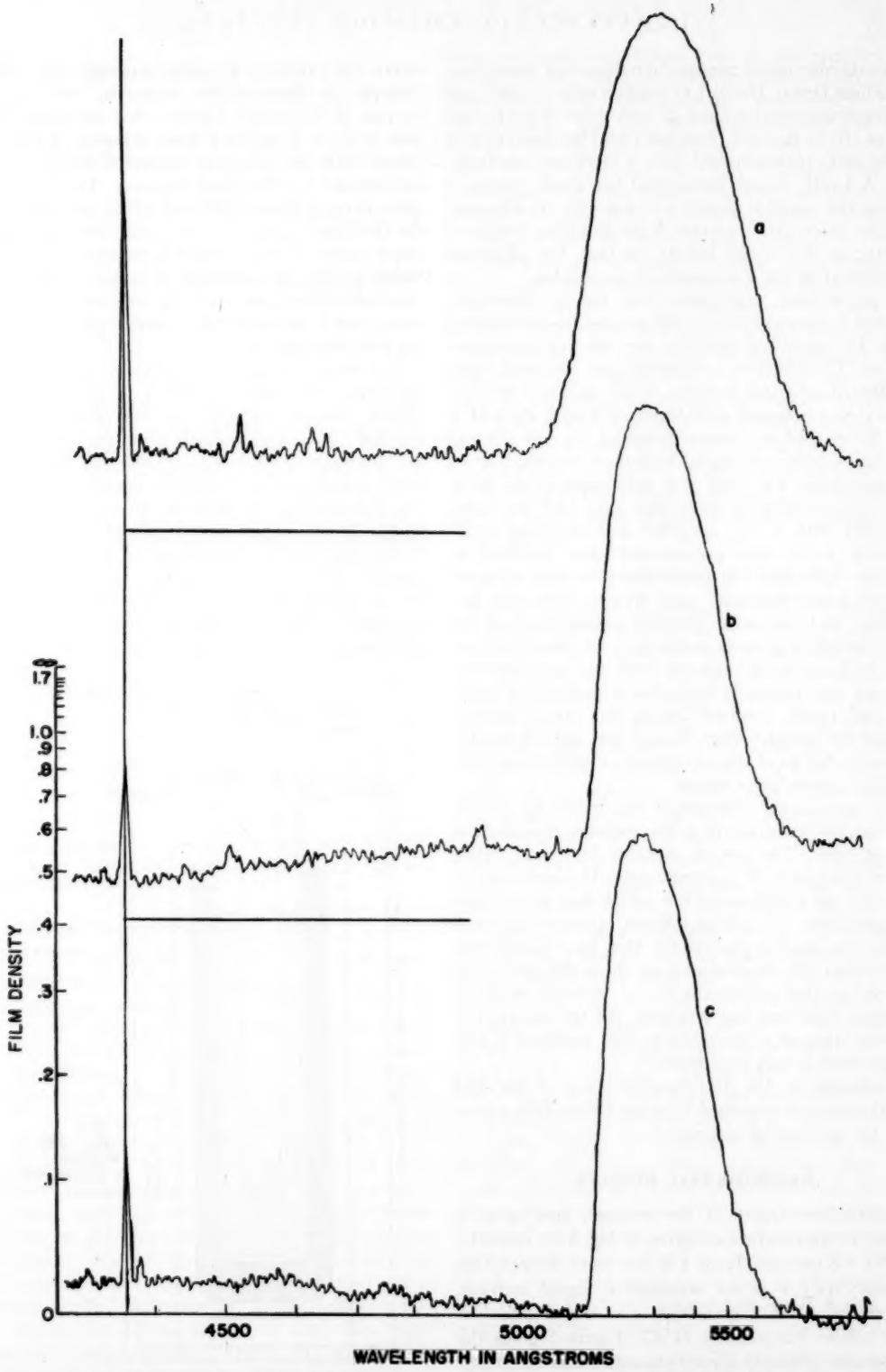

FIG. 4. Densitometer trace of the emission spectrum of Zn_2SiO_4–Mn_2SiO_4 6.8 percent at *a* 300°K, *b* 90°K, *c* 4°K.

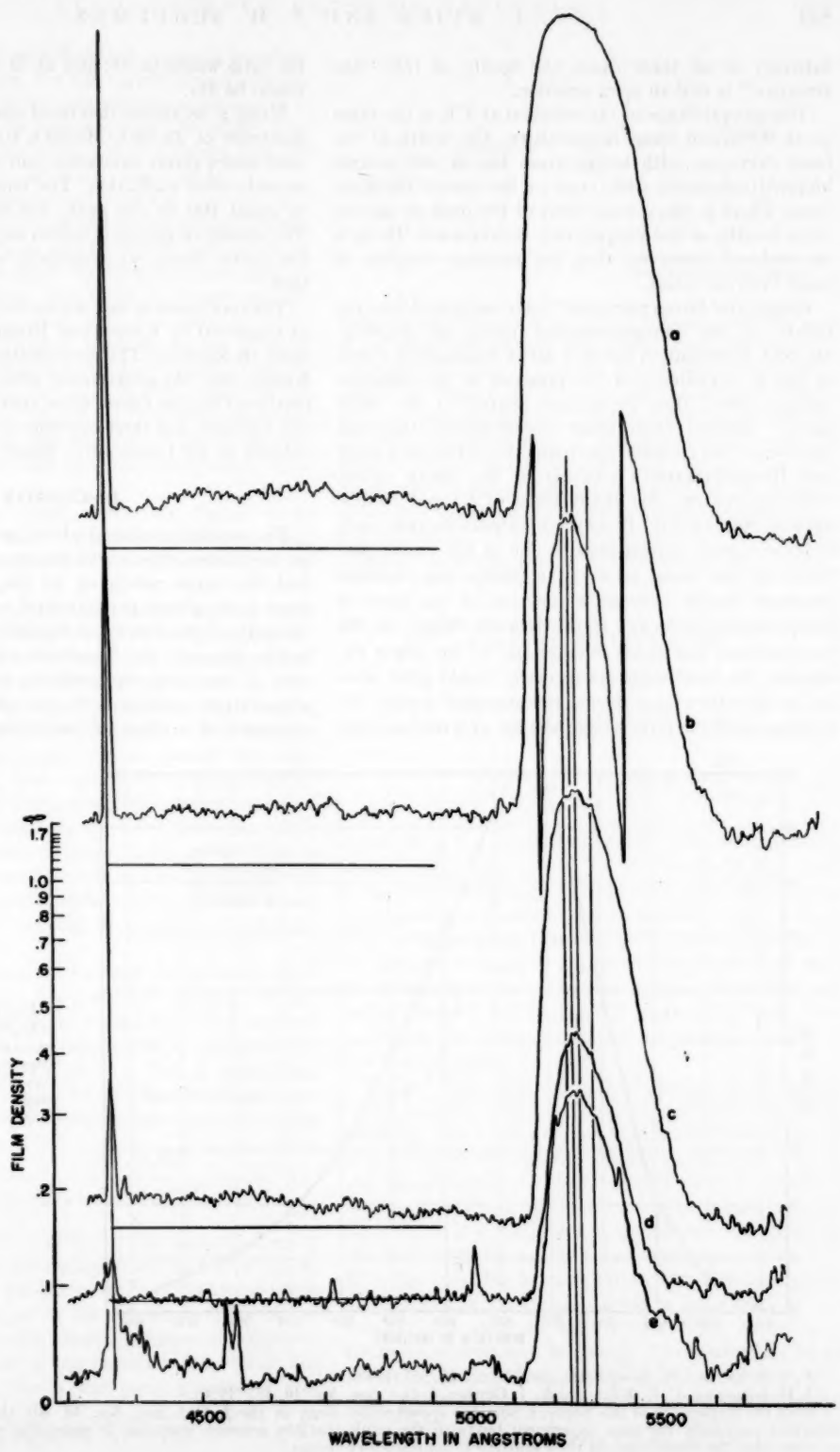

FIG. 5. Densitometer traces of the emission spectra of Zn_2SiO_4–Mn_2SiO_4 6.8 percent taken at 4°K. a. 2 hour exposure. b. 2 hour exposure. c. 1 hour exposure. d. ½-hour exposure. e. 1-hour exposure with phosphor immersed in liquid helium.

intensity in all these cases, the reality of this "line structure" is still an open question.

The general shape of the emission at 4°K is the same as at 90°K and room temperature. The width of the band decreases with temperature but is still several hundred angstroms wide even at the lowest temperatures. There is also a small shift of the peak to shorter wave-lengths as the temperature is decreased. There is no evidence, however, that the emission consists of more than one band.

Kröger and Hoogenstraaten[10] have suggested that the failure of the phosphorescence decay of Zn_2SiO_4–Mn_2SiO_4 5 percent to follow a strict exponential curve at 300°K is evidence of the presence of two emission centers which, they imply, are related to the "sub-bands" derived from other investigators' Gaussian analyses of the emission spectrum. According to Kröger and Hoogenstraaten's analysis of the decay curve, these two centers have decay times of 3.3 and 2 milliseconds, respectively. If, as these authors suggest, each of these centers corresponds to one of the bands predicted by the Gauss error curve theory, the emission spectrum should vary as a function of the time of phosphorescence decay. If the relative height of the two supposed sub-bands is taken as "r" for direct excitation, the band with slower decay would grow relative to the other band during the afterglow period. At 3 milliseconds the ratio would be $1.8r$; at 8 milliseconds the ratio would be $5r$; and at 22 milliseconds the ratio would be $81r$.

Using a technique described elsewhere[11] the emission spectrum of Zn_2SiO_4–Mn_2SiO_4 6.8 percent was measured under direct excitation and at 3, 8, and 22 milliseconds after excitation. The energy curves, adjusted to equal 100 at the peak, are reproduced in Fig. 6. The spread of points is within experimental error, and the curve shows no systematic variation with decay time.*

The conclusion is that if two emitting centers do exist as suggested by Kröger and Hoogenstraaten, the emissions are identical. The identification of these centers by Kröger and Hoogenstraaten with the emission bands predicted by the Gauss error curve theory is therefore not justified, and their existence is not evidence for the validity of the Gauss curve theory.

DISCUSSION

The results presented above seen to bear seriously on the Gauss error curve theory. First, the failure to find the bands predicted by the theory means that there is no direct experimental evidence for the universality of this theory or its ability to find submerged bands. Second, the broadness of the emission band even at very low temperatures means that the room temperature emission, of this phosphor at least, is composed of a range of wave-lengths inherent in the

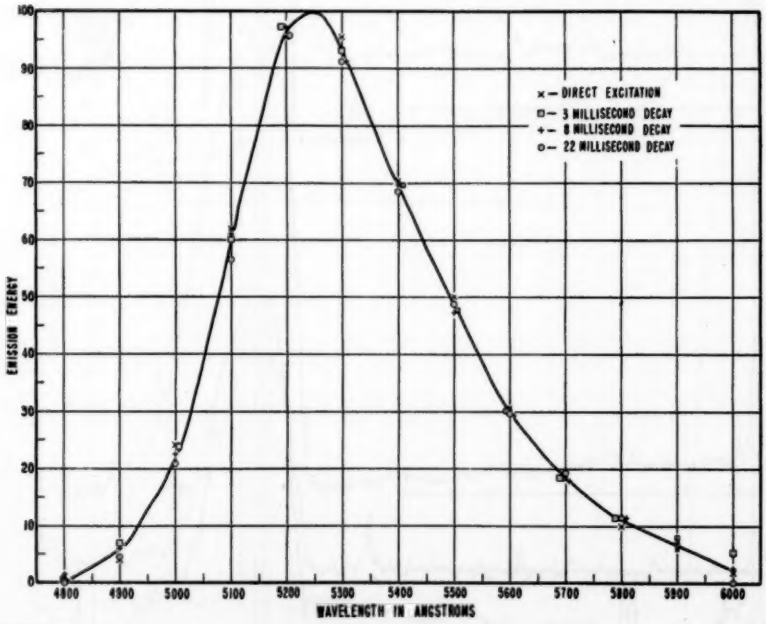

FIG. 6. Emission spectra of Zn_2SiO_4–Mn_2SiO_4 6.8 percent taken at varying times after end of excitation. All curves adjusted to 100 at peak.

[10] F. A. Kröger and W. Hoogenstraaten, Physica **15**, 557 (1949).

[11] J. H. Schulman, C. C. Klick and R. J. Ginther, J. Opt. Soc. Am. **40**, 337 (1950).

* Since the preparation of this paper, a note has appeared by Nagy in the J. Opt. Soc. Am. **40**, 407 (1950), in which he has performed essentially the same experiment but with the result that the emission spectrum *is* dependent on the decay time. It is not clear what the reasons are for these apparently contradictory results.

emission process, and superimposed on this a broadening due to temperature. For the Gauss curve theory to be generally true, the low temperature emission of a band would have to be Gaussian and the influence of temperature would have to be of such a nature that the Gaussian shape of the curve was maintained.

Finally, the invariance of the spectral emission as a function of the time after excitation implies that if the emission is composed of several bands they all have the same decay time. Since the probability of an electron transition between two levels is in general dependent on both the initial and final state, it would appear unlikely that pairs of levels giving rise to separate emission wave-lengths would have identical transition probabilities. This difficulty is emphasized by the results[11] with a similar phosphor, manganese-activated zinc beryllium silicate, the emission of which in contrast, consists of two definite component bands with different decay times.

The experimental evidence for the Gauss curve theory remains that some materials, chiefly the tungstates, have an emission which may be fitted by a single Gauss error curve.

It may be well to review here the theoretical work that has been done on the shape of emission and absorption curves in order to determine what theoretical evidence there is for Gaussian emission curves.

Peierls[12] has made perhaps the most rigorous attempt in this direction by analyzing the process of absorption in a pure solid leading to an electron transfer from one band to another. He finds that in the neighborhood of the absorption peak the transmitted energy varies as the square of the frequency deviation from the peak frequency. The inverse problem of luminescence in a pure solid he found too difficult for a complete solution but he felt the results would be similar to that for absorption. He did not attempt an analysis of impurity activated phosphors.

Smakula[13] has derived an equation for the absorption curve of alkali halide color centers (*F*-centers). He assumed that the complex polarizability of the electron in the color center can be represented by the polarizability for a single absorption line. This is superposed on the polarizability of the lattice. The resulting equation which fits the experimental points quite closely is,

$$k=\frac{n_0 f e^2}{18\pi m}\,\frac{(n'^2+2)^2}{n'}\,\frac{\nu_d'(\nu_F+\Delta\nu)}{\Delta\nu^2(2\nu_F+\Delta\nu)^2+\nu_d'^2(\nu_F+\Delta\nu)^2}, \quad (1)$$

where k is the coefficient of absorption, n_0 is the density of color centers, f is the oscillator strength and should be almost unity, e is the charge on the electron, m is the mass of the electron, n' is the refractive index of the pure material, ν_d' is the damping frequency approximately 10^{14} sec.$^{-1}$, $\Delta\nu$ is the variation from peak absorption frequency, ν_F is the peak absorption frequency. This equation is not a Gaussian function and is not even symmetrical about the center frequency.

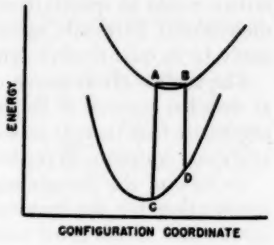

FIG. 7. Configuration coordinate diagram for emission.

Szigeti and Nagy[1] give the unpublished results of a somewhat similar analysis made by Gombas and Hoffman of emission spectra. They analyze the transitions between two bands each of energy width $h\Delta\nu$ with the centers of the bands separated by energy $h\nu_0$. The assumption is made that $\Delta\nu \ll \nu_0$ and that the allowed states and vacancies are uniformly distributed throughout the bands. The transition probability is assumed, constant for all transitions. This results in the equation

$$N(\nu)=-\frac{c}{\nu}\left\{\tfrac{1}{2}\log\frac{(1+a^2b^2)^2}{[1+(a+1)^2b^2][1+(a-1)^2b^2]}-ab\arctan\frac{2ab^3}{(1+a^2b^2)^2+b^2(1-a^2b^2)}+b\arctan\frac{2b}{1+a^2b^2-b^2}\right\}, \quad (2)$$

where N is the number of quanta emitted, c the velocity of light, a is $(\nu-\nu_0)/\Delta\nu$ and b is $\Delta\nu/d$ where d is a damping coefficient. This equation can be made to approximate a Gaussian curve within 2 percent over most of its range by choosing $b=7$. The representation of emission in impurity activated phosphors as an electronic transition between two narrow bands of equal energy width is admittedly not a general picture. Furthermore, the authors can find no physical basis for the relation $\Delta\nu/d=7$.

Butler[14] has proposed a justification for Gaussian curve analysis based on the configuration coordinate diagram, Fig. 7. He assumes that an electron in an excited state of an impurity center moves from A to B and that in analogy with the ground state of the simple harmonic oscillator, its distribution with time is Gaussian. There is a maximum of energy released when the electron jumps from A to C and a minimum from B to D. If the variation in energy from A to B in the excited state is negligible, and if the curve from C to D is a straight line then on this picture there would be a Gaussian distribution of energy. There seems to be no reason why, in general, the line CD should be straight. Also, while an impurity atom in a three-dimensional

[12] R. Peierls, Ann. d. Physik. **13**, 905 (1932).
[13] A. Smakula, Zeits. f. Physik **59**, 603 (1930).
[14] K. H. Butler, J. Electrochem. Soc. **95**, 267 (1949).

lattice would be qualitatively similar to the simple one dimensional harmonic oscillator, it would not necessarily be in quantitative agreement.

The review given above of the theoretical attempts at detailed analysis of emission and absorption curves emphasize that there is no solid theoretical argument for analyzing emission curves into Gauss error functions.

In view of the meager experimental and theoretical justification for the procedure of analyzing emission curves into Gauss error curves it may be well to use the technique with great caution. Considering the wide variety of luminescent types such as pure and impure solids, photo-conducting and nonphoto-conducting materials, and permitted and forbidden transitions; and considering that the phosphor investigated here shows both an inherent broadness of emission at low temperatures as well as a broadening effect due to temperature, it would perhaps be surprising if a simple mathematical function could represent all emission bands under all circumstances.

The width of the emission band in manganese-activated zinc silicate at low temperatures may be the result of various mechanisms: interaction of activator atoms, effect of lattice distortions and imperfections, zero point energy of the activator, or quantum-mechanical interaction between an excited electron of the activator and the lattice vibrations. Decisions between some of these explanations may be made on the basis of low temperature experiments on other phosphors which are now in progress.

ACKNOWLEDGMENTS

We wish to express our indebtedness to many people who have assisted in this work: To R. L. Dolecek and C. J. Grebenkamper for supplying liquid helium to us; to R. L. Dolecek and J. R. Clement for advice on the design of the helium Dewar; and to J. D. Purcell, E. W. Claffy and R. J. Ginther for assistance with the experiments.

JOURNAL OF THE OPTICAL SOCIETY OF AMERICA VOLUME 40, NUMBER 8 AUGUST, 1950

Theory of the Luminescence of Sulfide Phosphors

SHEPARD ROBERTS AND FERD E. WILLIAMS
General Electric Research Laboratory, Schenectady, New York

(Received May 12, 1950)

Assuming the existence of a killer center with an unoccupied electronic ground state above the Fermi level and explicitly including the metastable emitting state of the activator and the electron traps in the formulation, the dependence of emission intensity on excitation intensity for sulfide phosphors is comprehensively treated. The data of Nail, Urbach, and Pearlman, which demonstrate that over an intensity range the emission intensity of the $Zn_{0.5}Cd_{0.5}S$:Ag, Ni phosphor is proportional to the 3.5 power of the excitation intensity, are quantitatively reproduced by the theory. The adjustable parameters used to fit the data are shown to be reasonable and to be in accord with other measurements and are used to evaluate the energies of the various electronic states involved. In addition, it is shown that the relation of Klasens and Wise between excitation and emission intensity may be derived as a special case of the general theory.

I. INTRODUCTION

IT has been known for some time that the fluorescence brightness of certain sulfide phosphors is in some cases more than proportional to the intensity of the exciting ultraviolet radiation.[1] In studying silver activated zinc sulfide compositions Klasens, Ramsden, and Quantie[2] found a linear relation between the reciprocal of the efficiency and the inverse square root of the brightness of luminescence. This result appeared to be satisfactorily explained[3] by the existence of cobalt killer centers which could lose an electron by hole conduction in the filled band and could then receive an electron from the conduction band thereby by-passing the radiative process. The electronic energy of the killer center would in this case be below the Fermi level.

Experimental data for zinc-cadmium sulfide compositions recently reported by Nail, Urbach, and Pearlman[4] indicate an approach to constant efficiency at high intensities and a much lower constant efficiency at very low intensities with an extremely rapid change of emission intensity *versus* excitation in the intervening range. When the logarithm of brightness of luminescence is plotted *versus* the logarithm of exciting intensity a slope of almost 3.5 is observed. A slightly different type of killer center was suggested which could capture an extra electron with a resulting energy state above the Fermi level. However, even so, the above authors could not account for a slope greater than 2.

[1] N. Riehl, Zeits. f. Tech. Physik **20**, 152 (1939); J. H. Gisolf and F. A. Kroger, Physica **6**, 1101 (1939); F. Urbach, A. Urbach, and M. Schwartz, J. Opt. Soc. Am. **37**, 122 (1947).

[2] H. A. Klasens, W. Ramsden, and C. Quantie, J. Opt. Soc. Am. **38**, 60 (1948).

[3] M. E. Wise and H. A. Klasens, J. Opt. Soc. Am. **38**, 226 (1948).

[4] N. R. Nail, F. Urbach, and D. Pearlman, J. Opt. Soc. Am. **39**, 690 (1949).

A more detailed theoretical interpretation is now proposed. The presence of killer centers with vacant electronic ground states above the Fermi level is assumed, and the metastable emitting state of the activator and electron traps, both of which are known to exist in these phosphors, are explicitly included in the formulation. The theoretical treatment successfully explains the experimental data of Nail, Urbach, and Pearlman and permits the quantitative evaluation of significant parameters of these phosphors.

II. THEORY

The processes being considered are shown schematically in Fig. 1. Luminescent centers may be excited to a metastable emitting state M by ultraviolet radiation. From the metastable state electrons may either be thermally activated into the conduction band C, or they may drop back to the ground state L accompanied by light emission. In the conduction band, electrons may be caught again in the metastable states of vacant or ionized luminescent centers or they may be caught by empty killer centers K or by electron traps T. The traps are emptied by thermal activation to the conduction band, but the killer centers are too deep for this process. The ground state of vacant luminescent centers may also be filled without emission of light by electrons activated from the filled band F. The hole thus produced migrates in the filled band until it is caught either by an occupied killer center or by another luminescent center.

Let N_2 represent the concentration of killer centers, and let X be the fraction of these which are filled with electrons. Then XN_2 is the concentration of filled k.c. and $(1-X)N_2$ is the concentration of empty k.c. Similarly let YN_2 represent the concentration of filled traps. Then, recognizing from conductivity data that there is a negligible concentration of electrons in the conduction band and of holes in the filled band, the concentration of empty luminescent centers will be $(X+Y)N_2$. At low and moderate excitation intensities $(X+Y)N_2$ is small compared to the total number of luminescent centers and to the total number of traps. In this case the exchange of electrons between traps and the conduction band greatly exceeds the competitive processes so that an equilibrium is maintained between the concentration of electrons in the conduction band, n_c, and the concentration in traps.

$$n_c=\alpha Y N_2, \tag{1}$$

where α is the constant of proportionality.

Similarly the rate of recombination of holes in the filled band with luminescent centers greatly exceeds the rate of combination with filled killer centers, hence the concentration of holes in the filled band n_F is in equilibrium with the concentration of vacant luminescent centers.

$$n_F=\gamma(X+Y)N_2, \tag{2}$$

where γ is the constant of proportionality.

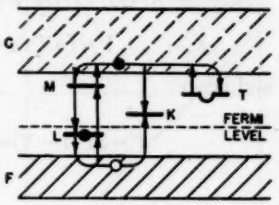

FIG. 1. Energy level diagram showing processes being considered.

Let J represent the rate at which incident ultraviolet light produces metastable luminescent centers. Then if I represents the rate at which light quanta are emitted and I' represents the rate at which quanta are lost in the non-radiative process, conservation requires:

$$J=I+I'. \tag{3}$$

The non-radiative process is equal to the rate at which conduction electrons are captured by killer centers.

$$I'=\sigma_2(1-X)N_2 n_c v_c, \tag{4}$$

where σ_2 is the effective capture cross section of the killer center and v_c is the effective velocity of conduction electrons.

In a steady-state condition this must also be equal to the rate at which holes in the filled band combine with filled killer centers.

$$I'=\rho_2 X N_2 n_F v_F, \tag{5}$$

where ρ_2 is the effective capture cross section of the killer center for holes and v_F is the effective velocity of hole migration.

An electron in the metastable level of a luminescent center may either be thermally activated into the conduction band or return to the ground level by the emission process. Let (k_1-1) be the ratio of probability of the former process to that of the latter. If G is defined as the total number per unit time of electrons that either are excited to the metastable level or are captured by the metastable level from the conduction band, the emission intensity is:

$$I=G/k_1. \tag{6}$$

The difference between G and J is equal to the rate at which conduction electrons are caught by empty luminescent centers.

$$G-J=\sigma_1(X+Y)N_2 n_c v_c=(k_1-1)I-I' \tag{7}$$

where σ_1 is the electron capture cross section of the metastable level.

Equations (4), (5), and (7) may be rewritten substituting the values of n_c and n_F from Eqs. (1) and (2).

$$I'=\sigma_2\alpha v_c N_2^2(1-X)Y=aY(1-X) \tag{8}$$

$$I'=\rho_2\gamma v_F N_2^2(X+Y)X=bX(X+Y) \tag{9}$$

$$(k_1-1)I-I'=\sigma_1\alpha v_c N_2^2(X+Y)Y=cY(X+Y) \tag{10}$$

where $a=\sigma_2\alpha v_c N_2^2$, $b=\rho_2\gamma v_F N_2^2$, $c=\sigma_1\alpha v_c N_2^2$.

Solving (8) and (9) for Y gives:

$$Y=[bX^2/a-(a+b)X] \tag{11}$$

and hence:

$$I'=aY(1-X)=\frac{abX^2(1-X)}{a-(a+b)X}. \tag{12}$$

Eliminating $(X+Y)$ from (9) and (10) gives

$$(k_1-1)I-I'=\frac{c}{b}\frac{Y}{X}I'=\frac{cX}{a-(a+b)X}I'$$

or

$$(k_1-1)\frac{I}{I'}=\frac{cX}{a-(a+b)X}+1. \tag{13}$$

The final parametric equations for I and J, obtained from Eqs. (3), (12), and (13) are:

$$I=\frac{ab}{k_1-1}\cdot\frac{X^2(1-X)}{a-(a+b)X}\left[\frac{cX}{a-(a+b)X}+1\right]$$
$$J=\frac{ab}{k_1-1}\cdot\frac{X^2(1-X)}{a-(a+b)X}\left[\frac{cX}{a-(a+b)X}+k_1\right]. \tag{14}$$

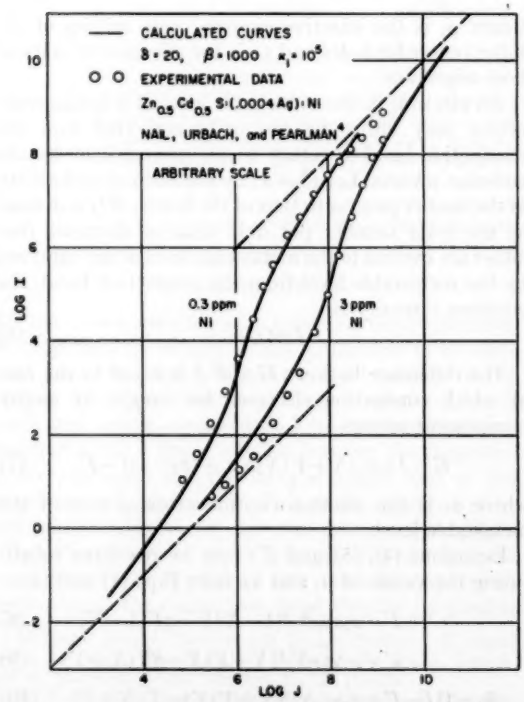

FIG. 2. Luminescent intensity *versus* excitation for zinc-cadmium sulfide phosphors.

These equations may be simplified by substituting a new variable Z instead of X.

$$I=B\frac{Z^2(Z+\beta)(Z+1)}{(Z+\delta)^2},$$
$$J=B\frac{Z^2(Z+\beta)(Z+k_1)}{(Z+\delta)^2}, \tag{15}$$

where:

$$Z=\frac{cX}{a-(a+b)X}$$
$$\beta=\frac{c}{b}=\frac{\sigma_1\alpha v_c}{\rho_2\gamma v_F}$$
$$\delta=\frac{c}{a+b}=\frac{1}{\sigma_2/\sigma_1+1/\beta},$$
$$B=\frac{a^2b^2}{c(a+b)^2(k_1-1)}=\frac{\sigma_2}{\sigma_1}\cdot\frac{\delta^2}{\beta^2(k_1-1)}\sigma_2\alpha v_c N_2^2.$$

The efficiency of luminescence, derived from Eqs. (15) is simply:

$$I/J=(Z+1)/(Z+k_1). \tag{16}$$

Incidentally, this result applies precisely only with homogeneous excitation. However, corrections arising from integrating over the non-homogeneous excitation at the different depths of penetration are found to be trivial, therefore (15) and (16) will be used in interpreting experimental data.

III. INTERPRETATION OF EXPERIMENTAL RESULTS

At very low intensities, $Z\ll 1$, the efficiency is constant and equal to $1/k_1$, while at very high intensities, $Z\gg k_1$, the efficiency is also constant but equal to unity. These limiting cases appear as straight lines of unity slope on the curve of log brightness *versus* log exciting intensity, and correspond to the asymptotes in Fig. 4 in the paper by Nail, Urbach, and Pearlman.[4] The logarithm of k_1 is simply equal to the vertical distance between the two lines. In this way the value of k_1 is determined to be 10^5.

The determination of β and δ is less direct since these parameters control the actual shape of the curve. A trial and error method has been used to obtain agreement between theory and experiment. The values chosen in this manner are $\delta=20$ and $\beta=1000$. δ is approximately equal to the capture cross section ratio for conduction electrons by the ionized activator and by the killer center. The large value of β indicates that there is a correspondingly greater probability for an electron to leave a trap, pass through the conduction band and combine with a vacant activator than for a hole to be released from an ionized activator, pass

through the filled band and combine with an occupied killer center.

A change in the multiplying factor B has the effect of shifting the whole curve an equal amount horizontally and vertically. Since the measurements of brightness and intensity are not on an absolute scale, the value of B cannot be determined from the experimental results. B is proportional to N_2^2, and is the only parameter in Eqs. (15) which depends on N_2 at all. Thus a change in the concentration of killer centers does not change the shape of the curve but merely shifts it equal amounts vertically and horizontally.

Two curves calculated from the above values of k_1, δ and β are shown in Fig. 2, the second curve being shifted to correspond to a tenfold change in concentration of killers. The experimental data of Nail, Urbach, and Pearlman[4] for Ni concentrations of 0.3 and 3 p.p.m. are superimposed on the calculated curves, indicating that the theory accounts satisfactorily for the effect of change in killer concentration as well as for the general shape of the curves.

Wise and Klasens[3] determined a somewhat different relation between brightness and excitation intensity, which was in agreement with the experimental results of Klasens, Ramsden, and Quantie[2] for similar phosphors poisoned by Co instead of Ni. Their expression may be put in the form

$$J/I = a + bI^{-\frac{1}{2}}. \tag{17}$$

This is approximately equivalent to Eqs. (15) when $Z \gg \beta$. Then

$$I \cong BZ^2, \quad J \cong BZ(Z+k_1)$$
$$J/I \cong 1 + k_1 B^{\frac{1}{2}} I^{-\frac{1}{2}}. \tag{18}$$

The data calculated from the present theory for $Z \gtrsim 10^4$ are plotted in the manner of Klasens, Ramsden, and Quantie in Fig. 3. The calculated points closely approximate a straight line, although there is some deviation from Eq. (18) since neither the intercept nor the slope corresponds exactly. The curve plotted in this manner deviates more noticeably from a straight line if extended to smaller values of Z or lower intensity.

IV. CALCULATION OF ENERGY LEVELS

The values determined for k_1, δ and β may be used, along with other information, for estimating the relative energy levels of the different states which participate in the luminescent processes. The energy differences so determined are indicated in Fig. 4, with the same symbols as used in Fig. 1. The primary excitation process is not shown on Figs. 1 and 4 because there are two alternative possibilities which are both compatible with the calculations of the preceding sections.

It is clear that the primary excitation process takes place either directly in the luminescent center or indirectly by exciton formation followed by efficient transfer of the excitation energy to the luminescent center. The

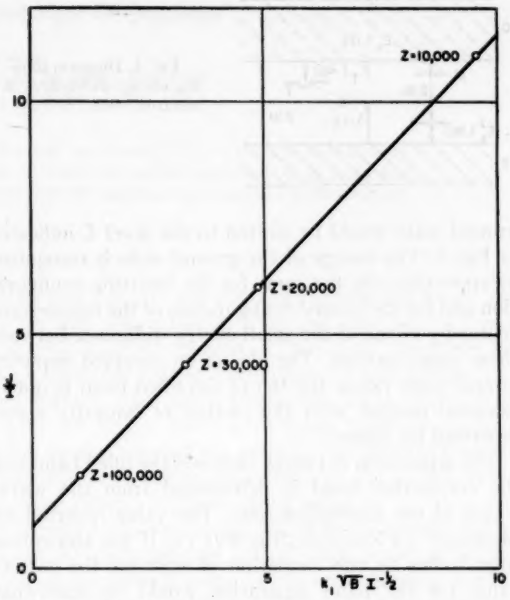

FIG. 3. Calculated reciprocal efficiency *versus* inverse square root of brightness.

postulated presence of excitons in ZnS is supported by the observation of a series of emission bands at low temperatures.[5] The wave-lengths of these bands are at or near the absorption edge in accord with the concept of excitons. Furthermore, the presence of small traces of Ag or Cu completely suppresses these emission bands, indicating that excitons are captured by these impurities before they can release their energy in emission. Dr. F. J. Studer of this laboratory has measured the excitation spectra of several ZnCdS phosphors. For $Zn_{0.5}Cd_{0.5}S$:Ag and ZnS:Ag the maxima occur at 4000A and 3400A respectively. These values are very close to the absorption edges and thus support the exciton theory.

On the other hand in ZnS:Cu the maximum excitation occurs at 3800A, which corresponds to too low an energy for production of excitons. It seems much more likely, therefore, that the Cu luminescent center is excited directly by the ultraviolet radiation. Furthermore, both the excitation and emission spectra are shifted 0.4 ev when Ag is used as the activator instead of Cu. This fact supports the theory that Ag may be excited in the same way as Cu. Possibly both impurity and exciton excitation occur simultaneously in the Ag activated phosphor. The direct excitation of the Ag activator would require the luminescent center to have a ground state somewhat below the top of the filled band when in the unexcited atomic configuration. When the luminescent center is excited, the energy of the

[5] P. Pringsheim, *Fluorescence and Phosphorescence* (Interscience Publishers, Inc., New York, 1949), p. 608.

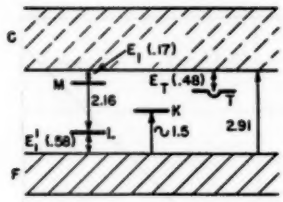

FIG. 4. Diagram showing energy differences in electron volts.

ground state would be shifted to the level L indicated in Fig. 4. The energy of the ground state is recognized as approximately the same for the emitting configuration and for the ionized configuration of the luminescent center by virtue of the small energy difference between these configurations. The idea of an occupied impurity ground state below the top of the filled band is not in essential conflict with the picture of impurity states described by Slater.[6]

The separation in energy between the filled band and the conduction band is determined from the wavelength of the absorption edge. The value reported by Melamed[7] for $Zn_{0.5}Cd_{0.5}S$ is 2.91 ev. If the absorption edge is due to the formation of excitons the correct value for the band separation would be somewhat greater, probably by one or two tenths of an electron volt. The emission spectrum has a maximum corresponding to 2.16 ev. Some of the other energy values may be determined, or at least estimated, with the aid of the values for k_1 and β.

To evaluate the energy difference E_1 let k' be the rate constant for thermal activation from the metastable level to the conduction band and let A be the transition probability for emission. Then

$$\frac{k'}{A}=k_1-1=\frac{se^{-E_1/kT}}{A}, \tag{19}$$

where s is the frequency factor estimated to be about 10^{13} sec.$^{-1}$ and kT is 0.025 electron volt at 25°C. The value of A, reported by Strange and Henderson,[8] is about 10^5 sec.$^{-1}$, which was determined by studying the decay of luminescence under pulsed cathode-ray excitation. The value of E_1 calculated from these data is 0.17 ev. The value of E_1' is then 0.58 ev.

By making assumptions regarding the relative values of σ_1, ρ_2, v_e and v_F, one can estimate the ratio α/γ from the value of β.

$$\frac{\alpha}{\gamma}=\beta\cdot\frac{\rho_2 v_F}{\sigma_1 v_e}=\frac{e^{-E_T/kT}}{e^{-E_1'/kT}}. \tag{20}$$

From which:

$$E_1'-E_T=kT\log_e(\alpha/\gamma). \tag{21}$$

To evaluate this result we suppose $\rho_2 \cong \sigma_2$ and $v_F \cong v_e$. The velocities of holes and electrons are presumed to be of similar magnitude since their mobilities are of the same order. Then:

$$\rho_2/\sigma_1=\sigma_2/\sigma_1=1/\delta=0.05,$$

and

$$\alpha/\gamma=1000\times 0.05=50.$$

Then

$$E_1'-E_T=0.025\times 3.9=0.10 \text{ ev}.$$

Therefore E_T is 0.48 ev. From thermoluminescence data the energy depths of the electron traps active at room temperature in $Zn_{0.5}Cd_{0.5}S$:Ag are found to be in good agreement with this value.

Klasens, Ramsden, and Quantie[2] determined a value of E from their experimental results such that the parameter b in Eq. (17) was proportional to $\exp(-E/kT)$. The value obtained in this manner for ZnS:Ag phosphors with Co killer centers was 0.37 ev. The theoretical value of E may be evaluated by expanding the term $k_1B^{\frac{1}{2}}$ in Eq. (18). It turns out to be $E=E_1'+\frac{1}{2}E_1-\frac{1}{2}E_T=0.42$ ev for $Zn_{0.5}Cd_{0.5}S$:Ag, Ni.

There is no direct experimental evidence for the energy of the lowest unoccupied state of the killer centers in $Zn_{0.5}Cd_{0.5}S$:Ag, Ni. Hill and Klasens[9] report a reflection minimum at 1.74 ev in ZnS:Ag, CO, and Melamed[7] reports quenching peaks at 1.58 ev for ZnS:Cu, Ni and at 1.5 ev for $Zn_{0.9}Cd_{0.1}S$:Ag, Co, therefore it is concluded that the killer center in Fig. 4 is of the order of magnitude of 1.5 ev above the filled band.

CONCLUSION

From a general theoretical treatment of the marked dependence of luminescent efficiency of sulfide phosphors on excitation intensity, it is concluded that the killer centers are normally unoccupied and that the metastable emitting states and electron traps play an important part in this phenomenon.

[6] J. C. Slater, Phys. Rev. **76**, 1592 (1949).
[7] N. T. Melamed, J. Electrochem. Soc. **97**, 33 (1950).
[8] J. W. Strange and S. T. Henderson, Proc. Phys. Soc. (London) **58**, 369 (1946).
[9] C. G. A. Hill and H. A. Klasens, J. Electrochem. Soc. **96**, 275 (1949).

Lens Centering in Microscope Objectives*

GLENN WOOTERS
Bausch and Lomb Optical Company, Rochester, New York
(Received March 30, 1950)

When a lens is decentered in a microscope objective the most noticeable defect is coma in the center of the field. A method is given for computing the central coma by using the transfer coefficients of M'Aulay and Cruickshank. The results for a typical microscope are given and the experimental means of verification are described.

A MICROSCOPE objective with an eccentric or tilted lens will produce an unsymmetrical image in the center of the field. The lack of symmetry on the axis appears the same as off-axis coma and to distinguish it from off-axis coma which may be inherent in the design, we will call it central coma. Other aberrations also arise from eccentric or tilted lenses. Among them are distortion, astigmatism, and lateral chromatic aberration. The general cases have been well covered.[1] In microscope objectives, however, central coma is the first aberration to be shown by eccentric or tilted elements.

Central coma can be apparent when a lens element is decentered only a few microns. This means that proper alignment is a serious problem in assembly of microscope objectives. This is not a new problem in manufacturing microscopes. In 1677 Father Cherubin[2] demonstrated the effects of defective centering. Many improvements have been made in centering and mounting lenses but the problem is still great. More microscope objectives are rejected for central coma than for any other single defect. In order to aid the production of microscope objectives, a study of lens centering in microscope objectives has been made.

Figure 1 shows how central coma can arise from a decentered surface. The single surface shown has a large amount of spherical aberration. When the entering beam is centered with reference to the surface, the upper and lower rays cross the axis as is shown by the full lines. Now, if the single surface is displaced, it is equivalent to displacing the entering beam of light as shown by the dashed lines. The ray nearest the axis will cross the axis just short of the paraxial focus. The upper ray is now farther from the axis so it will cross the axis closer to the surface. Similarly, the lower ray is closer to the axis so it will cross the axis farther from the surface. The upper, lower, and central rays of the beam no longer have a common intersection point after passing through the surface. The distance from the intersection of the marginal rays to the central ray is a measurement of the resulting coma.

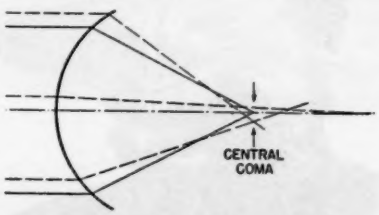

FIG. 1. A single surface with spherical aberration will show central coma when displaced laterally.

Figure 1 also shows that if the single surface had no spherical aberration no central coma would arise. The dashed lines would come to the same focus as the full lines. This suggests the general rule that the amount of central coma arising from a displaced surface is directly related to the spherical contribution of the surface. Also, a system with no spherical aberration will show no coma when displaced. It has been suggested at times that widely separated elements compensate one another for spherical aberration. Such suggestions have been made with microscope objectives and eyepieces, or with telescope objectives and lens erecting systems. If such a scheme were attempted, the alignment problems would be greatly magnified.

The data needed for establishing centering tolerances, and for determining which operation should be more closely controlled, ought to be in a convenient form. The effect of eccentric elements, untrue doublets, and tilted lenses was determined. The data could have been given as central coma arising from the tilt of a surface about its vertex. Such data would be difficult to combine, for example, to give the effect of a sideward shift of a doublet. The data was obtained as the central coma arising from the lateral shift of a single surface. Such a shift cannot be obtained experimentally, but the data can be used to predict any experimental change. The lateral shift of a surface is equal to the lateral shift of its center of curvature. The lateral shift

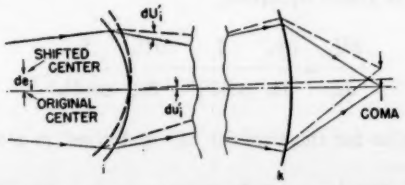

FIG. 2. Effect of displacing one surface laterally in a train of lenses.

* Presented at the Buffalo meeting of the Optical Society of America, October, 1949.

[1] L. Ivan Epstein, J. Opt. Soc. Am. 39, 847 (1949).

[2] Père Cherubin, "Vision Parfaite," II, pp. 25, 109 (1677).

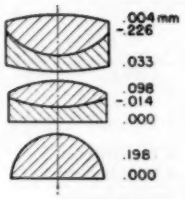

FIG. 3. Four-millimeter dry objective with effect of decentration indicated for each surface.

of a doublet would then cause central coma equal to the sum of the central coma given by shifting each surface, with due regard to sign. The method which was found to be the most convenient was developed from the transfer coefficients of M'Aulay and Cruickshank.[3] An additional advantage of the transfer coefficients was that other tolerances could also be computed.

The transfer coefficients express changes in the image space in terms of either an angle change, dU_i', of the ray in the system, or a displacement, dp_i, of the ray in the system. Now, if a surface, or more precisely, its center of curvature is displaced the differential distance de, then a marginal ray is changed only in the amount it is refracted at the surface. The displacement of the ray will be of the second order and can be neglected. The change in angle we will call dU'. The change in angle is the same as would result from displacing the ray instead of the surface, see Fig. 2. The displacement of a ray, however, is measured perpendicular to the ray while the displacement of a surface is measured perpendicular to the axis. The relationship between the displacement of the ray, dp, and the displacement of the surface is

$$\partial p/\partial e = -\cos U.$$

Thus

$$\frac{\partial U'}{\partial e} = \frac{\partial U'}{\partial p}\cdot\frac{\partial p}{\partial e} = -\cos U\frac{\partial U'}{\partial p}.$$

The effect upon the final angle and height of ray can then be written by using the transfer coefficients.

$$\frac{\partial U_k'}{\partial e_i} = \frac{\partial U_k'}{\partial U_i'}\cdot\frac{\partial U_i'}{\partial e_i}$$

$$\frac{\partial p_k'}{\partial e_i} = \frac{\partial p_k'}{\partial U_i'}\cdot\frac{\partial U_i'}{\partial e_i}.$$

The height of intersection of the marginal rays follows from the above equations.

$$\frac{\partial H_m}{\partial e_i} = \frac{\partial p_k'}{\partial e_i}\cdot\frac{1}{\cos U_k'} - \frac{\partial U_k'}{\partial e_i}\cdot\frac{S_k'}{\cos U_k'}.$$

The value for the paraxial ray is derived in a similar fashion

$$\frac{\partial H_{ax}}{\partial e_i} = \frac{\partial p_k'}{\partial e_i} - L_k'\frac{\partial u_k'}{\partial e_i}.$$

The central coma arising from a displacement of the ith surface can be found from the equation

$$\frac{\partial \text{ coma}}{\partial e_i} = \frac{\partial H_m}{\partial e_i} - \frac{\partial H_{ax}}{\partial e_i}.$$

A similar procedure can be used for finding the coma arising from tilting a plane surface.

The procedure for computing the central coma due to an eccentric or tilted element is straightforward. A marginal ray and paraxial ray are traced. The transfer coefficients are computed for both marginal and paraxial rays. The partial derivative of central coma with displacement of each surface is computed. Then, the effect of any decentered or tilted lens is found directly from the data.

The ordinary four millimeter, 0.65 numerical aperture, microscope objective can be used to illustrate the computation of central coma. Figure 3 shows construction and the partial derivative of central coma in the object space referred to the displacement of each surface. These values can be transferred to the image

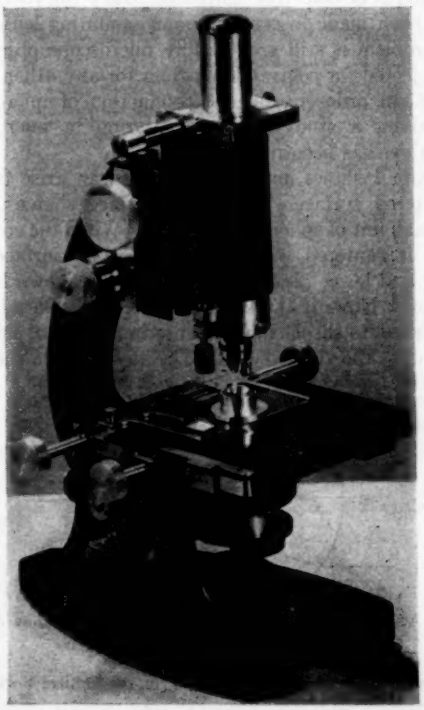

FIG. 4. Microscope used for experimental study of central coma.

[3] A. L. M'Aulay and F. D. Cruickshank, Proc. Phys. Soc. 57, 302 (1945); F. D. Cruickshank, Proc. Phys. Soc. 57, 350 (1945).

space by multiplying by 43, the magnification of the objective. The two plano surfaces have to be treated differently since a lateral displacement of a plano surface has no meaning. The plano surfaces can introduce central coma by being tilted. The data given in Fig. 3 plus the effect of tilting the two plano surfaces is sufficient to establish centering tolerances. The Rayleigh limit for sagittal coma[4] is $0.64\lambda/\sin U_M'$. The central coma which is found by the present method is tangential coma. Tangential coma is equal to three times the sagittal coma. The amount of central coma allowable in the 4 mm objective is 0.0015 mm. We can apply the information to the upper doublet and see how far it can be decentered. Adding the three partial derivatives and dividing into 0.0015 mm we get 0.008 mm. The upper doublet of the four millimeter can be decentered no more than eight microns and give a suitable image. In a similar fashion the effect of any centering or tilting error can be found. In all cases the allowable movements are extremely small.

The study of lens centering was undertaken to establish definite tolerances on each operation which affected centering. Such information clearly shows which operations must be done with greater accuracy. There would be little use in making investments to do a better job on some operation where only small returns could be expected. Thus, the study showed where better equipment could be used to advantage. In addition to the above expected gains there were some which were unexpected. One of these will be given as an example.

In computing the effect of tilting a lens the displacement of a surface is the displacement of its center of curvature. Generally, it will make a great difference as to what point the lens is rotated about. In the upper doublet of the four millimeter objective, the cemented surface contributed by far the greatest amount of central coma. If the lens is rotated about the center of curvature of the cemented surface, little central coma is introduced. The only amount which is introduced must come from the two rather insensitive surfaces. Should the lens be rotated about a point far removed from the center of curvature of the cemented surface, a large amount of central coma would be introduced. There must be with this doublet some point about which it can be rotated and introduce no central coma. The point is easily found. The partial derivatives can be considered analogous to forces perpendicular to the axis and acting at the centers of curvature. The point at which these forces would have no moment is the point about which the lens can be rotated a small amount without introducing central coma. This point for the top doublet of the 4 mm objective is 0.32 mm above the vertex of the crown air surface. This means, that if the bearing surface of the lens cell is about this point, a small tilt of the cell will produce no central coma. A tilt of the cell can easily take place in assembly through a burr on the cell or a small particle of dirt. The lenses of the four millimeter objective can be mounted in cells so that a small tip of any cell will introduce no central coma.

Again the relation between central coma and spherical aberration can be shown. If a lens has no spherical aberration, the partial derivatives will add to zero, since a small displacement of the lens would introduce no central coma. Such a lens would, most likely, introduce central coma if it were tilted. Since the partial derivatives would add to zero there would be no point about which the lens could be rotated and introduce no central coma. There is such a point for any lens with spherical aberration.

An experimental study was made to verify the computations. Figure 4 is a photograph of the altered microscope. The stage can be tilted, the objective tilted, and the eyepiece displaced. In the photograph the objective is a 4 mm objective. The upper doublet is attached to the body tube while the hemisphere and other doublet are resting on the stage. The movement of the stage is equivalent to moving the upper doublet alone. This movement was measured with a micrometer eyepiece. The star slide used was prepared by depositing a small amount of magnesium oxide on a slide (by holding over a burning magnesium ribbon) and then evaporating aluminum onto the slide. The photographs of the star images verified the computational work. The photographs were similar to those already published.[4,5] In addition to star images, pictures were taken of diatoms. Central coma corresponding to several Rayleigh limits did not seem to affect adversely the resolving power. Central coma was most noticeable in that the contrast was reduced.

[4] R. Kingslake, Proc. Phys. Soc. **61**, 147 (1948).

[5] L. C. Martin, Trans. Opt. Soc. **24**, 1 (1922–3).

Measurement of Photographic Transmission Density*

K. S. WEAVER
Kodak Research Laboratories, Eastman Kodak Company, Rochester, New York
(Received April 13, 1950)

This investigation was carried out in 1943 and 1944 and was undertaken primarily to determine the relation between the sphere and pot-opal types of densitometers, and the factors which affect their reproducibility from specifications, preliminary to the formulation of an American Standard specification for the measurement of photographic transmission density.

The two sources of error which have been given the greatest consideration are the directional variation in the luminance of the sphere or opal glass used to illuminate the test sample, and the "build-up" of the luminance of the illuminator by light reflected back from the test sample.

The net difference between the pot-opal and sphere densitometers was found to be about 0.04 at low densities, decreasing to about 0.01 to 0.02 at high densities.

The differences in density as measured by the sphere and the pot-opal densitometers were determined by computations based on the optical properties of the instruments and the test materials, with final checks by direct measurement. The differences between the pot-opal and sphere densities determined by these two methods agree within about 0.005 between 0 and 2.0, and within about 0.01 from 2.0 to 3.0.

It is concluded that the inherent difference between the sphere and pot-opal densitometers is small and that either can be readily reproduced from specifications.

I. INTRODUCTION

ALTHOUGH more than fifty years have passed since Hurter and Driffield laid the foundations of photographic science by their fundamental researches on the chemistry and sensitometry of the silver emulsion, at the time this work was undertaken, there was still no generally accepted standard method of measuring density.

The gradient ratio method of speed determination had been adopted as standard by the American Standards Association. The unit of intensity of radiation used in photographic sensitometry had also been standardized by the International Congress of Photography. It seemed very desirable, therefore, that a standard method or methods of measuring density be adopted. The present communication, which is primarily concerned with the visual pot-opal and integrating-sphere types of densitometer, is intended to cover some of the important questions upon which the choice of standard methods of measuring density depends.

Hurter and Driffield,[1] at an early point in their photographic researches, discovered the fundamental importance of the density concept.

They defined optical density as

$$D=\log_{10}(1/T),$$

in which D is the density and T is the transmittance of a photographic negative. This expression is of general application; no restriction is placed on the way in which the photographic material is illuminated or on the way in which the transmitted light is measured. Hence, for any value of T resulting from measurements made under specified conditions there will be a corresponding value of D, as determined by this equation.

It soon became evident that density depends to a very important degree upon the type of instrument used in its measurement. The result was an extended controversy between Hurter and Driffield[2–6] on the one hand, and Abney[7–10] on the other, regarding the relative merits of their photometers. Hurter and Driffield's photometer was so arranged that very little of the light scattered by the silver deposit was collected at the grease spot which formed their comparison field. Abney placed his densities in contact with a diffusing material, first paper and later opal glass, with the result that his measurement depended to a large extent upon the scattered light. The densities measured by Abney were much lower than those measured by Hurter and Driffield.

Hurter and Driffield correctly pointed out that interreflection between the density and the diffuser in the Abney photometer would reduce the observed density, but they did not at once realize that the loss of scattered light in their photometer was responsible for most of the discrepancy. Both Hurter and Driffield and Abney checked the densities by photographic printing methods. These tests convinced Abney that the lower values found with his photometer were correct, but led Hurter and Driffield to point out that the effective density of a negative depends to a large extent upon the geometrical arrangement of the printing apparatus and that under certain conditions the higher densities were more nearly correct.

In 1909, Callier[11] investigated the effect of scattered light on density. He used a Martens densitometer and measured the densities, first in contact with an opal glass and then with the diffusing glass at some distance

* Communication No. 1339 from the Kodak Research Laboratories.

[1] F. Hurter and V. C. Driffield, J. Soc. Chem. Ind. **9**, 455 (1890).

[2] See reference 1, p. 725.

[3] F. Hurter and V. C. Driffield, J. Soc. Chem. Ind. **10**, 20 (1891).

[4] F. Hurter and V. C. Driffield, J. Soc. Chem. Ind. **10**, 98 (1891).

[5] F. Hurter and V. C. Driffield, J. Soc. Chem. Ind. **10**, 100 (1891).

[6] F. Hurter, J. Soc. Chem. Ind. **10**, 318 (1891).

[7] W. deW. Abney, Phot. J. **11**, 38 (1887).

[8] W. deW. Abney, Phot. J. **13**, 2 (1888).

[9] W. deW. Abney, J. Soc. Chem. Ind. **9**, 722 (1890).

[10] W. deW. Abney, J. Soc. Chem. Ind. **10**, 18 (1891).

[11] A. Callier, Phot. J. **49**, 200 (1909).

from the film, so that most of the scattered light was lost. The first measurement he designated by the symbol $D\#$, for diffuse density, and the second by $D\|$, for specular density. He showed that for each photographic material tested the ratio, $D\|/D\#$, was approximately constant. He called this ratio "Q" and it has become known as the Callier Q factor. The important implication of Callier's work, in its application to densitometry, lies in its demonstration that the amount of light scattered by a photographic silver deposit is far from small. In fact, a coarse-grained material of high density may scatter nearly all of the light transmitted.

Although it was realized that no single method of measuring density could be applicable to all photographic printing processes, the trend in standardization in the years following Callier's work was toward a method which simulated contact printing. The trend was influenced partly by the obvious importance of the contact method of making positives and partly because the measurement of diffuse density appeared to be more reliable and convenient than the measurement of specular density. This led to the development by many different workers of opal-glass densitometers in which the density was measured in contact with an opal glass illuminated by a suitable source.[12]

The earlier forms of these instruments were visual. Later, as better photo-tubes became available, several photoelectric pot-opal densitometers were constructed.[13] At the time this study was started, the various pot-opal instruments had shown some differences in their measurement of density, but they had been found generally satisfactory, and although no precise specification of the optical constants of the opal glass had been made, they were the most widely used.

The arrangement of density and opal glass in the opal densitometer is very similar to the arrangement of negative and positive material in contact printing. There are, however, certain fundamental differences between the two which lead to differences in effective density.

These had been studied by several investigators,[14] with the hope that a simple relation between them might be found. The results of these comparisons show considerable variation, and it is uncertain to what extent the differences between the photographically determined densities and those determined by the opal densitometers were due to differences in the various densitometers and to what extent they were due to variations in the photographic methods.

Koerner and Tuttle[15] made a comparative study of densities determined by the pot-opal method, by a precision contact printing optical system and by a certain arrangement of a sphere densitometer in which a barrier-layer cell was used as the measuring device.

Later,[16] they proposed the use of a visual integrating-sphere photometer as a standard method of measuring diffuse density, listing the factors which are of importance in the complete specification of such an instrument. The numerical values were left for future determination. The sphere densitometer was adopted in 1938 as recommended practice by the Society of Motion Picture Engineers.

Since the measurement of diffuse density has come to have a predominantly important place in sensitometry, it seemed desirable to examine further the performance of the opal-glass and integrating-sphere densitometers. Although we shall here deal primarily with visual densitometers, much of the material will be found equally applicable to photographic or photoelectric methods.

II. CAUSES OF VARIATIONS IN THE VALUE OF DENSITY

In this section the most important factors which affect the measurement of density are reviewed. While most of the present work concerns the first two topics, scattered light and interreflection, the others are discussed briefly in order to give a more complete idea of the whole problem.

A. Light Scattered by the Silver Deposit

Scattered light is important because the way in which the light, transmitted by the photographic deposit in different directions, is collected and evaluated may affect the measured density to a very marked degree. This is potentially the greatest source of variation.

B. Interreflection

When the test density is in contact with the diffuser as it is in the pot-opal type of densitometer, the light reflected back to the opal glass by the photographic material results in an appreciable increase in luminance of the opal glass and hence in a lower value of density. This effect is greatest in the measurement of low densities and decreases to a nearly constant value at densities above 1.0.

C. Cover Glass Used in Contact Printing

In contact printing from a negative film, a cover glass is required to hold the negative in contact with the positive material. The cover glass causes an increase in the effective density of the negative amounting to about 0.02. It would be quite possible to duplicate this optical element in the pot-opal densitometer, but since the effect is small it has not been considered necessary.

[12] L. A. Jones, J. Opt. Soc. Am. **7**, 231 (1923).
[13] F. C. Toy, J. Sci. Inst. **7**, 252 (1930).
[14] F. C. Toy, Phot. J. **49**, 164 (1925). M. H. Sweet, J. Phot. Soc. Am. **7**, 126, 176 (1941); J. Opt. Soc. Am. **33**, 143 (1943).
[15] A. M. Koerner and Clifton Tuttle, J. Opt. Soc. Am. **27**, 241 (1937).
[16] Clifton Tuttle and A. M. Koerner, J. Soc. Mot. Pict. Eng. **29**, 622 (1937).

D. Diffuse Illumination with Diffuse Collection

Another factor which may have a considerable influence on the effective density of a negative material is the diffusion of the light which occurs in certain kinds of contact-printing boxes. In this case, the negative is, in effect, between two diffuse elements, the illuminated box and the positive paper. Koerner and Tuttle[16] have shown, for a sample of positive film, that when illuminated by a narrow beam, the density increases as the angle of incidence is increased (measurements cover the range 0 to 60 degrees) and that the increase can be estimated by computing, from the refractive index of the emulsion, the light path for oblique incidence and from this the increase in density due to the increased light path by applying Beer's law, which states that "the density should be directly proportional to the length of path."

Tuttle[17] has also described an experimental study of the effect of contact printing with diffuse light obtained from an opal cover glass. The increase in the contrast of the negative was ascribed to interreflection.

Similarly, increase in average light-path accounts for the change in the distribution of relative luminance of a piece of opal glass when illuminated from behind and observed through a photographic density, as reported by Bull and Cartwright[18] and by Selwyn and Pitt.[19]

An examination of a number of contact printers used in present-day commercial photo-finishing indicates that in most cases the illumination is very nearly specular. Consequently, the type of densitometer which measures diffuse density under normal illumination may be considered to represent the prevailing practice quite well in this respect. This type of densitometer may also be considered to represent fairly well the arrangement in many projection printers, in which the negative is backed by a diffusing glass while the lens collects light over only a small angle as viewed from any point on the negative.

E. Reversal of the Test Specimen

It is customary in measuring diffuse density to turn the emulsion side of the film toward the diffuser; in the case of the opal densitometer, the emulsion is in contact with the opal glass, corresponding to the way the negative is placed in contact printing. Koerner and Tuttle[15] have determined the effect of reversing the film in both the sphere and opal densitometers. They found a small increase in density when the base side of the film was turned toward the diffuser; an increase in the measured density of about 0.03 at a density of 2.0, and an increase of lower value at lower densities. In projection printers in which a diffusing glass is placed in back of the negative, the usual arrangement is reversed, since the emulsion side of the negative must be turned toward the lens.

[17] Clifton Tuttle, J. Opt. Soc. Am. **24**, 272 (1934).
[18] A. J. Bull and H. M. Cartwright, J. Sci. Inst. **1**, 74 (1923–24).
[19] E. W. H. Selwyn and F. H. G. Pitt, Phot. J. **77**, 397 (1937).

F. Spectral Selectivity

Finally, the effective density will depend upon the spectral selectivity of the material being measured. The films selected for test in this study are all slightly selective in their transmission. The densities will therefore depend upon the energy distribution of the light source used, on the selective transmission of the optical components of the densitometer or printer, and upon the spectral-response characteristics of the receiving element whether it is the eye, a photo-tube, or a positive photographic material.

In the comparison of the sphere and pot-opal densitometers to be described, check computations indicated a density difference of about 0.001 due to their differences in spectral selectivity.

In view of the many factors which may alter the effective value of a photographic density in printing processes, it is obviously impossible to set up any system of densitometry which will directly measure contact-printing density, since this itself is subject to so many variables. Hence, the pot-opal densitometer, or the sphere densitometer which has been given more recent consideration represents about as satisfactory a compromise with photographic requirements as can be achieved in a reasonably simple apparatus. In using these instruments, it has been the practice to omit the cover glass, to use either diffuse illumination with narrow angle collection or its approximate equivalent, narrow angle illumination with diffuse collection, and to turn the film with the emulsion side toward the diffuser. Further, any effect of spectral selectivity has generally been kept within small limits by the fact that tungsten lamps, radiating throughout the visible spectrum, have been used as the light source, and the selective transmissions of the opal-glass and sphere illuminators are comparatively small.

In comparing visual and photoelectric instruments, the inherent differences between the spectral response of the eye and that of photo-tubes is a source of error that is not easily eliminated. However, the use of suitable filters in connection with the photoelectric densitometers can be considered a fairly satisfactory solution to this problem, although the filter factor will depend to a certain extent upon the kind of film being tested.

III. THE REVERSIBILITY PRINCIPLE

Applied to Densitometry

A comparison of densitometers and photographic printers shows that in many cases the geometrical arrangements are similar, except that in one apparatus the negative is illuminated by a diffuser and the light is accepted from the negative through a narrow cone angle, while in other apparatus the negative is illuminated normally and the transmitted light is collectde or partially collected by a diffuse element which more or less completely accounts for all of the scattered light

as well as that directly transmitted. When considered from the point of view of the principle of the reversibility of path of a ray in an optical system, we may expect that the effective densities of a photographic negative in such systems will be approximately the same. For example, the sphere densitometer has often been so arranged that the sphere collects the light transmitted by the test density while under normal illumination, the value of the density being determined by measuring the luminance of the sphere through a second aperture. In the alternative arrangement, the sphere is illuminated by projecting a beam of light into it (the projector now replacing the photometer) and the test density is placed over the aperture through which the luminance of the sphere is observed. In the first arrangement, the criterion for correct integration is that measurement of the transmitted light shall be independent of the direction in which it leaves the film, and in the second, the criterion is that the test aperture shall have the same luminance viewed from any direction. In the present work, the sphere will be used in the second way, and the completeness with which the light transmitted by the density is integrated will be estimated from measurements of the luminance of the test aperture.

IV. DEFINITION OF TOTALLY DIFFUSE DENSITY

It is desirable to introduce here a definition of "totally diffuse visual density" to be used as a standard of comparison in describing the work which follows.

For our purpose, "totally diffuse visual density" is defined as the negative logarithm to the base ten of the transmittance, the light being incident normally on the base side of the test density, all of the transmitted light being collected and *equally measured*.

This definition corresponds to the density which would be measured by a sphere densitometer in which the response to the transmitted light is independent of the direction of emergence from the density, or reciprocally, to the density which would be measured by a sphere densitometer, the sphere acting as illuminator of uniform luminance, and in which the angle of observation is limited to a narrow cone normal to the surface of the test density.

Koerner and Tuttle[15] have shown on theoretical grounds, as well as experimentally, that the specification of normal illumination is sufficiently well met if the extreme rays are at an angle not greater than 10 degrees from the normal. In the present work, this condition has been met in all the measurements of diffuse density.

V. ESTIMATION OF ERROR CAUSED BY SCATTERED LIGHT FROM THE TEST SAMPLE AND INCOMPLETE DIFFUSION OF THE ILLUMINATION

A. Data Required

Correction is required because the luminance of illuminators used in densitometers will, in most cases, show some falling off at angles away from the normal. As a result, the measurement of light scattered by the silver deposit will not be entirely independent of the direction in which it is transmitted. To estimate the error in the density determination due to this cause, it is necessary to determine the polar distribution of the scattered light and the luminance variation of the illuminator. From these two sets of data the density correction can be computed.

B. Polar Distribution of Light Transmitted by a Photographic Density

1. Relative Polar Distribution of Scattered Light

The relations which are to be taken up next may be illustrated by a graph such as Fig. 1. If a photographic density is illuminated by a narrow beam of light concentrated within a few degrees of the normal to its surface, and the transmitted light is collected by a receiver, such as an integrating sphere, in such a way as to include spherical zones of various magnitudes from 0 to $\pi/2$, the density and transmission plotted against the half-angle θ subtended by the spherical zones will form a curve indicated by the symbol ⊙. The circular angle θ is measured along the axis of abscissas and the ordinates are transmissions in logarithmic units, and the corresponding densities in arithmetical units.

Define D_d = diffuse density†
D_s = specular density.
Then $D_{0°} = D_s$ and $D_{90°} = D_d$.

Data of this kind have been published by Tuttle[17] and McFarlane[20] and by Boutry[21] for part of the angular region from 0 to 90 degrees. Tuttle and McFarlane used a photo-tube with a 1-in. window and varied the cone angle of collection from about 20 to 90 degrees by varying the distance between the window and the density. Boutry collected the transmitted light by means of a lens of variable aperture and in this way made observations from 0 to 70 degrees. These were supplemented by a density measurement using an opal glass in contact with the film, thus obtaining nearly complete collection. The value obtained in this way was used to continue the curve between 70° and 90°. Bull and Cartwright[22] estimated the amount of light scattered by two photographic densities. They arranged two integrating spheres in tandem; the scattered light was received by the first sphere and the unscattered light passed through the apertures at the point of

† Callier used $D\|$ and $D\#$ to designate specular density and diffuse density, respectively. In more recent usage, the symbols D_s and D_d seem to be preferred, and they will be used in the remainder of this report.

[20] Clifton Tuttle and J. W. McFarlane, J. Soc. Mot. Pict. Eng. 15, 345 (1930).

[21] G. A. Boutry, "Sur la Definition et la Mésure des Densités Photographiques," IX^e Congrès International de Photographie, Paris, p. 484 (1935).

[22] A. J. Bull and H. M. Cartwright, Phot. J. 65, 177 (1925).

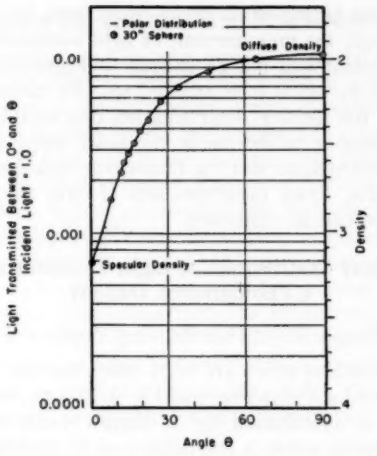

FIG. 1. Chart shows the relation between the transmission, T_θ, and the density, D_θ, for angles from 0 to 90 degrees. At zero degrees, D_θ becomes D_s, the specular density, and at 90 degrees it becomes D_d, the diffuse density.

tangency of the spheres into the second, and was measured there. They found that scattered light amounted to 7.1 percent for one sample having a density of 0.08, and 13.8 percent for the second sample having a density of 0.95.

The fraction of the transmitted light for any angular zone θ_1 to θ_2 can be computed from a curve of this kind. Such a computation requires the determination of a density or transmission difference, small errors in which may lead to relatively large errors in the estimation of the light flux in a small interval, θ_1 to θ_2. It is preferable to use a more direct method in the determination of the light flux in small angular intervals.

For this purpose, polar curves were taken of the intensity of the transmitted flux while the sample was illuminated normally with a collimated beam of light. Data of this kind are taken on the goniophotometer. The sample is held perpendicular to the axis of the collimated beam of light. The sample and illuminator are moved together around a vertical axis, the position being indicated by a graduated circle. The transmitted light is received by a photo-tube at a fixed position. Readings were taken at angles from about 2 to 85 degrees. A barrier-layer cell fitted with a green filter to approximate the sensitivity of the eye was used in part of the measurements. Some measurements of intensity at angles near 90 degrees, on films of high density or at other angles with very small apertures, were made using an RCA 929 cell and an *FP*54 amplifier.

The relative amount of light per unit circular angle is derived from the intensity‡ measured at a given angle by multiplying by the sine of the angle. Figure 2 is a curve representing the distribution of the scattered light transmitted by a piece of negative film. The amount of light scattered in an angular region such as that from 20 to 25 degrees is proportional to the area under the curve within these limits.

Since the sine of zero degrees is equal to zero, the ordinate will be zero at zero degrees. This fact is of help in drawing in the curve. However, in measuring the distribution of light for low densities, in which the scattered light is largely concentrated at small angles, difficulty is found in taking measurements sufficiently close to the axis and with sufficiently small apertures actually to determine the maximum of the distribution curve. This difficulty is more apparent than real, since in the final calculation of the diffusion errors the correction for such densities is so small that no important uncertainty results from this factor.

In Fig. 1 the solid line shows the relation between the density and the angle θ over which the light is collected determined from the goniophotometric data. The circles show the densities and transmittances measured directly by varying the solid angle subtended at the sample by the sphere illuminator. Figure 2 as shown represents only the relative distribution of scattered light. The absolute scale of ordinates is found by computation from the diffuse and specular densities measured independently.

The diffuse densities in the present work were measured on the sphere densitometer described later, and the specular densities on the photoelectric apparatus which will be the subject of the next section.

2. *Measurement of Specular Density*

An accurate determination of specular density is difficult. Although light is scattered by a photographic deposit over the whole anterior hemisphere, it is largely concentrated near the direction of emergence of the directly transmitted light and it is therefore necessary

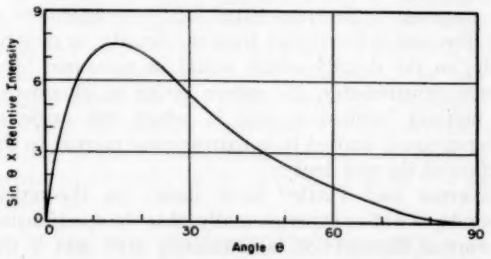

FIG. 2. Plot of galvanometer readings after multiplication by sine θ against θ. Curve represents relative distribution of the transmitted light which is scattered. Negative film of diffuse density, 2.

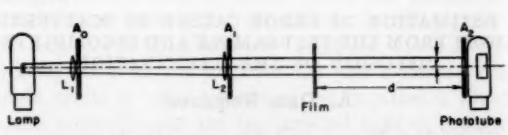

FIG. 3. Arrangement of apparatus used in measuring specular density.

‡ Intensity as used here is equivalent to "candlepower" as applied to ordinary light sources.

TABLE I. Average light distribution by 5-degree zones.

Zone	Density 0.100	0.200	0.400	0.600	0.800	1.000	1.200	1.400	1.600	1.800	2.000	2.200	2.400	2.600	2.800	3.000
0– 5[a]	0.879	0.702	0.441	0.289	0.204	0.151	0.115	0.091	0.072	0.058	0.046	0.037	0.031	0.026	0.023	0.020
0– 5[b]	0.049	0.098	0.155	0.154	0.135	0.114	0.095	0.079	0.067	0.058	0.052	0.047	0.042	0.038	0.034	0.030
0– 5[c]	0.928	0.800	0.596	0.443	0.339	0.265	0.210	0.170	0.139	0.116	0.098	0.084	0.073	0.064	0.057	0.050
5–10	0.032	0.081	0.142	0.168	0.170	0.163	0.148	0.134	0.123	0.111	0.102	0.094	0.087	0.081	0.075	0.070
10–15	0.015	0.047	0.092	0.123	0.140	0.144	0.143	0.136	0.129	0.122	0.117	0.112	0.108	0.103	0.098	0.094
15–20	0.009	0.025	0.056	0.080	0.098	0.111	0.118	0.121	0.121	0.119	0.116	0.114	0.111	0.109	0.106	0.104
20–25	0.005	0.015	0.035	0.053	0.068	0.082	0.092	0.099	0.104	0.106	0.107	0.107	0.108	0.108	0.107	0.107
25–30	0.004	0.009	0.022	0.036	0.049	0.060	0.071	0.080	0.087	0.091	0.094	0.096	0.098	0.100	0.101	0.102
30–35	0.002	0.006	0.016	0.026	0.036	0.045	0.054	0.063	0.070	0.075	0.079	0.083	0.086	0.090	0.092	0.094
35–40	0.002	0.005	0.011	0.019	0.027	0.034	0.042	0.049	0.056	0.061	0.066	0.070	0.074	0.077	0.080	0.084
40–45	0.001	0.004	0.008	0.014	0.020	0.027	0.033	0.039	0.045	0.050	0.055	0.059	0.062	0.065	0.069	0.072
45–50	0.001	0.003	0.007	0.011	0.015	0.020	0.026	0.031	0.036	0.041	0.045	0.048	0.052	0.055	0.057	0.060
50–55	0.001	0.002	0.005	0.008	0.012	0.015	0.020	0.024	0.029	0.033	0.036	0.039	0.042	0.044	0.047	0.049
55–60	0.001	0.002	0.004	0.006	0.009	0.012	0.015	0.018	0.022	0.026	0.029	0.031	0.033	0.035	0.036	0.037
60–65	0.001	0.001	0.003	0.005	0.007	0.009	0.011	0.013	0.012	0.020	0.022	0.024	0.025	0.026	0.027	0.028
65–70	0.000	0.001	0.002	0.003	0.005	0.006	0.008	0.010	0.011	0.014	0.016	0.017	0.018	0.019	0.020	0.021
70–75	0.000	0.001	0.001	0.002	0.003	0.004	0.005	0.007	0.008	0.009	0.010	0.011	0.012	0.013	0.014	0.015
75–80	0.000	0.000	0.001	0.001	0.002	0.003	0.003	0.004	0.005	0.005	0.006	0.006	0.007	0.007	0.008	0.008
80–85	0.000	0.000	0.000	0.001	0.001	0.001	0.002	0.002	0.002	0.002	0.003	0.003	0.003	0.003	0.004	0.004
85–90	0.000	0.000	0.000	0.000	0.000	0.000	0.000	0.000	0.001	0.001	0.001	0.001	0.001	0.001	0.001	0.001

[a] Unscattered.
[b] Scattered.
[c] Total (0 to 5 degrees).

to use a very small angle of collection in order to approximate the true specular density.

The apparatus used is shown in Fig. 3. A lens, L_1, images the lamp filament on L_2; L_2 images the aperture, A_0, at A_2; A_1 and A_2 have the same diameter, 1.3 cm, and the diameter of A_0 is so chosen that its image at A_2 is 1.3 cm in diameter. The density is placed at various distances, d, between A_1 and A_2 and is large enough to cover the light beam completely. The only area of the density which is illuminated is that required to transmit the unscattered light. The specularly transmitted light will fall upon the cell, together with the light scattered within the angle, $\pm r/d$.

The photo-tube was an RCA 929 combined with a Kodak Wratten No. 16 Filter. This combination is not sensitive over the whole visible spectrum, but the response for the tungsten light which was used is fairly well centered within the visual range. The densities were measured with this apparatus for angles of 0.28, 0.5, 1.0, 1.5, and 2.0 degrees. The observed densities were plotted against the angles and the curve was extrapolated to 0 degrees. The value so found was taken as the specular density, D_s.

3. *Calculation of Scattered Light as Fraction of the Total Transmitted*

In Fig. 1, the total transmitted light is represented by T_d and the specularly transmitted light by T_s. The fraction of T_d which is scattered will be called P and is given by

$$P=(T_d-T_s)/T_d=1-(T_s/T_d), \qquad (1)$$

from which is derived[23]

$$P=1-[1/\log_{10}^{-1}(D_s-D_d)]. \qquad (2)$$

[23] Toy (see reference 14, p. 294), in his analysis of the relation between specular and contact-printing density, has arrived at an expression equivalent to this. He used f to designate the fraction of the transmitted light which is scattered.

4. *Calculation of Polar Distribution of Transmitted Light*

The determination of the relative polar distribution of transmitted light has been described, and the result is represented by a curve, Fig. 2. This figure represents, to a scale as yet undetermined, the scattered light per unit circular angle. The whole area under the curve, when drawn to the correct scale, will be equal to P. The required adjustment of the scale of ordinates is made from a trial calculation of the area of Fig. 2, made by adding the ordinates for the mid-zone angle for each of eighteen 5-degree zones from 0 to 90 degrees, and then multiplying the eighteen ordinates by a factor which will reduce their sum to P.

Space does not permit presentation of all the distribution data used in the final determination of the average correction curves.

The average distribution data for the five kinds of film tested most completely are given in Table I. These

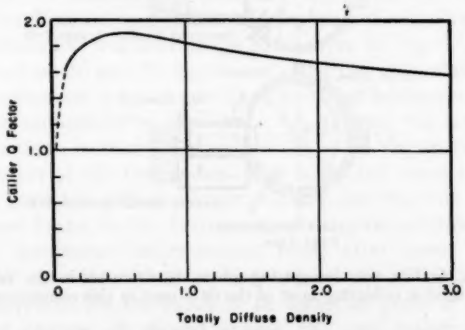

FIG. 4. Average relation between Callier Q factor and totally diffuse density for five test films.

data have been obtained by averaging and plotting the densities and distribution data and reading the final values from the curves at density intervals of 0.2.

In Fig. 4, the average Callier Q factors, corresponding to the data of Table I, are plotted as a function of the totally diffuse density. The five individual curves from which Fig. 4 was derived all have the same general shape. The curve has been extrapolated (by a dotted line) to 1.0 at a density of 0.03, representing the clear base.[24]

VI. SPHERE AND OPAL-GLASS DENSITOMETERS

A. The Sphere and Its Luminance Characteristics

The practical application of the photometric integrating sphere to a particular kind of measurement is not as simple as the elementary theory of the device would lead one to expect. In practice, the performance is complicated by the presence of many elements, such as screens, apertures, and test specimens which more or less interfere with the internal reflections. Further, the perfectly diffuse sphere coating assumed in certain mathematical investigations of the sphere is still to be discovered. Consequently, when high accuracy is required, recourse is generally had to some means of direct experimental check of the performance under the conditions of actual use.[25]

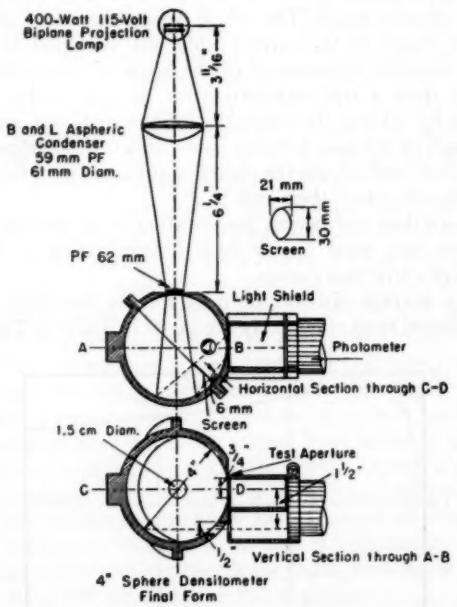

FIG. 5. The 4-in. integrating-sphere densitometer in the final form used in collecting most of the data used in this communication.

[24] A large number of photoelectrically determined Q factor curves may be found in a paper by J. G. Streiffert, J. Soc. Mot. Pict. Eng. **49**, 506 (1947).

[25] H. J. McNicolas, Bur. Stand. J. Research **1**, 35 (1928).

Since Ulbricht,[26] following the theoretical work of Sumpner,[27] demonstrated the usefulness of the sphere as a photometric integrator, an extensive literature on the subject has appeared; this has largely been concerned with the problem of determining or eliminating the errors found in specific applications.

Sharp and Millar[28] have described the use of the integrating sphere in general photometry. Of particular interest is their use of a translucent screen in place of an opaque one to shield the observation window from the direct light from the lamp or luminaire. Chaney and Clark[29] checked the performance of their sphere by the use of a narrow beam of light which, when directed at different points, indicated the irregularities in the integration characteristics and thus enabled them to make a suitable arrangement of screens and test lamps. They pointed out some difficulties that they found in the use of translucent screens and recommended opaque screens.

Karrer[30] has described a number of applications of the integrating sphere in the measurement of reflection and transmission. He shows one arrangement (his Fig. 7) in which the sphere serves as a diffuse illuminator. A Martens polarization photometer is used to compare the luminance of the sphere interior viewed directly with the luminance viewed through the sample. Since the light spot and the test aperture are adjacent, a very small (opaque) screen is used. The arrangement of the sphere adopted for the present work is similar in principle to that of Karrer.[30] Referring to Fig. 5, it is seen that the sphere is illuminated by a projected beam from a lamp and condenser system. The condenser is imaged on the sphere wall by a lens in order to reduce the spread of the light spot. A translucent screen of pot-opal glass, transmitting about 30 percent, was used. The translucent screen has nearly the same luminance as the sphere wall and is almost invisible when viewed through the test aperture.

Figure 5 represents the final form of sphere densitometer, after several variations had been tried in the preliminary experiments.

B. Size of Sphere

There is no good reason why a sphere of almost any size could not be used in the construction of a densitometer.

In general, two densitometers which are duplicates in all respects, except in the scale to which they are built, should give the same results. In order to obtain the same illumination in both, the lamp wattages would be proportional to the spherical areas. However,

[26] R. Ulbricht, Elektrotech. Zeits. **21**, 595 (1900).

[27] W. E. Sumpner, Phil. Mag. **35**, 81 (1893).

[28] C. H. Sharp and P. S. Millar, Trans. Illum. Eng. Soc. **3**, 502 (1908).

[29] N. K. Chaney and E. L. Clark, Trans. Illum. Eng. Soc. **10**, 1 (1915).

[30] E. Karrer, J. Opt. Soc. Am. **5**, 96 (1921).

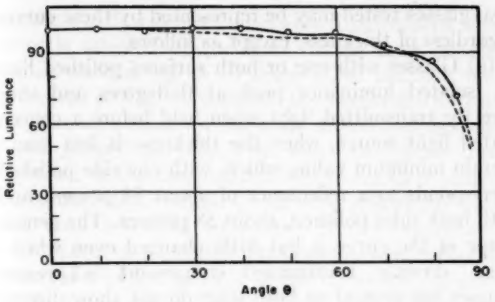

FIG. 6. Polar distribution of luminance of 4-in. sphere No. 1. - - - with nine percent screen and 1.0-cm illumination aperture. ——— with 29 percent screen and 1.5-cm illumination aperture. ○ with 29 percent screen and 1.5-cm illumination aperture, after one year.

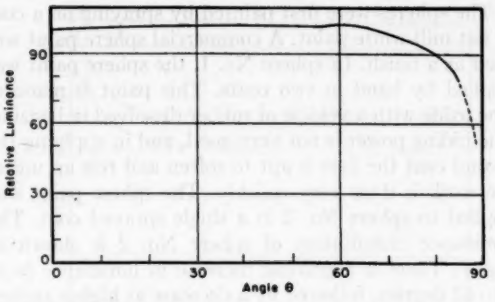

FIG. 7. Polar distribution of luminance of 4-in. sphere No. 2 suggesting incomplete paint coverage near 0 degrees.

certain practical considerations place maximum and minimum limits on the size of the sphere.

If a specified maximum density is to be read with a reasonably high precision, a fairly definite lower limit is placed on the required sphere luminance. If a very large sphere is used, an inconveniently large lamp may be required for its illumination. On the other hand, a very small sphere will necessarily have small apertures and difficulty might be experienced in adapting the sphere to a satisfactory photometer, either of the visual or the photoelectric type. Further, in order to minimize the effect of local variations in density, due to grain or imperfections, it is desirable to include an area of at least several square millimeters of the sample in the measurement.

All the measurements made up to the present time by the writer have been made with a 4-in. sphere, and a polarization photometer. The first set of measurements were made with a Schmidt and Haensch photometer, and later the sphere was modified to accommodate a Bausch and Lomb polarization photometer.

It is evident that the sphere densitometer used in this way is very similar to the pot-opal densitometer in many respects. In both instruments, the test density is illuminated with nearly completely diffused light. On the other hand, in this form of the sphere densitometer, the light reflected from the sample is so distributed that it has a negligible effect on the measurement. In the opal densitometer, the light reflected by the sample does not contribute to the luminance of the comparison side of the photometric field. Hence, it has an important effect on the measurement.

Many modifications of the sphere densitometer could probably be devised which would be just as satisfactory as the one described. A hemispherical illuminator is another possibility. In any arrangement of apparatus, a determination of the luminance distribution of the test aperture is the most significant check that can be made of the performance of the sphere as a diffuse illuminator.

Each of the several arrangements of the sphere which were used was checked for variations in the luminance of the test aperture throughout the whole hemisphere. Luminance measurements made at 10-degree intervals in azimuth around the diameter passing through the test aperture were averaged, giving curves of Figs. 6 and 7. The departure of these curves from unity at any angle is a measure of the extent to which, under normal illumination, light transmitted by the sample at that angle will be undervalued.

The test aperture in all cases had a diameter of $\frac{3}{4}$-in. This was large enough to clear both beams of the Schmidt and Haensch polarization photometer, with which the work was started. In the first arrangement of the sphere densitometer, the translucent screen was rather dense, having a transmission of nine percent, and the aperture through which the light was admitted to the sphere was 1 cm in diameter. The luminance distribution is shown by the dashed line of Fig. 6. After a few preliminary measurements of density had been made under these conditions, the illumination aperture was increased to 1.5-cm diameter and a screen of 29 percent transmission was used. A Bausch and Lomb polarization photometer then became available, and a second aperture was cut in the sphere to provide illumination of the comparison field, since the separation of the entrance apertures of this instrument was too great for observation through a single $\frac{3}{4}$-in. aperture. After these changes had been completed, the luminance distribution was that of the solid curve of Fig. 6. The dips near 50 and 70 degrees are caused by the enlarged illumination aperture and the comparison field aperture. The uniformity of luminance, in spite of the added apertures, is much improved owing to the higher transmission of the new screen. The computed corrections for imperfect diffusion are in this case less than one half those found in the first arrangement. A repetition of the luminance determination made after about one year gave the values represented by the circles. The differences are too small to be taken as proof of any real change. A second sphere (No. 2), which was intended to duplicate in all essential details the first sphere, was made in order to see how closely the performance could be determined by specification.

The spheres were first painted by spraying on a coat of flat mill-white paint. A commercial sphere paint was used as a finish. In sphere No. 1, the sphere paint was applied by hand in two coats. This paint is made of zinc oxide with a vehicle of rubber dissolved in benzine. The hiding power is not very good, and in applying the second coat the first is apt to soften and rub up unless the work is done very quickly. The sphere paint was applied to sphere No. 2 in a single sprayed coat. The luminance distribution of sphere No. 2 is shown in Fig. 7. There is a gradual increase in luminance from 0 to 62 degrees, followed by a decrease at higher angles. This is probably due to incomplete coverage at the lower angles; the luminance uniformity would probably be improved by a second coat of sphere paint. Some experiments have indicated that a much better paint can be made using titanium dioxide as the pigment. Such a paint has recently appeared on the market but was not available at the time these tests were made.

C. Opal Glasses and Their Luminance Characteristics

A large number of samples of pot-opal glass and a few pieces of flashed-opal glass have been tested. The measurements consisted of: (1) goniophotometric determination of relative luminance from 0 to 85 degrees, (2) measurement of reflectance for diffuse illumination and nearly normal observation, and (3) measurement of total transmission for collimated light incident normally.

The data obtained under (1) and (2) are used in calculating the errors in density measurement due to imperfect diffusion and interreflection, respectively. The transmission does not have any direct bearing on the value of density observed, but it does indicate the maximum density that can be read with a reasonably high photometric field luminance.

The results of a large number of tests on pot-opal glasses of various thicknesses and manufacture have been summarized in Figs. 8 and 9. Figure 8 shows the relative luminance by transmitted light of glasses having the emitting surface either polished or fine-ground with No. 904 emery. The data for all the cryolite opal glasses tested may be represented by these curves, regardless of thickness, except as follows.

(a) Glasses with one or both surfaces polished have an isolated luminance peak at 0 degrees and show directly transmitted light when held before a concentrated light source, when the thickness is less than a certain minimum value, which, with one side polished, corresponds to a reflectance of about 54 percent and, with both sides polished, about 58 percent. The general shape of the curve is but little changed even when a large, directly transmitted component is present. Glasses fine-ground on both sides do not show directly transmitted light, but the diffusion starts to decrease when the thickness is sufficiently reduced, the general shape of the luminance distribution curve being affected in this case. The thickness at which this occurs is rather indefinite, since the departure from maximum diffusion takes place very gradually. The corresponding reflectance is about 50 percent.

(b) The luminance distribution of the glasses with the fine-ground emitting surface varies slightly with the coarseness of the abrasive.

It would seem that for glasses of this general class, the distribution of transmitted light is almost entirely a function of the condition of the surface at which the light is emitted, once a certain degree of diffusion is attained in the internal illumination of that surface, either because of the presence of a sufficiently thick layer of diffusing glass behind it, or because of diffuse external illumination.

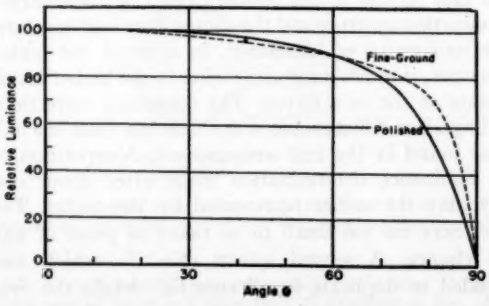

FIG. 8. Luminance distribution of polished and fine-ground pot-opal glasses of thickness sufficient to give maximum diffusion.

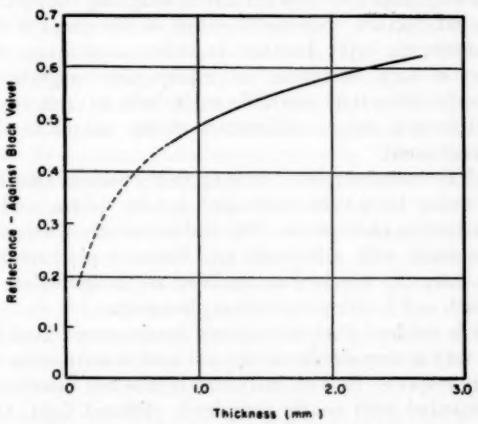

FIG. 9. Relation between reflectance and thickness of Monax glass.

Our experimental work on opal glasses confirms the conclusions of Selwyn and Pitt,[19] that: "It appears certain from the following experiments that a density close to its asymptotic value, so far as diffusion alone is concerned, is reached with a very small thickness of opal glass, and that the last stage in the reduction of the density reading is determined almost entirely by interreflection." Glasses of thickness sufficient to give

maximum diffusion have luminance distributions which are little affected by incidence of the light, whether normal, oblique (up to 60 degrees), or diffused. Since the curves of Fig. 8 represent the maximum diffusion that has been found in our tests of polished and fine-ground glasses, the data from which they were drawn were used in the computation of the errors in density due to imperfect diffusion, and only glasses for which these data are valid were used in the experimental densitometer on which the test densities were measured.

The most logical method of describing the complete-

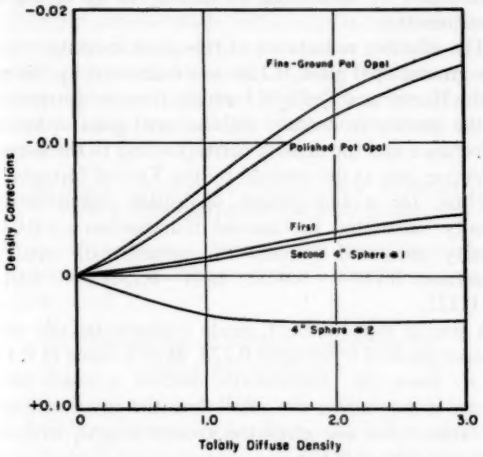

FIG. 10. Calculated density corrections required because of imperfect diffusion of some of the illuminators.

ness of the diffusion of opal glasses, by a single numerical value, is probably that devised by Halbertsma.[31] The Halbertsma diffusion power for the curves of Fig. 8 are 0.92 for the fine-ground glass and 0.91 for the polished glass. They may be computed most conveniently by averaging the twenty-five ordinates at the following angles:

8.1	28.0	40.4	51.9	64.9
14.2	30.7	42.7	54.3	68.0
18.4	33.2	45.0	56.8	71.6
22.0	35.7	47.3	59.3	75.8
25.1	38.1	49.6	62.0	81.9

In a densitometer, it is desirable to use an opal glass which has as high a transmission as possible, as long as diffusion is not sacrificed. At the same time, the glass should be thick enough for mechanical strength but not so thick that loss of light at the edges disturbs the luminance distribution over the area being used.

Monax glass was found to have about the characteristics desired. Figure 9 shows the relation between the reflectance and the thickness for the sample Monax used.§ This curve will be referred to later when the

[31] J. W. T. Walsh, *Photometry* (Constable, London, 1926), p. 118.

§ This glass appears to be unobtainable now, at least in the form of flat sheets, but other opal glasses are obtainable which show about the same characteristic relation between reflectance and thickness.

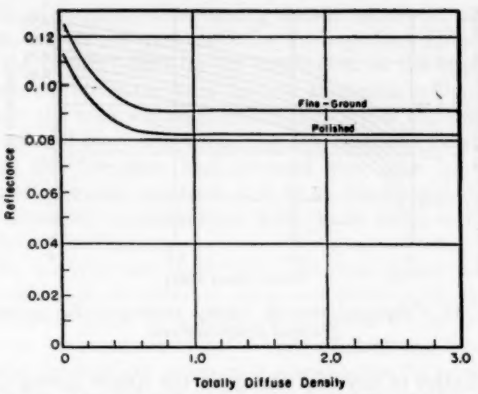

FIG. 11. Average reflectance of five films tested in contact with fine-ground and polished pot-opal glass as a function of totally diffuse density.

effect on density measurement of error in specified thickness is estimated. Opal-glass reflectance was measured with an integrating-sphere reflectometer of conventional design. The values obtained were total reflectance for normal incidence.

VII. ESTIMATION OF DENSITY CORRECTION REQUIRED BY REASON OF IMPERFECT DIFFUSION OF ILLUMINATORS

This correction is determined by considering the loss in the measured transmission in each of the eighteen 5-degree zones, for which the tabulation of the distribution of light transmitted by the average film of specified density is listed in Table I. The percentage of the total light in a zone is multiplied by the percent luminance deficiency of the illuminator (either sphere or opal glass) in that zone, and the sum of such products for the eighteen spherical zones gives the total percent by which the measured transmittance will be less than the correct value.

This method has been used to calculate the errors due to imperfect diffusion for the average data of Table I representing five kinds of film and for the following diffuse illuminations: polished pot-opal glass, fine-ground pot-opal glass, sphere No. 1 from first and second luminance determinations, and sphere No. 2. The final values are shown as curves in Fig. 10. Similar computations, made for the sphere in some phases of its development, have not been included in Fig. 10 since they were only of temporary interest.

The maximum density error (for densities up to 3.0) is found to be about 0.02 for the pot-opal glasses. The correction for the polished opal is slightly lower than for fine-ground glass because of the higher relative luminance of the polished glass between 0 and 60 degrees, which more than offsets the lower values beyond 60 degrees.

The maximum change with time in density correction for sphere No. 1 is about 0.001. This is too small to be

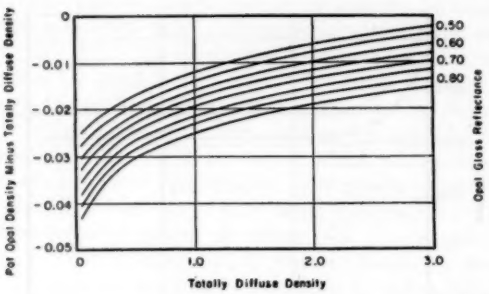

FIG. 12. Calculated over-all density corrections for polished pot-opal densitometers.

indicative of any real change in the sphere during the year which elapsed between the two determinations of luminance, and may be due to the experimental error in those determinations.

The corrections for sphere No. 2 are positive and are characterized by their rapid increase at low densities.

VIII. INTERREFLECTANCE CORRECTIONS

Hurter and Driffield[4, 5] showed that in the opal-glass densitometer the infinite series of reflections increased the luminance of the diffuser by the factor, $1/1-Rr$, in which R is the reflectance of the diffuser, and r is the reflectance of the test density. This formula has been used by Selwyn and Pitt[19] and in a modified but equivalent form by Tuttle and Koerner.[16]

This method of estimating the interreflection effect has been used in the present investigation, and the next section of this paper will deal with the determination of R and r.

A little consideration will show that this procedure involves assumptions which can be only approximately true. Nothing is stated about the distribution of the reflected light and the variation of R and r with the order of the reflection in the infinite number which occur. The results will further depend upon the method used in measuring R and r, and upon the extent to which the light reflected by the film contributes to the luminance of the illuminator in the direction of observation.

The whole matter could be disposed of very neatly if it were possible to determine the luminance distribution of the diffuse illuminator while in contact with the test density. If such data were available, the corrections for both imperfect diffusion and interreflection could be determined in one operation, using the method already described for the estimation of the error due to imperfect diffusion of the illuminator. No simple method of doing this seems possible at present.

A. Reflectance of Photographic Densities

In their estimation of the effect of interreflection on density measurement, Selwyn and Pitt[19] measured the total reflectance by the use of an integrating sphere. Since their results showed no regular variation in reflectance with density, they adopted the constant value of 0.11. Tuttle and Koerner[16] used an integrating sphere with which they measured the total reflectance for normally incident light.

In the present work, the reflectances were measured by placing the test density in contact with an opal glass and measuring the luminance increase on the surface on which the light was incident. The calibration factor was determined by measurements made on a piece of thin, clear glass, the effective reflectance of which was determined by measuring its density in an opal-glass densitometer.

The effective reflectance of this glass in contact with fine-ground opal glass, 0.125, was estimated by the use of the Hurter and Driffield formula, from measurements of the density in contact with an opal glass of known reflectance and the density corresponding to the normal reflection loss as determined by the Fresnel formula.

Thus, for a fine-ground opal-glass densitometer: density calculated for normal illumination $=+0.037$; density measured visually in contact with opal of reflectance $0.732=-0.0053$; $\log(1-0.732r')=-0.042$; $r'=0.127$.

A similar measurement, made photoelectrically with an opal glass of reflectance 0.774, gave a value of 0.124 for r'. Since the photoelectric method is much more precise in measuring the small densities involved here, the latter value was given the greater weight, with the final adoption of 0.125.

By a similar procedure, the reflectance of the standard glass for contact with polished opal-glass was found to be 0.113.

In measuring the reflectances by this method, very little difference was found for different kinds of film, and in no case were the differences significant in the final determination of density corrections; hence, the single set of data of Fig. 11 have been taken as representative of the five kinds of film used in these tests.

B. Reflectance with the Integrating Sphere

Light reflected from the test density has relatively less effect in the integrating-sphere densitometer than in the pot-opal type. In the pot-opal densitometer, the reflected light is confined to the area of the opal glass covered by the sample and does not contribute to the illumination of the comparison field. On the other hand, the light reflected from the sample into the integrating sphere is scattered over the whole area of the sphere and hence contributes relatively less to its illumination. When the comparison field of the photometer is illuminated by the same sphere through a second aperture, as in the present work, the effect of reflected light cancels out. Consequently, no corrections for reflectance have been made to the sphere densities reported here.

It is possible, in certain circumstances, for the light reflected into the sphere to have an important effect on the density observed. In the usual arrangement of a

photoelectric densitometer, the cell response first with and then without the test sample in place is measured in determining the density, and in this case the reflected light is added to only one of the two readings and hence is a factor in the measurement. Even in this case, the error is very small unless the area of the test aperture is a large fraction of the area of the sphere. The sphere used in this work is 4 in. in diameter and the test aperture is $\frac{3}{4}$ in. in diameter. Test show that in this case the light reflected from a piece of film, which has been fixed out without exposure, increased the sphere luminance by about 0.7 of one percent.

The aperture was made fairly large to facilitate some of the experimental work. For routine work, a much smaller aperture could be used and the reflectance error could easily be reduced to a negligible value, whether the measurement be made by simultaneous or successive comparison.

IX. ERRORS CAUSED BY IMPERFECT DIFFUSION AND INTERREFLECTION COMBINED

In the experimental check of the preceding analysis of densitometer performance, the following procedure has been used.

A. Correction of Sphere Densities for Imperfect Diffusion

The observed sphere densities were corrected to totally diffuse densities by subtracting the corrections taken from the appropriate curve of Fig. 10 for sphere No. 1. These corrections are about equal to the probable error in photometric observations taken under the best conditions and hence could have been neglected with some justification. However, since they depend upon a very definitely measurable departure of the sphere from perfect diffusion, they are significant and have been applied. In the cases of the sphere as used here, no corrections for interreflectance are required.

B. Combined Corrections for Opal-Glass Densitometer

The correction curves for the pot-opal densitometers have been calculated by combining the correction curves for imperfect diffusion of Fig. 10 with the interreflectance correction calculated from the Hurter and Driffield formula, for opal glasses based on assumed reflectances varying from 50 to 85 percent, Fig. 12.

The differences between the observed pot-opal densities and the corrected sphere densities are finally compared with the calculated correction curve for an opal glass of the proper reflectance, as determined in Section B.

X. EXPERIMENTAL DENSITOMETERS AND COMPARISON OF OBSERVED WITH CALCULATED DENSITIES

In the development of the sphere densitometer in the final form illustrated in Fig. 5, tests were made on a strip of negative film having sixteen steps. In each case, corrections were made for the imperfect diffusion of the incident light by the application of the appropriate correction curves of the type illustrated in Fig. 10. Later, the work was repeated in detail on four additional samples of black-and-white negative materials varying from the fine-grain high contrast slow type to the coarse-grain low contrast fast type. Next, opal-glass densitometer measurements were made using several different opal glasses.

In carrying out these tests, the opal glasses were mounted on an aperture plate and illuminated by a 1000-watt lamp at a distance of about 13 in. This simple arrangement is not a very efficient one in the use of the light. However, it is adequate for the present purpose. The Bausch and Lomb polarization photometer was mounted before the opal glass, the test samples being held in contact with the glass on the side toward the photometer. The illuminated area of the opal glass and the test sample were in all cases considerably larger than required to cover the field of view of the photometer, so that the densities observed may be considered as applying to infinitely extended areas. In densitometers which are required to measure the density of small areas surrounded by densities of lower value, it is at times necessary to use a small diaphragm, in order to keep light scattered between the two surfaces of the film from striking the density from behind and thus vitiating the measurement. Since such test samples are unsuited for use in standardization, the present arrangement has been adopted.

The results of tests on the five kinds of films for fine-ground and polished opal-glasses are shown in Fig. 13.

The differences between the average calculated and observed corrections are in all cases less than 0.01 and, except in the upper density range, compare favorably with the precision attainable in most photometric work.

The difference found between the calculated and observed corrections in the upper density range is probably real and may be the result of some of the approximations involved in the determination of the effective reflectance of the photographic materials.

It is possible that the greater spread of the observa-

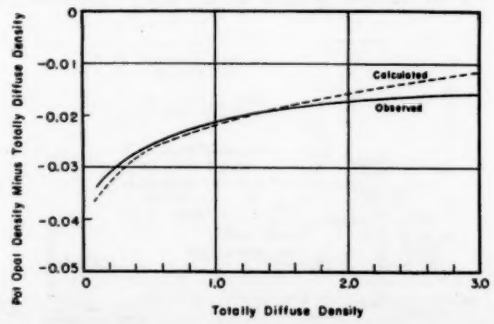

FIG. 13. Comparison of the calculated and observed correction curves for polished pot-opal glass.

tions for the high densities is due to small variations in the films; a variation of only one-third of one percent in the amount of silver deposited would account for a variation of 0.01 in a density of 3.0.

In view of the results of this analysis, it is not surprising that experience has shown that opal densitometers have, in general, agreed fairly well, although no complete specification of the necessary optical characteristics had previously been made. Where large discrepancies have been found, it would seem that the trouble is more likely to have been due to errors in the photometric equipment than to variations in opal glasses.

When this work was first started, all of the immediately available samples of opal glass that appeared to have possibilities as densitometer material were collected and the range of their reflectance determined. The range found, from 0.65 to 0.82, corresponds to a density difference of about 0.01. It would seem that with reasonable care in selection, no difficulty should be found in obtaining opal glasses of adequate uniformity.

XI. CONCLUSIONS

The work on the sphere densitometers described herein indicates that, with reasonable care in the mechanical details of construction and in painting the interior wall, it should be easy to duplicate the results obtained. While the detailed analysis of the luminance of the test aperture is necessary in a preliminary study of this kind, it should not be necessary to make such checks on each one of several spheres made from the same specification. The corrections required are so small that for practical purposes it may be said that a well-designed sphere densitometer can be used to determine directly American Standard totally diffuse density.

The duplication of the pot-opal densitometer should also be quite simple. Examination of Fig. 11 shows that a variation in the reflectance of the opal glass of five percent corresponds to a density error of about 0.002. Such a variation in reflectance corresponds to a relatively large variation in thickness, as shown in Fig. 9.

One set of twelve opal glasses was cut from Monax glass 1 in. in diameter and 2 mm thick, one side polished and the other fine-ground. These glasses have an average reflectance of 0.58 and the variation in reflectance is hardly measurable. The corresponding variations in density measurement are vanishingly small.

In the final specification of this opal glass, one side was fine-ground, in order to reduce the thickness required for adequate diffusion. The side turned toward the test density was polished in order to facilitate cleaning.

All the data shown here on polished opal-glass were duplicated with fine-ground glasses. The test results are but little different from those on the polished glasses.

ACKNOWLEDGMENTS

The author expresses his thanks to the following members of these Laboratories who cooperated in carrying out this work: Frank Milligan, for a preliminary comparison of opal densitometers in use here; R. N. Wolfe, who supplied all the test densities; E. M. Lowry, for his collaboration in planning and carrying out the investigation; and C. N. Nelson, as a representative of the American Standards Association, Sectional Committee Z38, Subcommittee 2, which prepared American Standard for Diffuse Transmission Density Z38.2.5-1946.

Recent Investigations in the Far Infra-Red

T. KING MCCUBBIN, JR. AND WILLIAM M. SINTON
Department of Physics, The Johns Hopkins University, Baltimore, Maryland
(Received April 26, 1950)

Experiments have been carried out in the far infra-red region from 100 to 600 microns using a grating spectrograph with crystal quartz optics. These experiments include measurement of the transmission of the atmosphere for paths up to 8 meters, the measurement of the transmission of various solid substances, and the observation of the longest wave-length pure rotation lines in the spectra of ammonia and hydrogen chloride.

THE FAR INFRA-RED GRATING SPECTROGRAPH

OUR far infra-red investigations were performed using the grating spectrograph shown in Fig. 1. Crystal quartz lenses of 8 cm diameter served as telescope lens and collimator lens in this instrument. These lenses have a focal length of 13 cm in the region beyond 100μ where the index of refraction of quartz is 2.2. Two echelette gratings were used, one with 66$\frac{2}{3}$ lines per inch for the region from 100 to 300μ and one with 25 lines per inch for the region from 300 to 600μ. These gratings were made on duraluminum by means of a milling machine. Each has four inches of grooves, each groove being three inches long. The echelette facets make an angle of 10° with the surfaces of the gratings. An Eppley-Golay cell was equipped with a crystal quartz window for use as detector. For some of the measurements, the 3 mm diameter aperture of the Golay cell served as exit slit. The effective exit slit width could be widened by means of the crystal quartz magnifying lens, or made narrower with metal slit jaws waxed to the Golay cell. Chopper blades provided modulation of the radiation at a frequency of 10 cycles per second. The 10-cycle electrical signal from the Golay cell was amplified, rectified, and displayed on a Leeds and Northrup Speedomax G Recorder.

A H-3 quartz mercury arc was used as source. In this lamp the arc takes place in a fused quartz tube of dimensions: 18 mm length, 4.5 mm inside diameter, and 8 mm outside diameter. It operates at 30 atmospheres pressure and consumes 85 watts. We broke away the outer glass envelope and replaced it with a test tube into which a hole had been blown.

The following precautions were taken to prevent short wave-length radiation from obscuring the far infra-red spectrum.

(1) The quartz optics were in focus for the far infra-red radiation for which quartz has an index of refraction of 2.2, whereas for visible and near infra-red radiation, where the index is about 1.5, they were out of focus.

(2) The radiation passed through about 35 mm of crystal quartz, a thickness which is opaque to radiation in the region from 4 to 100μ.[1] When obtaining spectra from 300 to 600μ with the 25 line per inch grating, we used a 1-mm thick rocksalt filter to eliminate radiation shorter than 300μ and chopped with a metal chopper.

(3) Four of the quartz lens surfaces, and also the grating surface, were smoked with turpentine soot. Such a soot filter does not transmit visible and near infra-red radiation, and yet is quite transparent to the far infra-red.

(4) The ground surface of the aluminum mirror and the machined facets of the gratings scattered the short wave-length radiation while reflecting the long wave-lengths specularly.

(5) For the first experiments, rocksalt plates were used for the chopper. Rocksalt is transparent to visible and short wave-length infra-red radiations and opaque for far infra-red radiation. This chopper modulated the visible and near infra-red radiations only slightly while giving complete square wave modulation to far infra-red radiation out to 300μ. We only used this selective chopper for the first few experiments because the other measures taken for the elimination of short wave-length radiation provided sufficient isolation to permit use of the more convenient metal bladed chopper.

(6) One reflection from a KRS5 crystal was used in some of the earlier experiments. Tests also indicated that pure radiation could be obtained without this reflection.

(7) The 66$\frac{2}{3}$ lines per inch echelette grating had its blaze at 135μ in the first order and the grating with 25 lines per inch had its blaze at 350μ in the first order. The higher order spectra in the blaze were eliminated by the filters of quartz for the finer grating and quartz plus rocksalt for the coarser grating. Beyond the blaze,

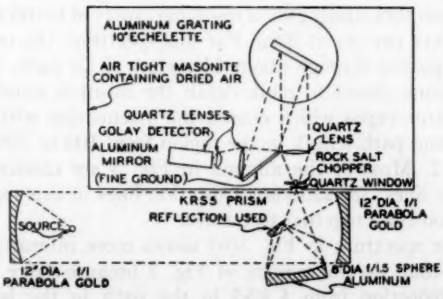

FIG. 1. Far infra-red spectrometer and transmission paths.

[1] R. B. Barnes and C. H. Cartwright, Zeits. f. Physik **90**, 430 (1934).

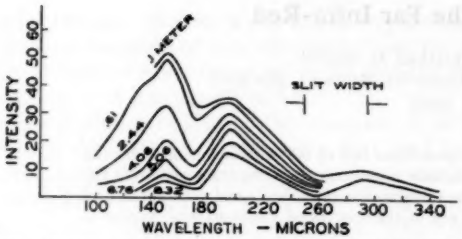

FIG. 2. Spectra of a H-3 mercury arc with various transmission paths through the atmosphere (relative humidity 53 percent, temperature 26°C).

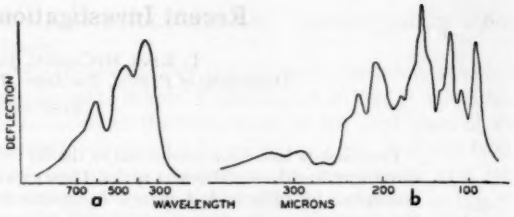

FIG. 3. Spectrum of a quartz mercury arc with atmospheric absorption. Relative humidity 70 percent at 29°C. (a) with 25-line-per-inch grating and 5-mm slits; (b) with 66⅔-line-per-inch-grating and 2.5-mm slits.

the efficiency of the gratings for higher orders fell so much faster than the efficiency in the first order that the shorter wave-length radiation in the higher order spectra did not obscure the first-order spectrum.

All of our experiments indicated that the grating spectrograph was isolating radiation of purity better than 80 percent throughout the region from 100 to 600μ.

ATMOSPHERIC TRANSMISSION IN THE SPECTRAL REGION FROM 100 TO 350μ

The optical system for measuring atmospheric transmission, shown below the spectrograph in Fig. 1, consisted of two 12-inch parabolas, a spherical mirror, and a KRS5 plane reflecting surface. Various atmospheric transmission paths were obtained by moving the first parabola and the source. The source used was a H-3 mercury arc. At path distances greater than 4 meters this optical system did not fill the $f/1.5$ aperture of the spectrograph without vignetting. We corrected for this vignetting for each transmission path by measurements of the visual illumination of a piece of filter paper at the entrance slit with a Macbeth illuminometer.

Figure 2 shows the spectra corrected by means of these illumination measurements. These spectra were obtained using a slit width of about 6 mm with a resulting resolving power of about 10 waves per cm at 200μ. Relative humidity was about 53 percent and room temperature 26°C on the September days when they were taken. For these measurements, the air in the box which contained the spectrograph was dried using silica gel and anhydrone.

Figure 3 shows a spectrum in this region taken with 2.5 mm slits which gave a resolving power of better than 3 waves per cm at 200μ. For this spectrum, the radiation passed through about $1\frac{3}{4}$ meters of air path. This spectrum shows in more detail the rotation structure of water vapor which caused the attenuation with increasing path length in the region from 100 to 200μ in Fig. 2. Most of the minima in Fig. 3 are clusters of water lines; the individual rotation lines in this region are too close together to resolve.

The spectrum in Fig. 3(b) shows more intensity at 100μ than do the spectra of Fig. 2 because there was one reflection from KRS5 in the path in the latter nstance.

The spectrum in Fig. 3(a) was obtained with the coarser grating and 5 mm slits. It exhibits a resolving power at 500μ of about 3 waves per cm. Two individual water vapor lines can be seen on this spectrum, one at 400μ and the other at 540μ. These are evidently the lines resulting from the rotational transitions of $J_\tau: 2_{-2}$ to 2_0 ($\tilde{\nu}=25.01$ wave numbers) and 1_{-1} to 1_1 (18.52 wave numbers).[2]

FAR INFRA-RED TRANSMISSION OF SOLID SUBSTANCE

Transmission spectra of some solid substances which we found to be transparent in the far infra-red are shown in Fig. 4. The maximum in the transmission of the mica at 300μ is evidently a channel spectrum maximum.

PURE ROTATION SPECTRA OF AMMONIA AND HYDROGEN CHLORIDE

The pure rotation spectra of ammonia and hydrogen chloride are shown in Fig. 5. All measurements at

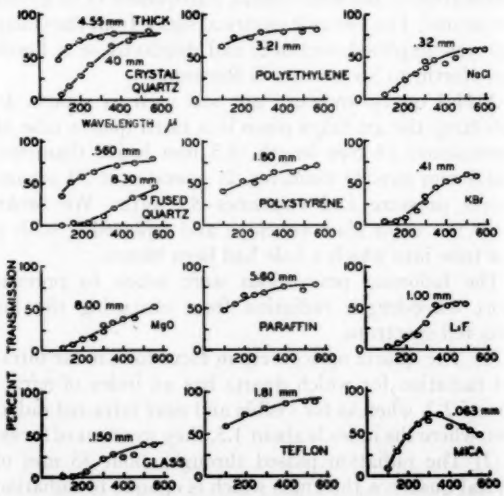

FIG. 4. Far infra-red transmission spectra of various solid materials.

[2] Water vapor absorption frequencies calculated from the constants of Randall, Dennison, Ginsburg, and Weber, Phys. Rev. 52, 160 (1937).

wave-lengths shorter than 300μ were made using a 5-cm cell with polyethylene windows which we placed in the beam between the collimator lens and the grating.

To obtain the longest wave-length line in each of the spectra, it was necessary to use a 13-cm path which we obtained by building a cardboard cell to enclose the space between the entrance slit and the collimator lens. The 1.3-mm rocksalt filter at the entrance slit and the quartz collimator lens served as windows for this cell. The five lowest frequency lines in the pure rotation spectra were observed for both gases.

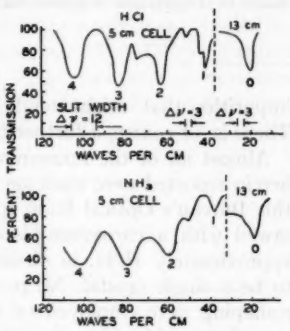

FIG. 5. Pure rotation spectra of ammonia and hydrogen chloride. (Numbers under transmission minima are the lower J values in the pure rotation transitions.)

THE FAR INFRA-RED TRANSMISSION OF ROCKSALT

In 1930 Czerny published a paper[3] in which he chose the constants in the formula for the complex index of refraction of rocksalt so that the values of n and k given by the formula:

$$(n-ik)^2=1+\sum_l \frac{C_l}{\omega_l^2-\omega^2+i\omega D_l}$$

would agree with the infra-red measurements which he and others had made. The dashed line in Fig. 6 is a plot of his calculated values for k in the far infra-red region. His calculations take into account the absorption frequencies in the ultraviolet, the main infra-red absorption at 61.0μ, and the weaker absorption which

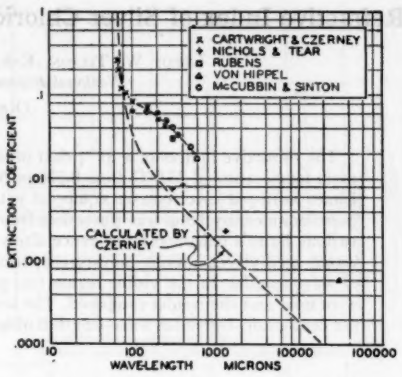

FIG. 6. The extinction coefficient of sodium chloride in the far infra-red.

is observed at 40.5μ. Measurements later made by Cartwright and Czerny,[4] using a grating spectrograph, showed greater absorption beyond 80μ than was given by Czerny's calculations. Our measurements, which are in agreement with those of Cartwright and Czerny, indicate that rocksalt has a third broad infra-red absorption line at about 150μ.

Other measurements of the far infra-red transmission of rocksalt have been made by Rubens[5] and Nichols and Tear[6] using radiation isolated by filters. Nichols and Tear made the measurement at 1300μ using a Hertzian oscillator as source. The 3-cm measurement was communicated to us by A. R. von Hippel.

ACKNOWLEDGMENT

This work was supported by Contract N5ori-166, Task Order 5, and was carried out under the supervision of John Strong. We are grateful to R. W. Wood for the loan of the crystal quartz lenses with which he and Rubens performed the original experiments on the focal isolation of far infra-red radiation.

[3] M. Czerny, Zeits. f. Physik **65**, 600 (1930).

[4] C. H. Cartwright and M. Czerny, Zeits. f. Physik **90**, 457 (1934).

[5] H. Rubens, Sitzungsberichte der Koniglich Preuss. Akad. der Wiss., 260 (1912).

[6] E. F. Nichols and J. D. Tear, Astrophys. J. **61**, 17 (1925).

Refractive Index of Silver Chloride for Visible and Infra-Red Radiant Energy*

LEROY W. TILTON, EARLE K. PLYLER, AND ROBERT E. STEPHENS
National Bureau of Standards, Washington, D. C.

(Received March 3, 1950)

The refractive indices of a 31° prism of silver chloride were measured at 30 wave-lengths at a constant room temperature of 23.9°C, from 0.578 to 20.6μ by use of a minimum-deviation spectrometer and a Perkin-Elmer infra-red spectrometer equipped with a calibrated screw for operation of the Littrow mirror. A cadmium-mercury lamp was the source from 1 to 2μ. From 2 to 20μ a Globar was used as the source with various Baird's reflection interference filters and the absorption bands of carbon dioxide, carbon disulfide, water, methylcyclohexane, polystyrene, trichlorobenzene, and chlorobenzotrifluoride for the identification of wave-lengths. In the visible region two prisms, one pressed and polished, the other sawed and lapped, were used and the results compared. The sensitivity of index to temperature is approximately -6.1×10^{-5} per centigrade degree for wave-length 0.610μ.

DURING World War II, progress was made in the United States in perfecting methods for growing crystalline silver chloride and in studies of its properties in order that it might supplement other available materials for windows, lenses, prisms, and other components for use in infra-red optical instruments and investigations. Silver chloride like thallium bromide-iodide is of the cubic system and has a high refractive index, 2.07 for sodium light. As grown, it is free from strain and not doubly refracting, but some low order strain can be introduced by pressing and otherwise reshaping the material.

We are informed by the Harshaw Chemical Company of Cleveland, where this silver chloride crystal was grown, that no commercial silver chloride is used in its preparation. Their silver chloride is specially prepared, starting with ingot silver and using only chemicals of reagent grade. All operations, including fusion of the silver chloride and loading of the furnace for growing the crystals, are carried out in light from tungsten bulbs protected by opalescent shades. Under these conditions the crystals are grown completely without color and the manufacturer feels that there are no impurities that might tend to form solid solutions. There is, of course, a further fining during growth.

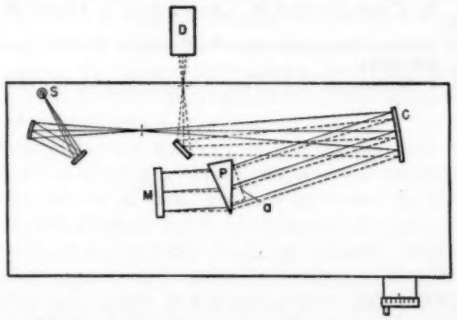

FIG. 1. Diagram showing installation of prism, P, on infra-red spectrometer. S represents the source, D the Golay detector, C the collimating mirror, M the Littrow mirror, and a an auxiliary prism for use in mounting the prism P for a definite angle of incidence.

Almost all of the measurements of refractive index herein reported were made on a 31° prism fashioned in this Bureau's Optical Shop with faces about 5×7 cm sawed with a chromium-plated blade from an ingot approximately 3½ in. in diameter and 2 in. long, said to be a single crystal. No pressing or other means of reshaping were employed on this prism. The surfaces were flattened by abrasion with a chromium-plated file and lapped to within a few wave-lengths of planeness on a clean dry Arkansas oilstone. The over-all degree of planeness by lapping had previously been found superior to that obtained by polishing. Some vertical scattering because of the fine horizontal marks produced by lapping was deemed less objectionable than the lack of planeness occasioned when the surfaces were polished.

The refractive indices of this prism were first measured in the visible region for five wave-lengths in the yellow and red. This was done by means of a minimum-deviation spectrometer, chiefly at temperatures near 23.4°C. Subsequent measurements of index at 27.3° for three of these same spectrum lines permit the evaluation of a temperature coefficient of -6.1×10^{-5} per degree centigrade for wave-lengths in the neighborhood of 0.61μ.

In attempting to get good optical surfaces a preliminary prism had been fashioned, from a different ingot, in a different manner involving some deformation, within a chromium-plated mold, under pressures approximating 2000 to 5000 lb./sq. in. at temperatures up to 295°C. The refractive indices measured on this preliminary prism, for five wave-lengths in the visible region, averaged higher by 36×10^{-5} than the indices for the second prism which was fashioned without application of heat or pressure.

The method used for index measurements in the infra-red is the same as that already described by the authors[1] for measurements on crystals of thallium

* The work described in this paper was carried out in part under Contract S and A 28658 between the Bureau of Ships and the National Bureau of Standards.

[1] L. W. Tilton, E. K. Plyler, and R. E. Stephens, J. Research Nat. Bur. Stand. 43, 81 (1949).

bromide-iodide. That is, briefly, the prism was installed with the aid of an auxiliary prism at an angle of known incidence on a Perkin-Elmer infra-red spectrometer (Fig. 1) equipped with a Littrow mirror; a Golay cell detector was used and a measure of the received energy was recorded on a Speedomax potentiometer. It is necessary, however, to refer the infra-red data to a known index in the visual region.

The refracting angle, A, of the prism was found to be $30°-49'-3.3''$, the visually determined refractive index, n, as adjusted for $t=23.9°C$, was 2.06931 for $\lambda=0.578\mu$ (mean of the mercury yellow lines), and the incidence angle, i, for which the prism was installed on the infra-red spectrometer was $33°-20'-45''$, which corresponds closely to $(A+D)/2$ at minimum deviation for these mercury lines. From these data, one computes an angle of emergence, E_0, of $33°-21'-49''$ for the initial conditions. An auxiliary prism was made in order to permit, by reflection of visible light, accurate installation of the silver chloride prism on the infra-red spectrometer.

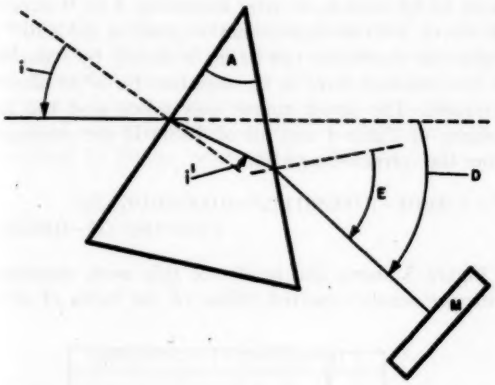

FIG. 2. Simplified relation of Littrow mirror, M, to deviation, D, and angle of emergence, E, produced by prism with angle, A, when light is incident at fixed angle i.

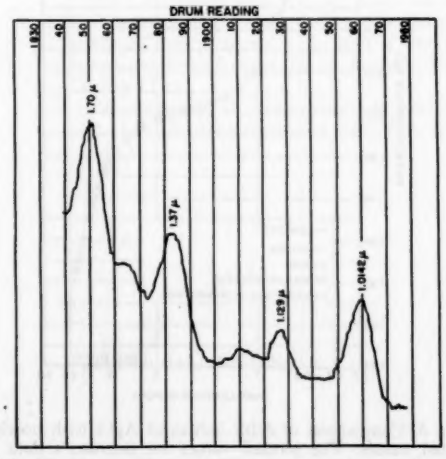

FIG. 3. Infra-red emission spectrum of mercury; silver chloride prism. An increment of 10 in drum reading (0.10 turn of screw) corresponds to an orientation of 162 seconds of the Littrow mirror.

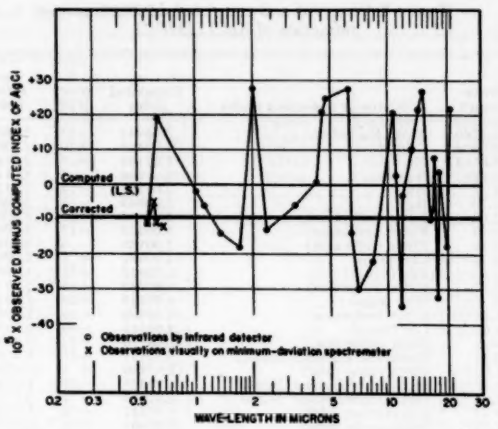

FIG. 4. Comparison of observed and computed indices of AgCl and evaluation of systematic error between visual and infra-red determinations.

The angular increments for the Littrow mirror, between the initially and the subsequently recorded energy maxima and minima, when applied to the initial E_0 give approximate values of E_λ for use in computing indices by the equations

$$\cot i' = \cot A + (\sin E / \sin A \sin i)$$

and

$$n = \sin i (1+\cot^2 i')^{\frac{1}{2}},$$

where the symbols have meanings as designated in Fig. 2.

It will be noticed in Fig. 1 that the entrance and exit slits of the infra-red spectrometer subtend a small angle (1.9636°) and thus the approximate values of index must be corrected[2] to compensate for the fact that $\delta E/2$, incidence angle on the Littrow mirror, is not zero (as it would be if entrance and exit slits subtended zero angle) or even constant for the different wave-lengths that are used.

The wave-lengths used in measuring the indices of the prism were identified in three different ways. For the region from 0.578 through 1.70μ the energy was obtained from a mercury-cadmium lamp of the Type FH4 manufactured by the General Electric Company. The wave-length 1.129μ is accurate to 0.001μ, and the wave-length at 1.70μ, the mean of several closely grouped lines, is accurate to 0.005μ. Figure 3 shows the recorded energy from the amplifier for these lines, for which the slit width was 0.25 mm.

The low dispersion of the silver chloride prism in the region from 2 to 6μ made it difficult to use narrow absorption bands for calibration. A series of reflection

[2] Reference 1, p. 84.

TABLE I. Observed and computed data on index of refraction of AgCl (23.9°C).

Wave-length	Source or absorbing media	Computed index	$(o-c)$ $\times 10^5$	Corrected index
0.5780	Mean Hg yellow	2.06942	−11	2.06932
0.6438	Cd red	2.05489	+19	2.05479
1.0142	Hg	2.02189	− 2	2.02179
1.129	Hg	2.01786	− 6	2.01776
1.37	Hg	2.01247	−14	2.01238
1.70	Hg	2.00843	−18	2.00833
2.02	Filter (reflection)	2.00613	+28	2.00603
2.43	Filter (reflection)	2.00422	−13	2.00412
3.39	Filter (reflection)	2.00138	− 6	2.00129
4.24	CO_2 in air	1.99937	+ 1	1.99927
4.62	CS_2 (liquid)	1.99847	+21	1.99837
4.87	Filter (reflection)	1.99787	+25	1.99777
6.26	H_2O (vapor)	1.99419	+28	1.99409
6.44	Filter (reflection)	1.99366	−14	1.99357
6.62	CS_2 (liquid)	1.99313	−30	1.99303
8.22	Filter (reflection)	1.98776	−22	1.98766
10.34	Methylcyclohexane (liquid)	1.97887	+21	1.97877
11.03	Polystyrene (film)	1.97550	+ 3	1.97541
11.47	Methylcyclohexane (liquid)	1.97323	−35	1.97313
11.86	Methylcyclohexane (liquid)	1.97113	− 3	1.97104
13.22	Polystyrene (film)	1.96312	+10	1.96303
14.32	Polystyrene (film)	1.95601	+22	1.95591
14.98	CO_2 in air	1.95137	+27	1.95127
16.40	1,2,4-trichlorobenzene (liquid)	1.94049	−10	1.94040
16.90	*p*-chlorobenzotrifluoride (liquid)	1.93636	− 7	1.93627
17.38	1,2,4-trichlorobenzene (liquid)	1.93224	+ 8	1.93215
17.80	1,2,4-trichlorobenzene (liquid)	1.92851	−32	1.92842
18.16	1,2,4-trichlorobenzene (liquid)	1.92522	+ 4	1.92513
19.80	*p*-chlorobenzotrifluoride (liquid)	1.90908	−18	1.90898
20.56	1,2,4-trichlorobenzene (liquid)	1.90093	+22	1.90083

interference filters was obtained from the Baird Associates and the maxima and minima were determined with a lithium fluoride prism. The error in determining the maxima is less than 0.02μ for the values 2.02, 2.43, 3.39, and 4.87μ. All the remaining wave-lengths listed in Table I were selected from the absorption bands of substances that have been previously measured. The center of the CO_2 absorption band is 4.255μ but the prism would not resolve the band into two peaks and it was found, by using wide slits with a NaCl prism, that the region of 4.24μ showed the maximum absorption. The 6.26μ band of water vapor in the air is well known, but this value applies to the center of the band which is practically free of absorption. An error of 0.02μ could result from lack of proper location of the center of the band on the observed curve. The atmospheric absorption of CO_2 at 14.98 gives rise to a very sharp peak which could be determined with this prism to 0.01μ.

The other wave-lengths were taken from measurements made on a Perkin-Elmer infra-red spectrometer using prisms of NaCl and KBr and are probably accurate to 0.02μ and in no case should the error exceed 0.04μ. The absorption bands of 1, 2, 4-trichlorobenzene, with wave-lengths of 17.38 and 18.16μ, have been checked by one of the authors on a grating instrument in the Physics Department of the University of Michigan and the values observed for these two bands were 17.42 and 18.16μ. The absorption bands at 17.42 and 17.80μ are broad and it is difficult to determine the region of maximum absorption accurately.

The index data were adjusted by least squares through determination of the parameters of the 5-constant Kettler-Helmholtz dispersion formula with the infra-red Sellmeier term expanded. The agreement between observed and computed values is shown by the residuals tabulated in Table I and also shown by Fig. 4 where 30 circles represent indices determined on the infra-red spectrometer and 4 crosses show visual determinations to which much higher weight should be given.

It is evident that the infra-red level is 9×10^{-5} too high but this discrepancy could be caused by an error of 12 seconds of arc in the basic or initial deviation assumed for the yellow lines of mercury, or by a difference of only 9 seconds in effective refracting angle in case the apertures of an imperfect prism as actually used were not exactly identical as installed on the two instruments. In other words, the difference in level shown in Fig. 4 is, under the circumstances, remarkably small.

For either error, or for a combination of each type, this small systematic net error could be corrected by recomputing all observations after reducing all deviations by 12 seconds, or after increasing A by 9 seconds. However, with an approximation good to $\pm5\times10^{-6}$ in index, the correction can be made simply by reduction of the constant term in the equation for n^2 as already adjusted. The latter course was taken and the last column of Table I and all of Table II are computed from the corrected equation

$$n^2=4.00804-0.00085111\lambda^2-0.00000019762\lambda^4 +0.079086/(\lambda^2-0.04584).$$

Figure 5 shows the results of this work compared with previously reported values of the index of silver

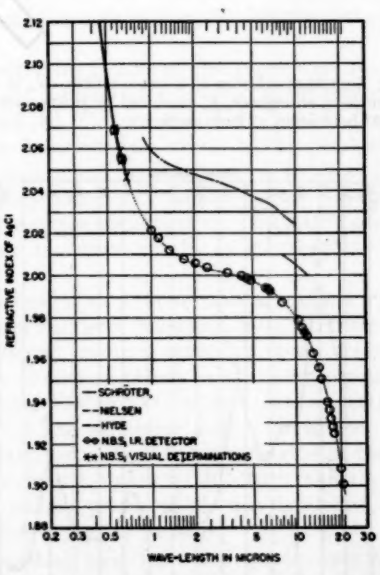

FIG. 5. Comparison of NBS indices of AgCl with previously reported values. The plotted values for Schröter's data were computed from his equation [Zeits. f. Physik **67**, 24 (1931)]. The values of Nielson and of Hyde were taken from the curves on p. 39 of *"Infra-red optical materials"* by Baird Associates, Inc. (1949).

TABLE II. Refractive index of AgCl at 23.9°C.

Wave-length	Tenths of microns 0	1	2	3	4	5	6	7	8	9
μ										
0	—	—	—	—	—	2.09648	2.06385	2.04590	2.03485	2.02752
1	2.02239	2.01865	2.01582	2.01363	2.01189	2.01047	2.00931	2.00833	2.00750	2.00678
2	2.00615	2.00559	2.00510	2.00465	2.00424	2.00386	2.00351	2.00318	2.00287	2.00258
3	2.00230	2.00203	2.00177	2.00151	2.00126	2.00102	2.00078	2.00054	2.00030	2.00007

Wave-length	n	Wave-length	n	Wave-length	n	Wave-length	n
μ		μ		μ		μ	
1	2.02239	6	1.99483	11	1.97556	16	1.94358
1.5	2.01047	6.5	1.99339	11.5	1.97297	16.5	1.93958
2	2.00615	7	1.99185	12	1.97026	17	1.93542
2.5	2.00386	7.5	1.99021	12.5	1.96742	17.5	1.93109
3	2.00230	8	1.99847	13	1.96444	18	1.92660
3.5	2.00102	8.5	1.98661	13.5	1.96133	18.5	1.92194
4	1.99983	9	1.98464	14	1.95807	19	1.91710
4.5	1.99866	9.5	1.98255	14.5	1.95467	19.5	1.91208
5	1.99745	10	1.98034	15	1.95113	20	1.90688
5.5	1.99618	10.5	1.97801	15.5	1.94743	20.5	1.90149

chloride, the present values being represented by circles and crosses. Schröter does not mention temperature and estimates his accuracy as $\pm 3\times 10^{-4}$ in index. The agreement between his results and ours is excellent for the small region in which our data overlap. The indices according to Hyde, measured by Talbot's bands, are probably valid only for the slope of the curve. The difference between Nielsen's curve and ours is large. His results have not been published but it is understood that his prism was practically opaque to visible radiation, and that the specimen may have contained impurities.

Group for the Advancement of Methods in Spectrography

The Groupement pour L'Avancement des Méthodes Spectrographiques is planning a symposium to be held in Strasbourg, France, October 12–14, 1950 at the University of Strasbourg. The symposium will deal primarily with problems in the field of spectroscopic analysis and the principal subjects treated will be Systematic Perturbations, Direct Analysis, Standards, Luminous Sources, and Analysis of Metalloids and Occluded Gas.

Persons wishing to present papers should communicate the exact title of their paper to the Secretary of G.A.M.S., 1 St. Thomas Aquinas Place, Paris 7, France. The official language of the conference will be French.

Letter to the Editor

A Method for the Determination of Optical Constants of Semitransparent Films

MAX S. OLDHAM,* L. G. MUNDIE, F. MATOSSI, AND B. F. CHEYDLEUR
Naval Ordnance Laboratory, White Oak, Silver Spring, Maryland
December 30, 1949

THE method of determining the optical constants of semitransparent films described in this letter is a modification of methods used by several other investigators in work with bulk materials.[1]

In 1947, Hadley and Dennison[2] presented a set of equations relating the optical constants of a semitransparent isotropic film between isotropic dielectrics to its reflectance, transmittance and thickness. Equations (28), (29), and (30) of Hadley and Dennison have been chosen as the basis of a method for determining the optical constants of such films. The method consists of the following two steps: (i) the film thickness, s, the reflectance at 10° angle of incidence, $R_{\perp 10}$, and the transmittance at normal incidence, $T_{\perp 0}$, are measured experimentally for radiation polarized with the electric vector normal to the plane of incidence; (ii) values of the optical constants of the film, n_2 and k_2, corresponding to these measured quantities are obtained from the Hadley-Dennison equations.

Because of the complexity of the equations, it is impossible to accomplish step (ii) above by direct solution. A numerical solution of the equations has therefore been performed with the aid of IBM machines. To do this, Eqs. (28), (29), (30) were first evaluated for $R_{\perp 10}$ and $T_{\perp 0}$ numerically for each of 10 parametric values of n_2, k_2 and s/λ, assuming one surrounding medium to be air and the other one a dielectric with refractive index 1.5, which can easily be approximated in practice. The range of the parameters was chosen as 0.1 to 10.0, 0.625 to 25.600, 0.0003 to 0.0993 for n_2, k_2 and s/λ, respectively. Interpolated solutions were then obtained for equi-interval values of $R_{\perp 10}$ and $T_{\perp 0}$ and arranged in the form of a table. Step (ii) can then be performed with the aid of this table. Space considerations permit the reproduction here of only a sample portion of the table† (Table I). In this table, the optical constants are listed at 4 percent intervals of $R_{\perp 10}$ and 1 percent intervals of $T_{\perp 0}$ for each of a range of values of the parameter s/λ.

As an example, suppose that $R_{\perp 10}$ and $T_{\perp 0}$ have been measured as 33 and 49 percent, respectively, at $\lambda = 1.0\mu$ and for $s = 100$A; $s/\lambda = 0.01$. In the groups for which $R_{\perp 10}$ is 33 and $T_{\perp 0}$ is 49, entries may be found corresponding to values of s/λ ranging from 0.06 to 0.0004. The entry nearest the measured value, 0.01, is 0.0102, for which the corresponding values of n_2 and k_2 are 0.8 and 4.9, respectively. In cases where the measured values are not so conveniently close to the tabular entries, standard interpolation procedures may be applied to obtain the corresponding values of n_2 and k_2.

TABLE I. Illustrative typical portion of table of numerical solutions of the Hadley-Dennison equations.

$R_{\perp 10}$ (%)	$T_{\perp 0}$ (%)	$s/\lambda \times 10^4$	$n_2 \times 10$	$k_2 \times 10$
.	.	.	.	.
.	.	.	.	.
.	.	.	.	.
33	49	648	003	011
33	49	356	005	023
33	49	248	005	030
33	49	152	007	039
33	49	102	008	049
33	49	070	010	060
33	49	049	012	072
33	49	036	015	086
.	.	.	.	.
.	.	.	.	.
.	.	.	.	.

It might be mentioned that the table, as originally[3] compiled, contained an additional column in which the values of reflectance at 70° angle of incidence, $R_{\perp 70}$, appeared. Using the table in this form, one could read off directly the values of n_2, k_2, and s/λ corresponding to measured values of $R_{\perp 70}$, $R_{\perp 10}$, and $T_{\perp 0}$. This method would have the advantage of being independent of any measurement of s/λ; it was, however, rejected as it was found to be considerably less accurate than that described in the foregoing paragraphs (because $R_{\perp 70}$ is, for a given value of $R_{\perp 10}$, practically independent of the parameters for a surprisingly large range of them), provided one can measure the film thickness with reasonable accuracy.‡

The entries in the table are accurate within 2 percent. Experimental errors in the measurements of $R_{\perp 10}$ and $T_{\perp 0}$ of, say, 2 percent generally lead to errors in n_2 and k_2 of less than 10 percent. A complete discussion of the accuracies obtainable in the determination of n_2 and k_2 by the use of the proposed method, as well as a detailed account of the procedure followed in obtaining the numerical table is given in reference 3.

Methods utilizing R and T have been used before, but either with approximations which are valid only for very small thicknesses[4] or with different methods of evaluation.[5]

* Now at the Strategic Air Command, Offutt Air Force Base, Omaha, Nebraska.

[1] G. Pfestorf, Ann. d. Physik **81**, 906 (1926); C. Boeckner, J. Opt. Soc. Am. **19**, 7 (1929); R. Tousey, J. Opt. Soc. Am. **29**, 235 (1939); J. R. Collins and R. O. Bock, Rev. Sci. Inst. **14**, 135 (1943).

[2] L. N. Hadley and D. M. Dennison, J. Opt. Soc. Am. **37**, 451 (1947).

† The complete table can be obtained by ordering Document 2831 from American Documentation Institute, 1719 N Street, N.W., Washington 6, D. C., and remitting $0.50 for microfilm (images 1 inch high on standard 35 mm motion picture film) or $1.30 for photocopies (6×8 inches) readable without optical aid.

[3] M. S. Oldham, "Determination of Optical Constants in the Near Infrared of Evaporated Metal Films from Reflectance, Transmittance, and Film Thickness Measurements" (unpublished Ph.D. Thesis, Iowa State College, Ames, Iowa, 1949).

‡ The interferometric method of Tolansky seems to give the most accurate values for film thickness at present. A description of this method is given in reference 3.

[4] H. Wolter, Zeits. f. Physik **104**, 269 (1939).

[5] M. Perrot, Ann. d. physik. **19**, 150 (1944).

Book Reviews

Structure et Propriétés des Couches Photographiques

L. P. Clerc. Second edition. Éditions de la Revue D'Optique Théorique et Instrumentale, Paris (15e), 1948. Pp. 193. Price 500 fr.

This book is a concise and clear account of present knowledge in its field. The first half deals with emulsion structure, latent image, development, and optical sensitization; the second with sensitometry, subdivided into density-exposure relations, reciprocity failure and other errors of integration, and photographic photometry; and with granularity and its effects. Photographic practice is omitted, and the treatment of theory is relatively brief; with these limitations it is possible to give an adequate treatment of the subjects mentioned in the space allotted. Illustrations are numerous and well chosen, but there is no index.

Burt H. Carroll
Kodak Research Laboratories
Eastman Kodak Company
Rochester, New York

Infrared Radiation Therapy Sources and Their Analysis with Scanner

Leopold Rovner. Charles C. Thomas, Springfield, Illinois, 1950. Pp. 34. Price $1.50.

This very brief monograph describes a scanning device utilizing a fast bolometer with amplifying equipment to measure radiation coverage patterns from various heat lamps used in therapy. Typical chart records are included. This material is essentially the same as published by the author with W. D. Paul and H. M. Hines, Arch. Phys. Med. **28**, 273 (1947). The introductory chapters give a brief but probably adequate discussion of the conditions to be met in infrared dosage. The book is directed to those interested in the use of radiant energy in therapy, but could possibly be useful in more general applications of heat lamps. The title could be improved.

Curtis J. Humphreys
National Bureau of Standards
Washington, D. C.

Fluorescence and Phosphorescence

Peter Pringsheim. Interscience Publishers, Inc., New York, 1949. Pp. 794+xvi. Price $15.00.

The author's approach has followed to some extent his earlier treatises on this subject (*Fluoreszenz und Phosphoreszenz im Lichte der neueren Atomtheorie*, 1921) although the expansion and composition of the present book and subject matter over the earlier 200-page book leaves little in common except the title.

The book emphasizes the fluorescence and phosphorescence of gases, vapors, organic liquids, and solids as compared with the emphasis on inorganic crystal properties in other recent books of the same general title. Nearly a third of the book is devoted to a critical survey of the fluorescence of gases and vapors which constitute Part I of the discussion. Part II on the fluorescence and phosphorescence of condensed systems in the liquid and solid state is divided between organic compounds, inorganic compounds and crystal phosphors.

The book is recommended as a comprehensive treatise and a critical literature survey on the subject of fluorescence and phosphorescence with an emphasis on the theoretical interpretation rather than technical applications. The more than 300 tables and figures supply ample data to support the discussions. The change in paper quality from rough to smooth stock with each halftone illustration is somewhat disturbing and considering the number of halftones the same stock might well have been used throughout.

Over 100 pages of bibliography are supplied in an alphabetical author arrangement with an author index which might have been more conveniently appended to the bibliographic references. The more than 2000 references covering the field of fluorescence and phosphorescence up to May 1948 may be considered as a comprehensive and well-selected coverage of the contemporary literature.

Wallace R. Brode
National Bureau of Standards
Washington, D. C.

News from the Local Sections of the Optical Society of America

New Officers of the Local Sections

During the months of April, May, and June each of the six local sections elects officers to serve for the forthcoming twelve-month period. The results of this spring's election are reported here, along with brief comments on the age and size of each of the sections.

The Rochester Section can be considered to antedate the National Society itself, since, as will be described in these columns next month, the Optical Society of America as a national society actually originated with the same group that founded the organization that is now known as the Rochester Section, which group first met during the winter of 1915–1916. At present the Rochester Section has a membership of about 400, which assures it of first place in size as well as age among the local sections. The affairs and activities of the section are directed by an executive council which consists of the usual officers plus the retiring president, four members-at-large, and the chairman of the program committee, who is appointed by the president with the approval of the remainder of the executive council. Officers for the coming year are:

President: James R. Benford, *Bausch and Lomb Optical Company.*

Vice President: Harold R. Condit, *Eastman Kodak Company, Research Laboratories.*

Secretary: Stephen M. MacNeille, *Eastman Kodak Company, Camera Works (Naval Ordnance).*

Treasurer: GORDON G. MILNE, *Institute of Optics, University of Rochester.*
Retiring President: ERNEST H. GREPPIN, *Wilmot Castle Company.*
Councillors: RALPH K. DAKIN, *Bausch and Lomb Optical Company;* ROBERT E. HOPKINS, *Institute of Optics, University of Rochester;* KONSTANTIN PESTRECOV, *Bausch and Lomb Optical Company;* ROBERT B. TACKABERRY, *Bausch and Lomb Optical Company.*

The Detroit Section came into existence in 1947 when the Michigan Society of Spectroscopy was recognized as the Detroit Section of the Optical Society of America. The present membership is 104. The executive council consists of the regularly elected officers, three councillors who are the last three chairmen to have held office, and the chairmen of the standing committees. The standing committees, which are appointed by the chairman of the Section and approved by the elected members of the council, are: membership, program, constitution and by-laws, and coordination. Newly elected officers for the coming year, and the three most recent chairmen, are:

Chairman: FORD R. BRYAN, *Ford Motor Company.*
Vice Chairman: WILLIAM R. O'NEILL, *Ethyl Corporation.*
Secretary: DANIEL L. HARMON, *University of Detroit.*
Treasurer: MARGARET E. GRIFFING, *Ethyl Corporation.*
Past Chairmen: HENRY A. TUTTLE, *Ford Motor Company;* DAVID L. FRY, *General Motors Research Laboratories;* G. M. RASSWEILER, *General Motors Research Laboratories.*

The Niagara Frontier Section also came into existence in 1947, as a result of a petition submitted to the Optical Society of America by the Spectrographic Society of the Niagara Frontier. This section now has 40 members. Its executive committee consists of the three elected officers and the two most recent past presidents of the section. The immediate past president serves as chairman of the executive committee. For the year 1950–1951 the Niagara Frontier Section will be guided by the following group of officers:

President: ERNEST SCHUSTIK, *Union Carbon and Carbide Works Laboratory.*
Secretary: TRUMBULL S. JACKSON, *Bethlehem Steel Company.*
Treasurer: JOHN T. WALLER, *Union Carbon and Carbide Research Laboratory.*
Past Presidents: GLENN E. SMITH, *National Aniline Division of the Allied Chemical and Dye Corporation;* GALEN PORTER, *Union Carbon and Carbide Chemicals Research Laboratory.*

The petition of the Ohio Valley Spectrographic Society was acted upon favorably early in 1948. The executive council of the Ohio Valley Section consists of three officers who are elected annually and four councillors elected for a two-year term, two being elected each year. This section has a membership of 55. Officers for the coming year are:

Chairman: C. H. ANESHANSLEY, *National Cash Register Company.*
Chairman-Elect: R. S. LAMBERT, *Proctor and Gamble Company.*
Secretary-Treasurer: CHARLES S. MILLS, *Armco Steel Corporation.*
Councillors (2 years): PAUL ROTHEMUND, *Kettering Foundation;* M. G. BOLINGER, *William Powell Company.*
Councillors (unexpired term—1 year): J. T. R. ANDREWS, *Proctor and Gamble Company;* M. L. STEINBUCH, *The Lunkenheimer Company.*

The New England Section represents the first group which was formed for the express purpose of petitioning for membership in the Optical Society of America. After an existence of just a few months, this "New England Optical Society" became the New England Section on May 5, 1949. Its present membership is 140, the second largest in the local section framework. Again, the section's day-to-day business is handled by an executive council, which consists of the regular officers and four members-at-large, all of whom are elected annually, the retiring president, and the (appointed) chairman of the program committee. The new officers of the New England Section are:

President: RICHARD C. LORD, *Department of Chemistry, Massachusetts Institute of Technology.*
Vice President: WALTER S. BAIRD, *Baird Associates, Inc.*
Secretary: JOHN T. WATSON, *Boston University Optical Research Laboratory.*
Treasurer: RUSSELL P. MAHAN, *Baird Associates, Inc.*
Past President: DUNCAN E. MACDONALD, *Boston University Optical Research Laboratory.*
Members-at-Large of the Executive Council:
STANLEY S. BALLARD, *Department of Physics, Tufts College.*
HAROLD E. EDGERTON, *Department of Electrical Engineering, Massachusetts Institute of Technology.*
DAVID S. GREY, *Research Department, Polaroid Corporation.*
HANS MUELLER, *Department of Physics, Massachusetts Institute of Technology.*

As reported in the June issue of this Journal, the Chicago Section was formally installed on May 24, 1950, when the active Optical Society of Chicago was recognized officially by the Optical Society of America. At the time of its installation this youngest section had 80 members. Its executive council consists of three elected councillors, the regularly elected officers, and the appointed chairmen of the standing committees. Officers for the year 1950–1951 are:

President: PAUL C. FOOTE, *Bell and Howell Company.*
Vice President and Program Chairman: WARREN J. SMITH, *Simpson Optical Manufacturing Company.*
Secretary: EUGENE PERRINE, *Armour Research Foundation.*
Treasurer: RALPH H. STEINBERG, *Carnegie Illinois Steel Company.*
Councillors: R. T. VAN NIMAN, *Motiograph, Inc.;* RUSSELL A. FISHER, *Northwestern University;* ROBERT A. WOODSON, *Consulting Optical Engineer.*

STANLEY S. BALLARD
Secretary for Local Sections

Announcements

Thirty-Fifth Annual Meeting of the Optical Society of America

THE thirty-fifth annual meeting of the Optical Society of America will be held at the Hotel Statler, Cleveland, Ohio, on October 26, 27, and 28, 1950. In addition to contributed papers covering all phases of optics, there will be a special program of invited papers on crystals. On Friday afternoon, October 27, the Society will be the guest of the General Electric Company at Nela Park. A tour of the Lighting Institute is being arranged as well as a program of invited papers by eminent authors on some phases of lighting and seeing.

Attendance at Optical Society of America meetings is not restricted to members of the Society and all interested persons are invited to attend and participate. Hotel reservation cards and an abstract blank will be mailed with the final meeting announcement to members of the Society the last of August. Those who wish to contribute papers at this meeting can assist in the arrangement of of the printed program by submitting their abstracts promptly on receipt of the blank. Additional blanks can be obtained from the office of the Secretary of the Society. The printed program and abstracts of papers to be presented will be mailed to members from Lancaster, Pennsylvania, October 7. In no case can an abstract be included in the program unless received in the office of the Secretary prior to noon on September 11. Abstracts should be addressed to Arthur C. Hardy, Secretary, Massachusetts Institute of Technology, Cambridge 39, Massachusetts.

In an attempt to save in publication charges and expedite publication, it will be helpful if authors will note any typographical errors in their abstracts and report these to the editor of the Journal upon receipt of their program. The abstracts of the meeting will be published in the November number of the Journal.

The program for the thirty-fifth annual meeting of the Optical Society is being arranged by a committee under the chairmanship of W. E. Forsythe and includes Stanley S. Ballard, B. T. Barnes, R. A. Beth, Hans Jaffe, Leonard Olsen, C. D. Spencer, and A. E. Taylor.

ASTM Emphasizes Spectroscopy and Optics in Its Annual Meeting—Wallace R. Brode Gives the Marburg Lecture

Dr. Wallace R. Brode, Editor of the *Journal of the Optical Society* and Associate Director of the National Bureau of Standards, was selected to present the Marburg Lecture at the 1950 Annual Meeting of the American Society for Testing Materials held in Atlantic City on June 27. The nomination to be the Marburg lecturer is an outstanding honor extended by the American Society for Testing Materials to a prominent scientist each year.

The purpose of the Edgar Marburg Lecture is to have described at the annual meeting of the American Society for Testing Materials, by leaders in their respective fields, outstanding developments in the promotion of knowledge of engineering materials. The Lecture honors and perpetuates the memory of Edgar Marburg, first Secretary of the Society and former Chairman of the Department of Civil Engineering of the University of Pennsylvania.

Following Dr. Brode's lecture he was presented with a scroll on recognition by the President of the American Society for Testing Materials, J. G. Morrow. The Marburg Lecture this year was the twenty-fourth lecture of this series; previous Marburg lectures since their establishment in 1926 have included a group of prominent engineers and scientists.

The committee on Emission Spectra (E-2) held a number of subcommittee sessions as well as a general meeting at which some 46 tentative methods of spectrochemical analysis were approved for publication. B. F. Scribner of the National Bureau of Standards was re-elected Chairman of the committee, E. B. Ashcraft of Westinghouse Electric Corporation Vice-chairman, and J. H. Coulliette of the University of Chattanooga Secretary, succeeding Mary Warga of the University of Pittsburgh who declined further continuance in this position after serving the committee for six years.

Of particular interest to Optical Society members was Report No. 4 of the Joint E-2—Society of Applied Spectroscopy on "Suggested Nomenclature in Applied Spectroscopy." This report was presented for discussion by the committee chairman, Dr. Harold K. Hughes. Although there appeared to be some terms upon which there was not a unanimity of opinion, it is hoped that some agreement will be reached so that an abstract of the final report of this committee may be published in this Journal.

The newly found committee on Absorption Spectra (E-13) held a steering committee meeting under its Chairman Wallace R. Brode, National Bureau of Standards. The other officers of this committee are Vice-chairman, E. J. Rosenbaum of the Sun Oil Company, and Secretary, W. S. Young of the Atlantic Refining Company.

Committee E-1 which is under the chairmanship of J. R. Townsend of Bell Telephone Laboratories is concerned with methods of testing and considered the field of optical instrumentation.

Activities of the Infra-Red Punch-Card Committee

The Punch-Card Committee, formed following an informal discussion at the 1948 Symposium on Molecular Structure and Spectroscopy at Ohio State University, had as its original function the survey of existing punch-card systems, with a view to producing a "standard" punch-card which would facilitate the exchange of infra-red data between laboratories. Using the data obtained from the cards submitted, the committee designed two cards, a "bibliography" card and a "compound" card.

The compound card includes the following: (1) A field for the wave-lengths of the absorption maxima. The scale (non-linear) runs from 2.70μ (3700 cm^{-1}) to 40μ (250 cm^{-1}) in 46 intervals, the size of the intervals varying from 25 to 200 wave numbers. (2) A field for functional groups. Fifty-seven functional groups are listed. (3) A field for either melting or boiling point, in 1° intervals from −300° to +300°C. (4) A field for the number of carbon atoms up to 39. The face of the card is to be used for recording the name of the compound, its empirical and structural formulas, and certain data which may be abstracted from literature references on the particular compound. The back of the card is to be used for a reproduction of the spectrum of the compound and a table of wave-lengths of absorption bands. The data from each of the literature references which appear on the face of the compound card are tied, by means of a reference number, to one or more bibliography cards.

The bibliography card may be sorted in the following fields: (1) The reference number, the first four numbers of which serve as an alphabetical index. (2) A subject field listing 39 subjects. (3) An apparatus field with 15 sub-headings. (4) A field for the year of publication. The face of the bibliography card is to be used for listing author, title, journal, and chemical abstract number. An abstract of the original paper may be reproduced on the front and, if necessary, continued on the back of the card.

Both the compound and bibliography cards have some unused holes in the inside row which are numbered serially and in the 1,2,4,7, SF code for use in individual laboratories for coding additional information if desired.

The punch-card system was presented at the 1949 Symposium on Molecular Structure and Spectroscopy and accepted, subject to a few minor revisions which are included in this presentation.

The Committee was responsible to no organized group; hence arrangements with the National Research Council for handling the Committee's finances are in process wherein the Punch-Card Committee will be a joint committee under both the Division of Physical Sciences and of Chemistry and Chemical Technology of the National Research Council. The present Committee consists of Chairman, Wallace R. Brode, National Bureau of Standards; Secretary, E. Carroll Creitz, National Bureau of Standards; and Bryce L. Crawford, University of Minnesota, Robert R. Hampton, United States Rubber Company, and James D. Stroupe, Rohm & Haas Company.

Paul Geary of the Smith, Kline and French Laboratories, has had a plate made for printing the compound card with cross-section lines on the back so that spectra may be plotted directly on the card. The Smith, Kline and French Laboratories have donated the use of this plate to the committee. The McBee Company will accept only large orders for cards printed from this plate but arrangements have been made with the Washington Branch of the McBee Company for the pooling of small orders.

The Wright-Patterson Air Force Base has, by means of a fund transferred to the National Bureau of Standards, initiated the production of punch-cards bearing infra-red spectra. This fund has made possible the preparation of multilith mats of spectra in advance of the official inclusion of the committee in the National Research Council.

Spectra of compounds of reasonably high purity and on which physical properties have been determined would be welcomed for inclusion in the punch-card file. General directions for the preparation of spectra for printing and correspondence concerning this committee should be addressed to the Secretary, E. Carroll Creitz, National Bureau of Standards, Washington 25, D. C.

German Glass Technology Society

THE German Glass Technology Society (Deutsche Glastechnische Gesellschaft) held its 24th annual meeting at Düsseldorf on June 6, 7, and 8, 1950. The program of the technical sessions included the following papers:

E. Jenckel, Organic Glasses and the Effect of Softening on their Congealing Temperature; H. W. Kohlschütter, Wetting and Cementing with Silicon-Compounds; W. E. S. Turner, Some Views on the Breaking of Glass Derived from the Examination of Fractured Surfaces (according to H. M. Bateson); Evidence Against Oriented Structure in Glass Fibers (according to F. W. Preston and W. H. Otto); J. E. Stanworth, The Physical Properties and Structures of Glasses; A. Dietzel, Reaction between Glass and Metal on Fusing; W. Klemm, Model Experiments for Polishing of Glasses; O. Gott, Technical Glasses with Various Spectroscopic Properties; H. J. Höfert, Methods for the Measurement of Spectral Transmission of Glasses; K. Flessa, Use of Cohart Blocks in Glass Tanks; G. Ribaud, The Thermal Exchange by Radiation in Gas Furnaces; E. V. Borel, Practical Results of Electrical Fusion; J. Dichter, Automatic Glass-Treatment Machines; T. Heim, Development of Blowers and Technical Air Problems in Glass Factories; W. König, Composition and Properties of Bottle Glass; H. Krippendorff, Rationalization in Glass Factories; R. Meister, Heat Control of Lehrs.

Trade Publications

Better Analysis. Baird Associates, 33 University Road, Cambridge 38, Massachusetts.

Baird Associates has initiated a quarterly publication on the technical application of their instruments under the title of *Better Analysis*. The first issue includes pictorial and descriptive information on grating productions, infra-red recording spectrophotometers, and incidental news items as well as equipment announcements. The next issue which is promised for about the middle of September will emphasize emission spectroscopy, some remarks about ammonium dihydrogen phosphate, and a note on the use of infra-red in the restoration of paintings.

Sensitized Materials for the Scientific and Industrial Laboratory. Eastman Kodak Company, Industrial Photographic Sales Division, Rochester, New York.

Eastman Kodak Company has recently issued a technical data circular with the above title, in which sensitivity range, emulsion characteristics, and other pertinent data are conveniently collected together for the research and industrial scientists and technicians. Other technical publications from Kodak which have been recently revised are **Kodak Materials for Spectrum Analysis, Kodak Photographic Plates for Scientific and Technical Use, Kodak Nuclear Track Plates and Kodak Nuclear Track Pellicles,** and **Autoradiography.** Other publications which are available are **Kodak Linagraph Films and Paper** and **Kodak Recording Materials.**